METHODOLOGIES FOR THE ANALYSIS OF MEMBRANE SYSTEMS USING LIPID NANODISCS

BY

IVAN LENKOV LENOV

DISSERTATION

Submitted in partial fulfillment of the requirements
for the degree of Doctor of Philosophy in Chemistry
in the Graduate College of the
University of Illinois at Urbana-Champaign, 2016

Urbana, Illinois

Doctoral Committee:

Professor Stephen Sligar, Chair
Professor Ryan Bailey
Professor James Morrissey
Professor Catherine Murphy

ABSTRACT

Membrane proteins are biologically significant targets of study due to their crucial roles in biochemical reactions, such as ion transport and cell signaling. Their study, however, is hampered by hydrophobic regions in their structures which cause aggregation without the presence of a membrane. For this reason, solubilization systems have been developed, but there are limitations to most. Nanodiscs were developed as an alternative platform that provides a native-like lipid bilayer for solubilizing membrane proteins with unparalleled control over lipid composition, exceptional monodispersity, and exceptional modularity. This dissertation details the coupling of Nanodiscs to multiple analytical platforms for the characterization of membrane systems, including Cytochrome P450s, blood coagulation factor proteins, and other membrane protein targets. The topology of three different Cytochrome P450 systems was characterized using linear dichroism spectroscopy. Methods were developed for the coupling of Nanodiscs to two different types of photonic biosensors, in atmospheric pressure and high pressure environments. The work further details the development of a microfluidic platform for the optimization of membrane protein incorporation into Nanodiscs as well as the development of a bimodal imaging construct utilizing Nanodiscs and a Gd(III) chelating molecule used as a contrast agent for the labeling of cells.

To Mom and Dad, for their love and support.

ACKNOWLEDGMENTS

This work represents the culmination of the last five years in my development both as a scientist and as an individual. This has by no means been a solitary journey and I have a lot of people to thank for their support. First, and foremost, I want to thank Prof. Stephen Sligar for his tremendous support and inspiration. The way he approaches scientific problems with an inquisitive instinct and a critical eye has presented an excellent example for me to follow. He has been an irreplaceable guide in this journey and his sage advice and direction will continue to influence me throughout my life.

I thank all of the members of the Sligar group, both past and present, for everything they have done for me including teaching, supporting, fruitful discussions, and at times constructive criticism. Having absolutely no experience in experimental biochemistry and molecular biology when I first joined the group, it was a steep learning curve with a lot of need for support. Dr. Ilia Denisov and Dr. Mark McLean initiated valuable discussions which provided me with the necessary fundamental background. Yelena Grinkova and Dr. Michael Marty taught me fundamental experimental and instrumental methods, Nanodisc assembly, basic molecular biology, and protein expression and purification, which have served me throughout my career here. Thank you to Dr. Abhinav Luthra, Michael Gregory, and Ruchia Duggal for the support with the Cytochrome P450 projects. Thank you to Xin Ye for the help with the high pressure project and for help with the HPLC. Thank you to Catherine Baker for being there with me from the onset - your support and friendship in and out of the lab has been a crucial and much needed part of this journey. I thank all lab members for all of their help in the lab, for the great company, and for the happy hour and ski trip escapades and shenanigans.

I want to thank all of my collaborators and former mentors, both on campus and off. I

have had the pleasure of working with Javier Baylon and Prof. Emad Tajkhorshid on the biophysical characterization of CYP enzymes and learning fundamental MD simulations. I thank James Wade, Ellen Muehl, and Prof. Ryan Bailey for all of their guidance on microring resonators and microfluidics. I thank Christiane Carney and Prof. Thomas Meade from Northwestern University for the guidance and collaboration on the MRI contrast agent project. Thank you to Scott Baker and Jared Bear at the Life Sciences Machine Shop for building custom designed parts for me. Thank you to the Core Facilities at the Carl R. Woese Institute for Genomic Biology for the providing training and help with the AFM.

I want to thank all of my friends outside of the Sligar group for making graduate school a great experience and for teaching me along the way. Thank you especially to my roommates - Daniel McCurry and David Wetzel - for putting up with me, for being great comrades, and for always being there when I needed you. Thank you to the wonderful Lisa Michigan for all the support and listening to my late night ramblings.

This work was funded in part by the National Institutes of Health Grant GM110432, the Ullyot Fellowship, the John and Margaret Witt Fellowship, and the Dow Chemical Travel Award. Thank you to all funding sources.

Lastly, I want to thank my entire family for all they have done for me, especially my parents, Lenko and Janeta Lenov. Without your unwavering belief in my abilities and continued encouragement and support I wouldn't have even come close to making it through graduate school. You have been there for me through everything and given me everything, even when it meant you were left without. Mom and Dad, I dedicate this work to you.

TABLE OF CONTENTS

LIST OF ABBREVIATIONS viii

CHAPTER 1 INTRODUCTION 1
1.1 Membrane Proteins 1
1.2 Strategies Addressing Membrane Protein Solubilization 3
1.3 Nanodiscs 5
1.4 Applications of Nanodiscs to Biochemical Problems 8

CHAPTER 2 ORIENTATION OF CYTOCHROME P450S WITHIN THE LIPID BILAYER 15
2.1 Introduction 15
2.2 Methods 17
2.3 Results and Discussion 22
2.4 Conclusions 23
2.5 Figures and Tables 25

CHAPTER 3 DEVELOPMENT OF THE HIGH PRESSURE LABEL FREE BIND ASSAY 31
3.1 Introduction 31
3.2 Theory 33
3.3 Methods 34
3.4 Results and Discussion 35
3.5 Conclusions 37
3.6 Figures and Tables 39

CHAPTER 4 INTERFACING DNA-LABELED NANODISCS WITH PHOTONIC MICRORING RESONATORS 45
4.1 Introduction 45
4.2 Methods 47
4.3 Results and Discussion 51
4.4 Conclusions 52
4.5 Figures and Tables 54

CHAPTER 5 DEVELOPMENT OF MICROFLUIDIC PLATFORM FOR THE ASSEMBLY OF NANODISCS 59
5.1 Introduction 59
5.2 Methods 61
5.3 Results and Discussion 64
5.4 Conclusions 68
5.5 Figures and Tables 69

CHAPTER 6 DEVELOPMENT OF A NANODISC DELIVERY PLATFORM FOR MRI-OPTICAL IMAGING 77
6.1 Introduction 77
6.2 Methods 79
6.3 Results and Discussion 81
6.4 Conclusions 84
6.5 Figures and Tables 85

CHAPTER 7 CONCLUSIONS AND FUTURE WORKS 89

REFERENCES 93

LIST OF ABBREVIATIONS

AFM	Atomic Force Microscopy
ApoAI	Apolipoprotein A-I
APTES	(3-Aminopropyl)triethoxysilane
BIND	Biomolecular Interaction Detection
BSA	Bovine Serum Albumin
BS3	Bis(sulfosuccinimidyl)suberate
CTB	Cholera Toxin B
CHAPS	3-[(3-cholamidopropyl)dimethylammonio]-1-propanesulfonate
CYP	Cytochrome P450
CYP17	Cytochrome P450 17A1
CYP19	Cytochrome P450 19A1
CYP3A4	Cytochrome P450 3A4
DMPC	1,2- dimyristoyl-*sn*-glycero-3-phosphocholine
DMPS	1,2-dimyristoyl-*sn*-glycero-3-phospho-L-serine
DMSO	Dimethyl Sulfoxide
EDTA	Ethylenediaminetetraacetic Acid
EGFR	Epidermal Growth Factor Receptor
G_{M1}	Ganglioside Glycolipid GM1
HDL	High Density Lipoprotein
HEPES	4-(2-hydroxyethyl)-1-piperazineethanesulfonic acid

HMMM	Highly Mobile Membrane Mimetic
IRE	Internal Reflection Element
MBS	*m*-maleimidobenzoyl-*N*-hydroxysuccinimide ester
MD	Molecular Dynamics
MRI	Magnetic Resonance Imaging
MS	Mass Spectrometry
MSP	Membrane Scaffold Protein
NHS	*N*-Hydroxysuccinimide
PBS	Phosphate Buffered Saline
PDMS	Poly(dimethylsiloxane)
POPC	1-palmitoyl-2-oleoyl-*sn*-glycero-3-phosphocholine
POPS	1-palmitoyl-2-oleoyl-*sn*-glycero-3-phospho-L-serine
rHDL	Reconstituted HDL
SAXS	Small Angle X-Ray Scatterring
SEC	Size Exclusion Chromatography
SPR	Surface Plasmon Resonance
ssDNA	Single Stranded DNA
SWS	Subwavelength-Structured Surface
TBS	Tris-buffered Saline
TCEP	Tris (2-carboxyethyl)phosphine hydrochloride
TE	Transverse Electric
TEV	Tobacco Etch Virus
TF	Tissue Factor
TIR	Total Internal Reflection
TM	Transverse Magnetic
TMR	Tetramethylrhodamine-5- (and -6) C2 maleimide

CHAPTER 1

INTRODUCTION

1.1 Membrane Proteins

Membrane proteins are a common class of proteins present in all organisms, along with soluble proteins, fibrous proteins, and disordered proteins.[1] It is estimated that 20-30% of the genes in most genomes encode membrane proteins[2] yet membrane proteins make up over 50% of the targets for currently available drugs.[3] Membrane proteins are responsible for a variety of biological functions including transport, signaling, catalysis, and energy conversion.[4] The membrane protein class is further divided into three different sub-classes, based on the topology in the membrane: integral membrane proteins, peripheral membrane proteins, and pore-forming toxins.[5] These proteins interact with the membrane in different ways, ranging from being fully embedded in the membrane for integral membrane proteins to temporarily interacting with the membrane in a non-covalent manner and then dissociating for peripheral membrane proteins. The membrane with which these proteins interact is an active and dynamic structure which regulates the function and the biochemistry of membrane proteins.

Despite the fact that membrane proteins are biologically significant, studies with traditional biochemical and analytical methods has proven challenging at best for several reasons. Primarily, membrane proteins are often poorly soluble in the aqueous buffers which are common in such methods. This is due to the fact that the proteins usually contain a hydrophobic residue region in order to associate with the hydrophobic cellular membrane. This can manifest as a full transmembrane region, such as a helix bundle or a beta barrel, or a region on the surface of the tertiary and quaternary protein structure which interacts with the membrane through a combination of hydrophobic and

electrostatic interactions. Membrane proteins tend to aggregate and lose activity in the absence of a membrane, rendering typical analytical methods useless without a strategy in which to solubilize the analyte.

Second, membrane proteins are usually expressed at low levels throughout the natural proteome of organisms and their recombinant overexpression in host cells is often difficult.[6] When the proteins are overexpressed in host cells, they are usually toxic to the host, express at lower levels than their soluble counterparts, and are often times misfolded and therefore inactive.[7, 8] This means that there is a limitation on active materials available for analysis and the small quantities available tend to be unstable for longer periods of time.[9] This inherently prioritizes analytical methods which have minimal sample volume requirements as the methods of choice in the study of membrane proteins. Additionally, method optimization is a required step which usually takes the form of serial trials and adjustments, increasing the requirement for materials. These considerations often preclude the study of membrane proteins that express at levels too low to be useful in analytical studies.

Finally, the interactions between the protein and the membrane are not negligible. Protein activity can be modulated by a number of factors, including membrane charge, membrane lipid composition, and even membrane thickness.[5, 10, 11, 12] Anionic lipids have been shown to aid in the insertion of Cytochrome P450's (CYPs) into the membrane and to facilitate the electron transfer between enzymes.[13] Additionally, the membrane-embedded domain of the protein can vary in length and structure, further complicating the picture. As discussed, the membrane bound region can take the form of a single helix, multiple helices, or even a barrel shape.[5, 14] This will can influence the depth of insertion of the protein as well as the topology inside the lipid bilayer. Another component of consideration when studying membrane proteins is that they are known for being intrinsically unstable and quickly degrading.[9] This characteristic necessitates the use of analytical techniques that are quick. While these issues have surely slowed down the study of these targets, efforts have gone into developing membrane mimetic systems and coupling them to established analytical methods in order to solubilize the target proteins and enable the elucidation of their underlying mechanisms.

1.2 Strategies Addressing Membrane Protein Solubilization

1.2.1 Detergent Micelles

One of the most common methods of solubilizing membrane proteins for analytical study is by using amphipathic detergents. By utilizing detergents, the protein is extracted from the natural membrane and encased in a micelle which provides a hydrophobic region for the protein to reside in and is still soluble in aqueous environments. There are multiple types of detergents which can be used for different biological systems, with optimized paramaters available for most. The detergents are categorized in several classes: nonionic, anionic, cationic, and zwitterionic, based on how they behave in solution. While these molecules are enabling in membrane protein studies and are very effective at solubilizing membrane proteins, caution must be exercised in order to prevent the detergents from denaturing the protein of interest. If the protein is denatured, as is the case with some detergents, the activity is lost and any experimemts are rendered moot. Additionally, there is not a single, all-encompassing detergent that can be used to effectively solubilize all systems.[15, 16, 17] This means that more material is used up in optimizing the detergent conditions of the system, as the process can take time and materials spent in serial iterations of trial and error.[6] Finally, detergents are intrinsically not representative of the natural lipid bilayer environment that membrane proteins require. The composition of the membrane can influence the activity of the protein therefore the ideal situation is that the protein remain in a lipid environment during the analytical studies.

1.2.2 Liposomes and Lipid Vesicles

An alternative to strategy for the solubilization of membrane proteins is the use of liposomes. Liposomes are bilayer lipid vesicles composed of one or more species of lipids. The membrane proteins are incorporated into liposomes by first solubilizing the proteins using a detergent and then removing the detergent either by dialysis or by hydrophobic detergent removal beads.[18, 19] This method causes the lipids to assemble into vesicles, incorporating the target membrane proteins in the process, due to hydrophobic

interactions. However, while liposomes do present a more native environment than detergent micelles for the membrane proteins, they also present several drawbacks. One of the primary concerns is that liposomes are polydisperse in size. Their sizes can vary widely and this doesn't allow for very precise control of stoichiometry. The lack of control means that multiple protein molecules are often incorporated into one vesicle and it is difficult to study monomeric forms of multimeric species. Furthermore, liposomes have a limited control of lipid composition, with data suggesting that lipid rafts often form within the membrane of the liposomes.[20] Additionally, liposomes do not allow access to both sides of transmembrane proteins. This property has been taken advantage of in some experiments involving transporter proteins.[21] However, extra work is required when studying signaling cascades which involve activating or monitoring both sides of transmembrane proteins. While liposomes have been commonly used in the study of membrane proteins, the issues outlined above render them unsuitable for some analytical techniques.

1.2.3 Lipoprotein Particles

Naturally occurring lipoprotein particles, such as high-density lipoprotein (HDL) particles, form discoidal structures that consist of a lipid bilayer, encircled by an alpha-helical amphipathic protein. Specially, in HDL particles, the encircling protein is Apolipoprotein A-I (ApoAI).[22, 23] A self assembly process can be initiated by introducing detergent solubilized lipids and ApoAI in a solution and proceeding to remove the detergent, forming reconstituted HDL (rHDL) particles.[24] If a membrane protein is introduced into the reconstitution mixture, the protein may preferentially assemble into the lipid bilayer and be in a soluble, native-like environment, facilitating the application of analytical techniques.[25] Additionally, other lipoproteins yield similar particles that can be used in the analysis of membrane proteins.[26] Nanodiscs, particles of the lipoprotein class derived from a genetically engineered ApoAI, have recently been growing in popularity among researchers for the many advantages over other solubilization systems.[27, 28, 29]

1.3 Nanodiscs

1.3.1 Nanodisc Development and Characterization

Nanodiscs are lipoprotein particles a discoidal lipid bilayer encircled by two amphipathic helical proteins, termed the Membrane Scaffold Protein (MSP). MSP is derived from the human ApoAI sequence, developed by the Sligar group in 2002.[30] The ApoAI sequence was truncated in order to remove the globular N-terminal domain and further optimized for expression in *Escherichia coli (E. coli)*. As described in Section 1.2.3, Nanodiscs follow a similar protocol of self assembly to rHDL particles by initially solubilizing components in detergent and then removing the detergent from the mixture. The lipid molecules self-arrange into a bilayer and the boundaries of the bilayer are stabilized by the MSP as it shields hydrophobic regions from the aqueous solvent environment. The Nanodiscs retain a hydrophilic surface due to the lipid head groups and residues on the MSP and remain soluble in aqueous buffers while offering an environment for the incorporation of hydrophobic molecules, such as membrane proteins.

The first MSP variant, termed MSP1, had 43 N-terminal residues removed from the original ApoAI sequence, contained a hexa-histidne tag used for purification, and a Factor X cleavage site on the N-terminal. A genetic fusion of two MSP1 molecules yielded the construct MSP2, which could avoid the need for biomolecular assembly.[30] Additional engineering of the protein found that the first 11 residues of MSP1 do not interact with the lipid bilayer and could be truncated. The truncation of these 11 residues and the addition of a tobacco etch virus (TEV) protease site between the hexa-histidine tag and the rest of the sequence yielded the MSP1D1 construct, currently the most common and widely used construct.[31] MSP has further been engineered by adding one or more 22-residue amphipathic helices.[28, 31] The additions of these helices have allowed for the creation of larger Nanodiscs, accommodating larger membrane proteins, oligomers, or multi-protein assemblies.

Nanodiscs have been characterized by a variety of methods, including atomic force microscopy (AFM), size exclusion chromatography (SEC), small angle X-Ray scattering

(SAXS) and native mass spectrometry (MS). Nanodiscs made with the MSP1D1 variant have been shown to be discoidal with a diameter of 10 nm and a thickness of 5-6 nm.[27, 31, 32, 33] The size of Nanodiscs has beeen further confirmed using SAXS, showing a discoidal shape with a diameter of 10 nm.[31, 34] Scintillation counting methods utilizing radiolabled lipids have been used to determine the average number lipids per Nanodic.[30] Furthermore, native MS has shown that Nanodiscs are very monodisperse, with the number of lipid molecules in each disc varying by 2-3 molecules per lealflet.[33] All of these methods have proven to be consistent and show a specific ratio of lipids to MSP for each species of lipids and MSP and a highly monodisperse construct with a defnied size.

Additionally, a number of membrane proteins have been shown to incorporate into Nanodiscs. Similar to the process of incorporating membrane proteins into rHDL particles, the proteins are solubilized using detergent and included in a reconstitution mixture consisting of lipids, MSP, and target protein. The removal of detergent by dialysis or hydrophobic beads facilitates a self assembly process which incorporates the membrane protein in a native-like lipid bilayer.[28, 35] The hydrophobic region of the membrane protein preferentially inserts into the lipid bilayer as the whole construct self-assembles. The incorporated proteins remain properly folded and exhibit native activity levels while incorporated into Nanodiscs.[31, 36] Nanodiscs have been used as the platform in multiple studies involving membrane proteins because they offer several a series advantages over other solubilization strategies, which will be outlined in the next section.

1.3.2 Nanodisc Advantages and Analytical Applications

The primary advantage of Nanodiscs is that they provide a native-like lipid bilayer environment for membrane proteins. This means that the membrane proteins experience an environment which is congruent to their physiological environment - a lipid bilayer, without the presence of detergents, and solubilized in an aqueous biological buffer. The lipid bilayer has been shown to to provide the environment for a better stability than detergent micelles. Epidermal growth factor receptor (EGFR) has shown significantly better stability in Nanodiscs when compared to detergent micelles.[37] Additionally, the

lipid-bilayer of Nanodiscs preserves the native conformation and ligand binding activity. The glycoprotein Ib-IX (GPIb-IX) complex, which is expressed on platelet plasma membranes and is involved in thrombosis and hemostasis was shown to adopt a native-like conformation and exhibit the ability to bind its natural ligands.[38] Furthermore, Nanodiscs offer a detergent-free environment for proteins that eliminates any of the detrimental effects of detergents. One example is that detergents can alter the binding of substrates to cytochrome P450 3A4 (CYP3A4). The incorporation of CYP3A4 into Nanodiscs allows for a characterization of activity, as well as a biophysical characterization, which is addressed in detail in Chapter 2.[39, 40, 41]

Nanodiscs additionally allow for a very precise control of stoichiometry of all components of the system - lipids, MSP, and target membrane protein. The surrounding lipid composition has been shown to affect the activity of embedded membrane proteins. One example of this is demonstrated through the lipid composition controlling the redox potential of membrane bound cytochrome P450 proteins.[10] Furthermore, it is known that lipid composition of the membrane can affect biophysical parameters such as binding to the membrane, as shown by blood coagulation factors binding tighter to charged lipids in comparison to uncharged lipids.[29, 42, 43] In order to be able to study these processes, the lipid composition of Nanodiscs can be exactly defined in the reconstitution mixture. The lipid content of the Nanodiscs can be modified and tailored to include conjugated lipids or even lipophilic molecules for analytical and therapeutic purposes as will be further detailed in Chapter 6.[44, 45] The stoichiometric control further extends to controlling the oligomeric state of embedded proteins. Nanodiscs were used to directly prove the physico-chemical and functional properties of monomers of bacteriorhodopsin, a protein which is found to prefer a multimeric structure *in vivo*.[36, 46] This study proves the ability of Nanodiscs to allow for control over the oligomeric states of target proteins.

The enabling properties of Nanodiscs require the coupling to analytical instruments in order to elucidate membrane protein mechanisms. Nanodiscs have been shown interface with a multitude of analytical techniques due to the fact that the MSP can be modified by attaching or engineering a variety of tags. These tags include epitope tags, fluorescent tags, and even using chemical crosslinkers to attach single stranded DNA (ssDNA), as will be

addressed in detail in Chapter 4. The advantage of modifying the MSP on the Nanodisc is that there is no need for modifying the membrane protein of interest, thereby eliminating the chance for altering the activity or structure of the target protein. The tags can be either genetically engineered so that they are expressed within the protein sequence, as has been shown for polyhistidine, FLAG, and other affinity tags[28], or they can be added chemically after expression. The chemical modification is achieved through two possible pathways - lysine residues on the MSP can be used as reactive amine residues, or a set of mutants of MSP1D1 which contain single point cysteine residue mutations can be used as reactive thiol residues. Labels using either N-Hydroxysuccinimide (NHS) ester or maleimide chemistry can be used to modify the MSP with fluorophores, targeting groups, or for surface immobilization.

1.4 Applications of Nanodiscs to Biochemical Problems

1.4.1 Microscopic and Spectroscopic Characterization of Membrane Proteins

Nanodiscs have been gaining ground as a platform used in structural biology techniques. Even though efforts in crystallizing the entire Nanodisc-protein complex for X-Ray crystallography have so far proven to be unsuccessful, Nanodiscs have been used in other imaging methods, such as AFM[27, 30, 36] and electron microscopy (EM)[35, 47, 48, 49] to obtain low resolution structures of membrane proteins as well as topological information about the membrane. In order to gain more structural information, Nanodiscs have been applied to a number of NMR studies[50, 51, 52, 53] as well as a variety of mass spectrometry (MS) studies.[33, 54, 55, 56] Additionally, Nanodiscs have been used with with spectroscopic studies because of their low scattering. Studies utilizing absorbance[36, 39, 57, 58], fluorescence[59, 60, 61], and Raman[62, 63] spectroscopy for membrane protein structure and function have utilized Nanodiscs as the platform. Nanodiscs were used in conjunction with resonance Raman spectroscopy to gain insights into the catalytic cycle of the membrane bound cytochrome P450 17A1 (CYP17) and

cytochrome P450 19A1 (CYP19) proteins.[62, 63] Of interest, recent efforts have gone into further engineering the MSP to exclude the aromatic tryptophan and tyrosine residues in order to minimize the optical fluorescence background present in Nanodiscs for the use of label-free fluorescence studies.

1.4.2 Biosensors Surface Plasmon Resonance and Silicon Photonic Resonators

Nanodiscs are a powerful technology for creating a well-defined cell membrane mimetic, but they are only part of the solution of investigating bilayer surface interactions. Biosensors have been have recently been at the forefront of the study and characterization of biomolecular interactions. These sensors are designed to have high sensitivity and to utilize label free techniques in order to eliminate any chance of altering the activity or structure of the biological analyte. Surface plasmon resonance (SPR) has been one of the widely used techniques to study the biomolecular interactions of membrane proteins with lipids, small molecules, or even soluble proteins.[64, 65] With SPR, an analyte is immobilized on the surface of a gold-coated sensor and a ligand is flowed over the surface of the chip, monitoring the change in refractive index on the surface as the ligand interacts with the immobilized surface. Nanodiscs have simplified the immobilization procedure by providing a polyhistidine tag on the N-terminal which can be immobilized to a Ni-chelating surface on the SPR chip. For example, polyhistidine tagged Nanodiscs containing different concentrations of phosphatidylserine (PS) were attached to a Ni-NTA modified surface chip to measure the binding affinity of Factor X to PS.[29] In a separate example, Nanodiscs were immoblized to chip using an anti-tetra-His antibody on the flow cell. Nanodiscs which contained G_{M1} were immoblized while a solution of CTB was flowed over the chip and the binding was monitored.[66] What this means is that the protein of interest can remain unlabeled, while the label used for attachment is placed on the Nanodisc, keeping the analyte completely unmodified.

Similar to SPR, silicon photonic resonators devices are an evanescent wave sensor that monitors the change in refractive index of the surface attached analyte. It is known that

phospholipid systems adsorb to silicon surfaces when there are divalent cations present in the solution.[30, 67] Nanodiscs are similar in that respect to other phospholipid containing systems, having the ability to directly physisorb to silicon oxide surfaces, such as those in microring resonator biosensors. In a previously published study, Nanodiscs were adsorbed to silicon photonic microring resonators employing this strategy.[68] There were four species of Nanodiscs Nanodiscs containing 1-palmitoyl-2-oleoyl-*sn*-glycero-3-phospho-L-serine (POPS) lipids, Nanodiscs containing biotinylated lipids, Nanodiscs containing ganglioside glycolipid GM1 (G_{M1}), and Nanodiscs containing CYP3A4. The specific substrate of each species was flowed over a single chip which had all 4 species immobilized on the surface and a specific response was observed for each analyte. This study demonstrated that Nanodiscs could be interfaced with these resonator biosensors in a simple physisorption fashion but at the same time exhibit specificity as well as multiplicity on the same sensor chip.

1.4.3 Therapeutic Delivery Agents

Nanodiscs are analogous to re-engineered rHDL particles in that they are biocompatible and antigenically neutral. Therefore, Nanodiscs can be considered as a viable option for therapeutic agent delivery *in vivo*. Liposomes have long been considered to be a leader in drug delivery agents for lipohilic molecules.[69, 70, 71] However, there are a lot of issues that arise from using liposomes, including those of heterogeneity, shelf-life, and stability *in vivo*. Liposomes can aggregate and fuse together, decreasing the efficacy of the delivery. Nanodiscs, on the other hand, have the advantages of having precise control of lipid composition, having homogeneous size, and stability during lyophilization and reconstitution.[45] Furthermore, Nanodiscs are much smaller than liposomes, having the ability to transport faster and more efficiently. A previously published study showed the utility of Nanodiscs used as carriers for therapeutic compounds. Nanodiscs containing 1-palmitoyl-2-oleoyl-*sn*-glycero-3-phospho-(1'-*rac*-glycerol) (POPG) lipids were used as therapeutic delivery agents against respiratory syncytial virus (RSV) in both *in vitro* and *in vivo* models. The lipids act as a surfactant and inhibit the binding of the virus to epithelial cells. The virus was found to be attenuated by the delivered lipids in both models

and the potency and effectiveness was evaluated. Nanodiscs were found to be effective in inhibiting RSV and thus a viable delivery option. This is the first work to show Nanodiscs being used as a delivery agent for therapeutic compounds and suggested that Nanodiscs can be further developed for the delivery of other lipophilic, therapeutic molecules.

1.4.4 Microfluidic Devices

Microfluidic devices are an attractive option when it comes to developing high throughput assays which involve the precise patterning of molecules of interest on a surface. The microfluidic technique has been applied to immunoassays[72] as well as protein analysis.[73] The advantages of using microfluidic platforms was also extended to Nanodiscs.[67] Using microfluidic channels patterned on a poly(dimethylsulfoxane) (PDMS) chip, Nanodiscs of different lipid compositions were patterned on a glass surface with precise spatial control. This work used two different systems, first a population of Nanodiscs with biotinylated lipids and streptaviidn, and the second system using PS lipids and annexin. The second population of Nanodiscs created a high density assay of Nanodiscs for the measurement of binding kinetics of annexin to various PS compositions. The patterning of Nanodiscs was evaluated using AFM to verify the generation of a tightly packed monolayer. The results showed that Nanodiscs could be coupled with microfluidic devices in order to create high throughput, multiplexed sensor devices. Taking a step forward from using microfluidic devices for patterning, Zahi Fayad and coworkers showed a system able to reconstitute rHDL particles in a microfluidic device.[74] The system employed in that study showed the assembly of lipoprotein particles, with hydrophobic molecules or quantum dots embedded within the lipid bilayer. This shows that methods which facilitate the assembly and use of well controlled lipid bilayer particles are being developed as an alternative to current standards, such as liposomes. Nanodiscs are well suited for being assembled on a microfluidic device due to the simplicity of the self assembly process. The required components - lipids, MSP, and a target membrane protein - are first solubilized in detergent and mixed together. The detergent is then removed to facilitate the self assembly process. Implementing the process on a microfluidic scale can exhibit multiple advantages

over traditional methods, such as a decrease in time of assembly and a decrease in sample volume requirements.

1.4.5 Dissertation Outline

The main focus of this dissertation is the application of the Nanodisc platform to a variety of analytical methods and techniques in order to gain a deeper understanding of biophysical processes as well as to develop methods for clinical applications. These topics include the study of the topology of membrane proteins inside the lipid bilayer, developing a high throughput biosensor array for diagnostics, developing magnetic resonance imaging (MRI) contrast agents, and exploring the assembly of Nanodiscs on a microfluidic platform. The work represents advancements in the understanding of crucial mechanisms behind protein-protein and protein-lipid interactions. It goes on to suggest future studies to build upon the platforms developed here.

Chapter 2 details the study of the orientation of CYPs incorporated into Nanodiscs. Three biologically significant enzymes are explored in this chapter. These enzymes are responsible for the metabolism of over half of the therapeutic compounds currently available as well as having a major role in the steroidogenesis pathways.[58, 75] However, there have been no crystal structures of these proteins within the lipid bilayer and the mechanism of substrate entry into the active site is not well understood. The chapter describes the building of an instrument which uses total internal reflection (TIR) in combination with linear dichroism (LD) in order to probe the orientation of the absorbing heme cofactor which is located in the active site of CYPs. This experimental study was coupled with a modeling study that gave insights into the topology of the enzymes and their substrate access channels.

Chapter 3 describes the development of a high pressure biosensor platform for the study of biomolecular recognition events. The system is based on a label free retroreflective biomolecular sensor, the BIND assay, which was developed by Brian Cunningham and coworkers.[76, 77] The assay is deployed in a high pressure bomb and a series of experiments show its utility in probing biological systems using hydrostatic pressure. The

system was validated using a series of salt solutions at different concentrations and pressures. The compressibility of each solution was calculated and compared to published values. The system can be used to monitor molecular interactions, as the peak wavelength shifts with a change in refractive index. Furthermore the biosensor is well suited to be implemented under high pressure because it does not require any specialized optics, which could shift under pressure.

Chapter 4 discusses the development of a multiplexed high throughput biosensor utilizing Nanodiscs and photonic waveguide microring resonator biosensors. Nanodiscs were immobilized using complementary single stranded DNA (ssDNA) labels. This chapter details the development of a method to label Nanodiscs with ssDNA and take advantage of complementary base pair recognition in order to immobilize Nanodiscs of different lipid composition on a single microring resonator chip. A single sensor with multiple populations of Nanodiscs can be used in a high throughput kinetic study of membrane protein interactions with minimal sample requirements. The studies in this chapter extend the previously published work which established the combination of the two novel technologies in order to create a highly multiplexed system for elucidating protein:lipid and protein:protein interactions in a high-throughput fashion.

Chapter 5 explains in detail the design and development of a microfluidic device used for assembling Nanodiscs in a quick and facile manner. This chapter addresses the specific issue of having small amounts of material when it comes to using and analysing membrane proteins. Using microfluidic devices, membrane protein incorporation into Nanodiscs can be accomplished quickly and use less materials than traditional methods. This is demonstrated by incorporating CYP3A4 into Nanodiscs. A gradient method of optimization is demonstrated, using less materials than traditional optimization studies. Additionally, this method enables the parallel screening of multiple detergents when optimizing the incorporation of a membrane protein. This in turn enables the optimization of membrane protein incorporation with a reduced requirement for reagent materials, a process that is often costly in both time and materials.

Chapter 6 addresses the development of a Nanodisc-based system for the incorporation and delivery of Gd(III) chelate MRI contrast agents. Lipophilic Gd(III) chelate molecules

were previously synthesized and used as MRI contrast agents *in vitro*. In this work, two lipophilic contrast molecules were incorporated into fluorophore labeled-Nanodiscs. The Nanodisc assembly was used as an imaging platform for labeling and tracking cells both optically and using MRI, exploiting the high modularity of the Nanodisc platform. The chapter details cell tracking studies, localization studies, as well as contrast enhancement studies. The system represents the first example in literature of using Nanodiscs for the delivery of imaging contrast agents.

Chapter 7 summarizes each of the individual chapters and suggests further experiments to be conducted in order to continue the work on biophysical characterization of membrane proteins, further applications of the biosensor systems, and continued work on the therapeutic delivery agents.

CHAPTER 2

ORIENTATION OF CYTOCHROME P450S WITHIN THE LIPID BILAYER

2.1 Introduction

Cytochrome P450s (CYPs) are a superfamily of heme-containing isoenzymes that are present in all organisms. CYPs are responsible the metabolism of external therapeutic compounds as well as the biosyntehsis of endogenous compounds via oxidation.[58] The enzymes are present in organisms in both soluble as well as membrane bound form and they are able to oxidize both hydrophilic as well as lipophilic molecules. A number of crystal structures have been solved for CYPs, both in their apo as well as substrate-bound form, but to date no crystal structure has been solved of a full length, membrane-bound form.[78] Human CYPs are comprised of a globular domain, which sits above the membrane, as well as an N-terminal alpha helix, which anchors the enzyme into the membrane. A large body of evidence suggests that the globular domain interacts with the lipid bilayer, which in turn raises the question of how substrates enter and exit the active site.[79] A school of thought suggests that the route of entry of lipophilic substrates into the active site is primarily through the membrane.[80, 81] However, the mechanism of substrate entry is not entirely understood and the topology of CYPs within the lipid bilayer requires further characterization.

The most abundant isoform in humans, cytochrome P450 3A4 (CYP3A4), is responsible for the metabolism of over 50% of the currently available clinical drugs.[82] Other isoforms, such as cytochrome P450 17A1 (CYP17) and aromatase cytochrome P450 (CYP19) are

Reproduced in part with permission from Baylon, J.L.; Lenov, I.L.; Sligar, S.G.; and Tajkhorshid, E. Characterizing the Membrane-Bound State of Cytochrome P450 3A4: Structure, Depth of Insertion, and Orientation *J. Am. Chem. Soc.* **2013** *135* (23), 85428551 Copyright 2013 American Chemical Society. The published version may be found online at http://pubs.acs.org/doi/abs/10.1021/ja4003525.

responsible for the synthesis of endogenous hormones.[83, 84] These enzymes can be found in the liver and small intestine for CYP3A4 and in the gonads and adipose tissue for CYP17 and CYP19.[75] The enzymes are primarily localized in the endoplasmic reticulum within the cell. The solved crystal structures of all three proteins have suggested that they present overall tertiary folds which are similar to one another as well as other CYPs, consisting of an N-terminal -sheet domain and a helical C-terminal domain, containing the cofactor heme in the active site.[85, 86] However, the published crystal structures are all of truncated forms, which exclude the N-terminal transmembrane helix as well as the membrane itself. This leads to a lack of understanding of the topology of the enzymes in the membrane and an explicit need for experimental data exploring this area.

Experiments have examined the interaction of multiple substrates and their homotropic and heterotropic cooperativity has been explored for CYP3A4.[31, 41, 87] The studies found that CYP3A4 has a very flexible active site and can accommodate up to three substrate molecules[83], with the number of bound substrates modulating the activity of the enzyme. Furthermore, the identity of the substrates can induce cooperativity, showing a stimulatory effect on the activity of the enzyme for other substrates present. High pressure studies have been conducted on the enzyme showing the enzyme displays conformational heterogeneity.[88, 89] These studies showed that the activity of CYP3A4 can be modulated by the oligomeric state of the enzyme. The high-spin state of the enzyme was observed to exhibit unusual stability under hydrostatic pressure, reflecting decreased accessibility of water into the active site, and suggesting specific interactions with the lipid bilayer.

In addition to crystal structures and catalytic activity experiments,the structural dynamics have been explored by molecular dynamics (MD) simulations. There have been multiple MD simulations which have explored how CYPs interact with a multitude of substrates. For example, studies have focused on examining the hydration of the active site and how that affects substrate binding.[90] Even further, active site gating has been explored by MD simulations for CYP17 and CYP19.[91, 92] While these simulations provide very useful information, they usually don't account for the interactions with the lipid bilayer. More recently, simulations have explored membrane interactions of CYPs,

specifically exploring the topology of the enzymes within the membrane.[93, 94, 95] Simulations have shown insights into the orientation of the enzymes but the results have given rise to speculation as some show the protein adopting two orientations or even a burial of the globular domain within the hydrophobic part of the lipid bilayer.

While MD simulations provide valuable information, there is still a need for experimental studies exploring the topology of these biologically critical enzymes. In order to reveal the topology of the protein in the phospholipid bilayer and gain an insight into the mechanism of hydrophobic substrate entry, CYP3A4, CYP17, and CYP19 were expressed, purified, and self-assembled into Nanodiscs of POPC lipid composition. A series of linear dichroism measurements were carried out on a custom built instrument by first adsorbing the Nanodisc-incorporated proteins onto a glass substrate and measuring heme absorbance using two orthogonal polarizations of linearly polarized light. The angle of the heme plane determines the relative orientation of the P450s with respect to the the laboratory z-axis, and therefore the lipid bilayer. The data from this work shows that CYPs adopt a specific structure and orientation within the lipid bilayer and do not adopt random orientations. The heme orientations calculated with this method, along with the MD simulations, show that the globular domain is responsible for interactions with the lipid bilayer and the protein-lipid interaction is not solely dependent on the transmembrane helix of the enzymes. These insights allow for a detailed description of the enzymes in their membrane-bound form and a better understanding of substrate entry into the active site.

2.2 Methods

2.2.1 Theory

As light is incident upon an interface between two transparent media, it is partially reflected as well as partially transmitted. However, light inside of an internal reflection element (IRE) is totally internally reflected, having no transmitted element. The angle of

reflection is known as the critical angle and is calculated by the following equation:

$$\theta_c = \sin^{-1} \frac{n_2}{n_1} \tag{2.1}$$

where n_2 and n_1 are the refractive indices of medium 2 and medium 1, respectively. This is a well-known phenomenon, which has been studied extensively.[96, 97] Using the ray-optics approximation, it is known that an electric field, known as the evanescent field, penetrates the surface of the rarer medium and decays exponentially with distance from the surface of the medium. The electric field interacts with material close to the surface and has amplitude of:

$$E = E_0 e^{-\gamma^2} \tag{2.2}$$

The amplitude can be separated into components corresponding to the magnitudes of the electric fields that extend along the laboratory axes, as given by the equations formulated by Harrick[98]:

$$E_x = \frac{2\left(\sin^2\theta_i - \left[\frac{n_2}{n_1}\right]^2\right)^{\frac{1}{2}} \cos\theta_i}{\left(1 - \left[\frac{n_2}{n_1}\right]^2\right)^{\frac{1}{2}} \left[\left(1 + \left[\frac{n_2}{n1}\right]^2\right)\sin^2\theta_i - \left(\frac{n_2}{n_1}\right)^2\right]^{\frac{1}{2}}} \tag{2.3}$$

$$E_y = \frac{2\cos\theta_i}{\left(1 - \left[\frac{n_2}{n_1}\right]^2\right)^{\frac{1}{2}}} \tag{2.4}$$

$$E_z = \frac{2\sin\theta_i\cos\theta_i}{\left(1 - \left[\frac{n_2}{n_1}\right]^2\right)^{\frac{1}{2}} \left[\left(1 + \left[\frac{n_2}{n1}\right]^2\right)\sin^2\theta_i - \left(\frac{n_2}{n_1}\right)^2\right]^{\frac{1}{2}}} \tag{2.5}$$

where θ_i is the incident angle and n_2 and n_1 are the refractive indices of medium 2 and medium 1, respectively. Knowing the electric field amplitudes along the laboratory axes, it is possible to calculate the absorbance of a chromophore which is adsorbed to the surface of the IRE. Cropek, et al. showed that the absorbance of the chromophore on the surface

can be calculated by the following equation: [99]

$$A = c_1 \left| \left\langle m \left| \vec{\mu} \cdot \vec{E} \right| k \right\rangle \right|^2 \tag{2.6}$$

where c_1 is a constant, m and k are the states of the transition, $\vec{\mu}$ is the absorption transition moment, and $\vec{E}$ is the electric field vector. This equation can be further broken down in terms of the laboratory axes:

$$A = kl \left(\mu_x E_x + \mu_y E_y + \mu_z E_z\right)^2 \tag{2.7}$$

where k is a constant and l is an effective path length. Two approximations are made to simplify the mathematical treatment. First, a heme ring can be approximated as a circular oscillator which means that it has two orthogonal dipole transitions. The dipole transitions are x,y polarized, and it follows that the two transition moments of the heme are degenerate.[100, 101] Second, the molecules on the surface are not artificially ordered along either the x or y axes and the samples are uniaxially symmetric. Applying this assumption to the mathematical treatment, the absorbance can be simplified and broken down into the three distinct components along the laboratory axes with the following three equations:

$$A_{TE} = \frac{1}{2} kl \left|E_y\right|^2 \left|\mu\right|^2 \sin^2\theta \tag{2.8}$$

$$A_{TM,x} = \frac{1}{2} kl \left|E_x\right|^2 \left|\mu\right|^2 \sin^2\theta \tag{2.9}$$

$$A_{TM,z} = \frac{1}{2} kl \left|E_z\right|^2 \left|\mu\right|^2 \cos^2\theta \tag{2.10}$$

where θ, the orientation angle, is the angle between the transition moment and the laboratory z-axis. The subscripts TE and TM refer to transverse electric polarized and transverse magnetic polarized light, respectively. TE polarized light is oriented only in the y direction and only absorbers with a transition moment component in the y direction will absorb TE polarized light. TM polarized light is oriented in the x and z directions, thus

only absorbers with transition moment components lying in the x or z direction will be able to absorb TM polarized light. The ratio of the absorbance of TE to TM polarized light, the dichroic ratio, can be used to determine the orientation of the absorber. The following equation relates the dichroic ratio to the orientation angle of the absorber:

$$\rho = \frac{A_{TE}}{A_{TM}} = \frac{|E_y|^2}{|E_x|^2 + 2\,|E_z|^2 \cot^2\theta} \tag{2.11}$$

where ρ is the dichroic ratio and is the angle between the transition moment vector and the laboratory z-axis. Since all of the proteins in this study, CYP3A4, CYP17, and CYP19 are heme-containing enzymes, it is possible to take advantage of the heme as the absorber and monitor the anisotropic absorbance of the Soret band in order to determine the orientation of the heme with respect to the z-axis and hence, the protein in the lipid bilayer.

2.2.2 Materials and Apparatus

The lipids 1-palmitoyl-2-oleoyl-*sn*-glycero-3-phosphocholine (POPC) were purchased from Avanti Polar Lipids (Alabaster, AL, USA). The scaffold protein, MSP1D1 was expressed and purified as described previously.[30, 31] CYP3A4 was expressed with a histidine affinity tag from the NF-14 construct in the pCWOri+ vector, purified, and incorporated into POPC Nanodisc lipid bilayers as previously described.[41, 83, 102, 103] Nanodiscs containing purified CYP17 and CYP19 were generously provided by Ruchia Duggal, Michael Gregory, and Dr. Abhinav Luthra. The Nanodiscs were stored in buffer before use (50 mM Tris/HCl pH 7.4, 0.3 M NaCl). Sodium cholate, Amberlite XAD-2 hydrophobic beads, and all other chemicals were purchased from Sigma Aldrich (St. Louis, MO, USA). Buffers were prepared with 18 MΩ deionized water and filtered prior to use.

The diagram of the instrument is shown in Figure 2.1 while a picture of the actual instrument is shown in Figure 2.2. A commercially available 405 nm laser diode was used in the laser module. The laser spot was reduced using a pinhole and any stray polarization was excluded by using a Glan-Taylor polarizer. The whole laser assembly, which includes the laser, pinhole, and the polarizer, was mounted on a rotational stage to precisely select

between TE and TM polarized light. The light was incident onto the slide assembly, which is composed of the IRE, posts at the four corners, and a microscope slide underneath. The solution was sandwiched between the IRE and a regular glass slide, separated by the four corner posts. Two BK7 prisms (Edmund Optics, Barrington, NJ) were used to to couple the light in and out of the IRE. The entire slide assembly was placed on a custom-machined, temperature-controlled, aluminum slide holder. The IRE substrates used were SuperClean 2 Microarray Substrates (Arrayit Corporation, Sunnyvale, CA) with dimensions of 25 x 76 x 0.940 mm. The out-coupled light passed through a 405 nm band pass filter and onto a light diffuser before being detected by a phototube (Newport Corp., Irvine, CA). The output of the phototube was amplified by a low noise current amplifier (Stanford Research Systems, Sunnyvale, CA) and subsequently measured by a digital multimeter (Hewlett Packard, Palo Alto, CA). The signal was averaged and recorded using a program developed in the LabVIEW programming environment (National Instruments, Austin, TX).

2.2.3 Experimental Procedure

In order to facilitate adsorption onto the substrate, $MgCl_2$ was added to the buffer before adding Nanodiscs to the substrate. The temperature of the slide holder was set to 20 °C. A background signal was measured on the slide assembly using tris buffered saline (TBS) buffer containing $MgCl_2$. Subsequently, Nanodiscs with CYP protein incorporated were added to the buffer on the substrate so that total concentration of CYP was 100 nM and the total concentration of $MgCl_2$ was 10 mM. The addition of Nanodiscs to the solution forms a monolayer at the silicon surface between the substrate and the bulk solution, with free Nanodiscs in the bulk solution. After incubating for 30 minutes, which is required for adsorption to the glass, the substrate was flushed with 2 volumes of buffer to wash away the free Nanodiscs. The final signal was measured and compared to the background signal to calculate the monolayer absorbance. The same procedure is repeated for both polarizations of light.

2.3 Results and Discussion

Each CYP isoform had multiple measurements conducted on multiple glass substrates. A total of 11 unique measurements were conducted for CYP3A4, which spanned three different preparations of protein assembled into Nanodiscs. A total of 15 separate measurements were conducted per enzyme for CYP17 and CYP19. Each sample was measured on a separate and different glas substrate and the signal averaged until an equilibrium was reached. The average orientation angle of the heme moiety in the 11 samples of CYP3A4 associated to Nanodiscs was 60 ± 4° with respect to the Z-axis. (Table 2.1) The average orientation angle of the heme in the 15 samples of CYP17 associated to Nanodiscs was 64 ± 4° with respect to the Z-axis. (Table 2.2) The average orientation angle of the heme in the 15 samples of CYP19 associated to Nanodiscs was 55 ± 4° with respect to the Z-axis. (Table 2.3)

These measurements are in close agreement with previously published work, both theoretical and experimental. Since CYP3A4 is responsible for the metabolism of over 50% of clinically available therapeutic compounds, it has been the subject of a multitude of studies. This experimental work was coupled with MD modeling work, employing a novel highly mobile membrane mimetic model (HMMM) which reported the orientation of the heme group to be 72°.[40] The simulation was then extended to fill in the lipophilic tails of the POPC lipid molecules so that the full length lipids are present in the bilayer. The protein was subsequently allowed to equilibrate with the presence of the full lipid tails. The results of the full length lipid simulation show that the heme of CYP3A4 lies at 57 ± 6° with respect to the Z-axis. These values are in very close agreement and show details of the protein associating with the membrane bilayer which are not able to be determined experimentally such as the position of the substrate access channels.

Additionally, other published studies report theoretical results for the orientation of CYP3A4 which fall between 52° and 72°.[93, 104, 105, 106] The orientation of CYP17 in liposomes was determined using the method of rotational diffusion with a flash photolysis depolarization apparatus, reporting either 47° or 63°.[107] The calculation of the results depends on a second-order polynomial, the solution of which yields the two possible values.

The orientation of CYP17 has also been explored theoretically, with one study finding that the protein equilibrates to two distinct orientations in the simulation, around 40° and around 60°.[94] A total of five simulations were conducted, each one starting at a unique heme angle and allowed to equilibrate. Two of the simulations converged to 40° and three of the simulations converged to 60° in 100 ns. Two simulations were extended to 150 ns, and no large scale fluctuations were observed. Additionally, Rommie Amaro and coworkers addressed the orientation of CYP19 using MD simulations, finding that the enzyme equilibrates at an orientation of 57° with respect to the Z-axis.[95] Two different structures, one with a protonated aspartate 309 and one with a deprotonated residue are examined and the heme angle determined for both. The structures were allowed to equilibrate for 250 ns and the values averaged.

2.4 Conclusions

Characterization of the membrane-bound form of CYP enzymes is crucial to the understanding of the topology of the proteins as well as the mechanism of substrate entry. Studies addressing these questions have employed simulations in the past, but few have addressed these questions experimentally. This chapter described the work that addresses the question through the use of Nanodiscs coupled with LD spectroscopy. The results show that the three different enzymes used in this work adopt slightly different orientations within the POPC lipid bilayer. However, each enzyme adopts a specific conformation within the membrane and the average is reported. This information is used a step in the direction of understanding the mechanism behind substrate access to the active site. The results show that there are slight differences in the orientation of all three enzymes. That would suggest that the interaction between the protein and the lipid bilayer are not merely through the transmembrane helix, but also through protein lipid interactions in the globular domain. Furthermore, the results would imply that the interactions are specific to each enzyme and help orient its position within the bilayer.

Theoretical treatment of CYP3A4 accompanying the experimental work comes in close agreement with the experimental values calculated using the LD method. (Figure 2.3) The

simulations further show that the globular domain of the proteins interacts with the lipid bilayer and suggest that the interaction is not merely nonspecific and based on proximity. Rather, the interaction is through a set of specific protein-lipid interactions which modulate the orientation the enzymes undertake when associated with the membrane. The simulations further show that the association of the enzyme has an effect on the substrate access channels, which cannot be seen in the crystal structures. Additionally, HMMM simulation studies are currently being conducted on CYP17 and CYP19.

We show that membrane binding of three different CYP enzymes has significant structural and dynamical impacts on its globular domain at the membrane interface. The presence of the membrane induces a each enzyme to adopt a specific orientation, suggesting that binding to the membrane might play a role in efficient recruitment of lipophilic ligands from the membrane to the active site. The fact that the orientations are slightly different for the three different enzymes prompts the question of how this orientation is controlled on a molecular level. The topology of the enzymes could be controlled primarily by the head group of the lipids. Since the globular domain interacts with the lipid bilayer it is plausible that the charge on the lipid head group, and the specific lipid:protein interactions, will affect how the protein orients itself. Furthermore, the length of the tail of the lipids could be another key factor in this regard. Not only does the length affect how deep the protein is embedded in the bilayer, but the length also dictates the transition temperature of the bilayer. These questions prompt further exploration into the topic of CYP orientation within the membrane and how affects the mechanism of substrate recruitment.

2.5 Figures and Tables

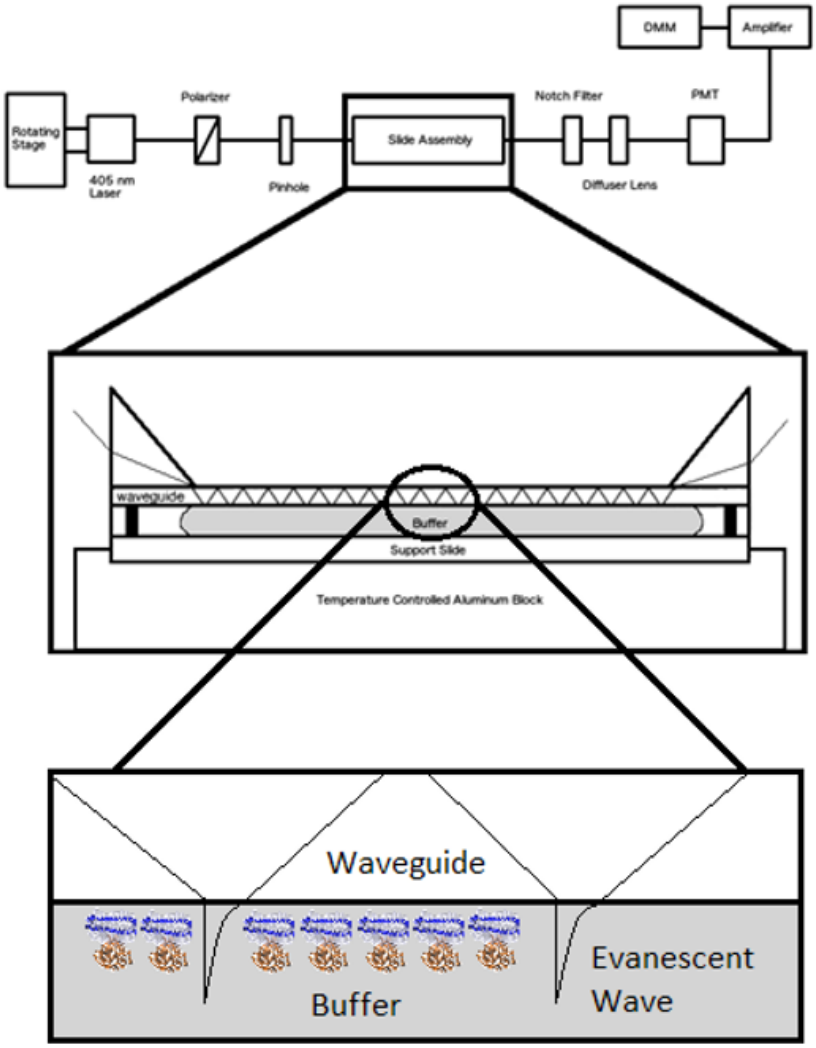

Figure 2.1: A diagram of the home-built instrument LD instrument used. The laser, polarizer, and pinhole are all mounted on the rotating stage. The notch filter, diffuser and PMT are all located within the PMT housing. The signal is routed through the amplifier into the DMM and then averaged and recorded by a LabVIEW program.

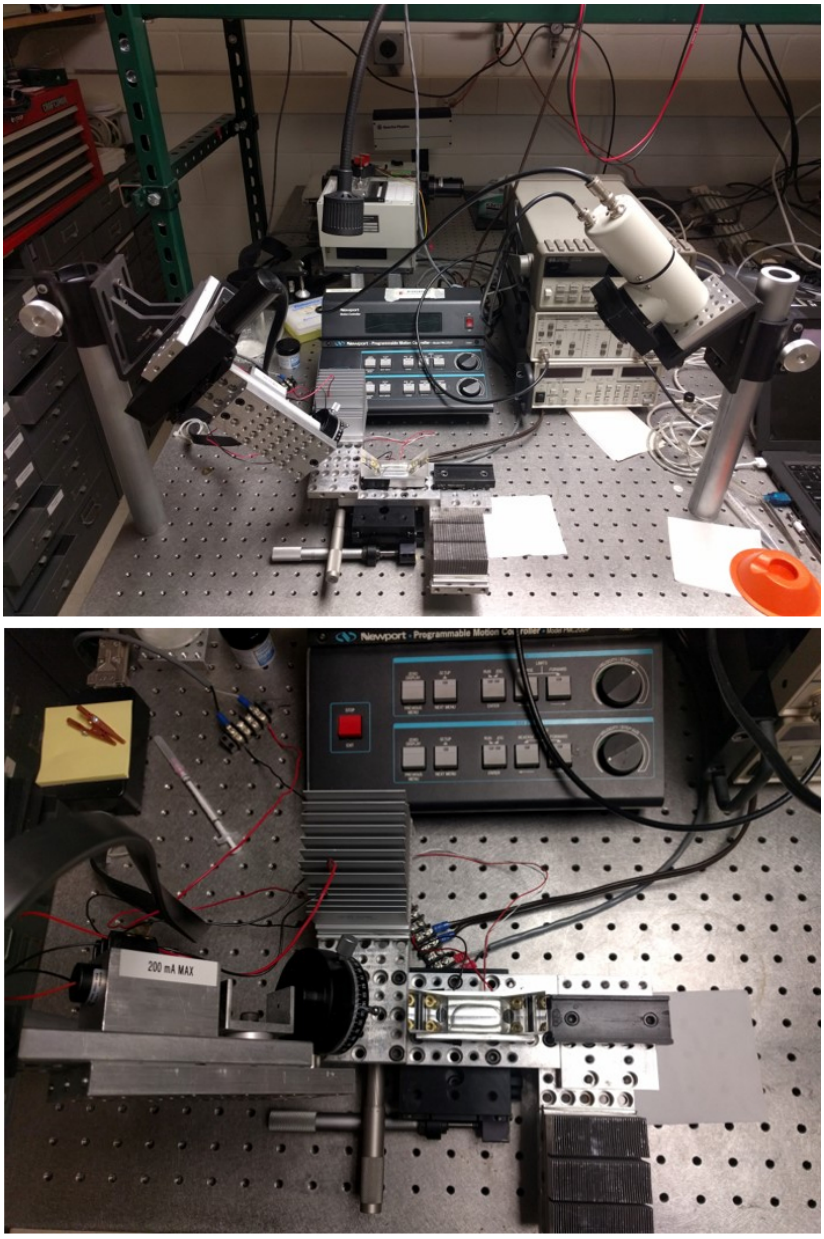

Figure 2.2: A side and top-down view of the actual instrument used in these experiments. The instrument was built based on the diagram above and it is all mounted on a laser table. The rotating stage is controlled by a separate module and the slide stage is controlled by hand using fine thread screws.

Table 2.1: Orientation of Heme in CYP3A4

Trial	**Angle**
1	61°
2	58°
3	58°
4	61°
5	59°
6	52°
7	60°
8	56°
9	63°
10	67°
11	63°
AVG	**60°**
Std.Dev.	**4°**

Table 2.2: Orientation of Heme in CYP17

Trial	**Angle**
1	60°
2	56°
3	62°
4	69°
5	65°
6	73°
7	60°
8	62°
9	63°
10	63°
11	59°
12	69°
13	64°
14	63°
15	65°
AVG	**64°**
Std.Dev.	**4°**

Table 2.3: Orientation of Heme in CYP19

Trial	**Angle**
1	48°
2	56°
3	57°
4	49°
5	52°
6	49°
7	59°
8	51°
9	63°
10	50°
11	59°
12	58°
13	57°
14	58°
15	56°
AVG	**55°**
Std.Dev.	**4°**

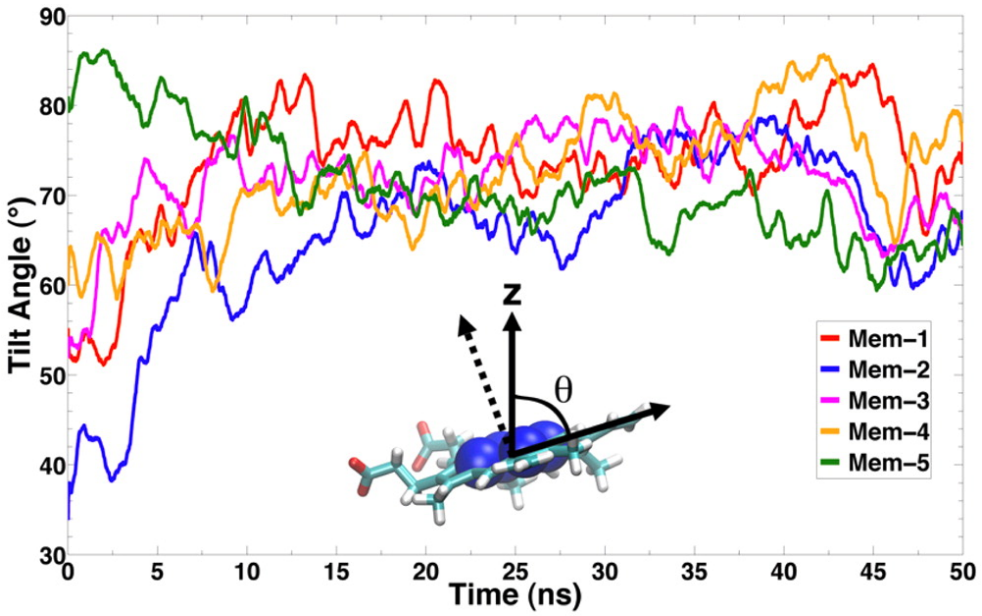

Figure 2.3: Trajectory traces of the heme orientation of five different simulations of CYP3A4 using the HMMMM model. This figure shows that the orientation of CYP3A4 started out at 5 different values and converged to one value. The heme plane was defined by fitting the position of the four porphyrin nitrogen atoms to a plane. The angle θ is defined as the angle between the membrane normal (z-axis) and the heme plane.

CHAPTER 3

DEVELOPMENT OF THE HIGH PRESSURE LABEL FREE BIND ASSAY

3.1 Introduction

Hydrostatic pressure modulation has been previously used in conjunction with surface plasmon resonance (SPR) and optical absorbance experiments to study the optical and physical properties of polymers and solutions of bio-molecules.[108, 109, 110] An advantage of SPR is the ability to observe biological interactions without the requirement of labels, such as chromophores, which can alter the folding and activity of bio-molecules. The technique is based on observing changes in refractive index and quantifying the change based on a shift the peak wavelength.[64, 111] However, using SPR in the Kretschmann[112] configuration requires the use of specialized optics, such as optical prisms and focusing lenses.[111] Optics such as these are prone to shifting, expanding, and contracting under hydrostatic pressure. Slight movements of the optics can cause a shift in the angle of incidence as well as change the critical angle. Furthermore, subjecting optics to external pressure can change the density of the optics, therefore changing the refractive index of the optics. For these reasons, SPR cannot be considered an ideal method for investigating pressure dependence and compressibility.

Ideally, an analytical method would not require complex coupling optics and would not depend on a very specific angle of excitation. A recent push for the development of bedside diagnostic tools has spurred the development of a multitude of optical biosensors.[113, 114] These sensors detect a change in the optical density of the medium in contact with the sensor, whether the change is caused by the binding of biological material or a change in the bulk analytite solution. Developed by Brian Cunningham and coworkers in 2002[76, 77] the Biomolecular INteraction Detection (BIND) Assay sensor utilizes a sub-wavelength

grating as a waveguide structure. The sensor is illuminated with white light at normal incidence using a fiber optic probe and a narrow band of resonant wavelengths is reflected back. The reflected band of resonant wavelengths can be modulated by a change in the dielectric constant of the material in contact with the grating - which is the result of an attachment of molecules directly onto the surface of the sensor.[76, 115, 116] Unlike optical detection approaches that rely upon interaction of detected molecules with an evanescent wave, the detection in this sensor actually occurs within the waveguide. This is due to the change of the optical path of the light that is coupled into the grating. A spectrophotometer collects the reflected light through a second fiber, which is at normal incidence to the sensor as well. As there is no physical contact between the readout system and the grating surface, no coupling prisms are required.

A system that utilizes BIND Assay grating sensors inside of a high-pressure optical cell used for measuring the pressure dependence of the refractive index of bulk solutions is described in this chapter. Using the BIND Assay gratings in a pressurized environment is possible since there is no need for coupling optics and the grating is both illuminated and read at normal incidence. In this chapter, the BIND sensors are first mounted inside a custom-made high pressure cuvette, which is filled with the analyte. The entire high pressure cuvette assembly is then put inside a high pressure bomb before being pressurized. The compressibility of several mixed, aqueous solutions is calculated using the BIND Assay in conjunction with high pressure. The theory of both the sub-wavelength grating and the use of hydrostatic pressure as a perturbant are first discussed, then the chapter describes how pressurizing different concentrations of sodium chloride (NaCl), sucrose, and ethanol affects the refractive index. These measurements allow for the calculation of compressibility at varying pressures up to 21,000 psi. The system is further designed to

3.2 Theory

3.2.1 Subwavelength-Structured Surface Relief Gratings

The sensor incorporates a subwavelength-structured surface (SWS) relief grating with the grating period being small compared to the wavelength of incident light. This ensures that no diffractive orders other than the reflected and transmitted zeroth orders are allowed to propagate. As the grating is illuminated, the incident light propagates into the waveguide as a leaky mode. The light propagates a very short distance - around 10 to 100 μm - and then undergoes scattering, coupling with the zeroth order light. This coupling condition results in a narrow band of reflected wavelengths, which can be modulated by a change in the dielectric constant of the materials that are in contact with the grating. Material that is in contact with the surface of the grating increases the optical path length of the coupled light and therefore changing the maximum wavelength of reflectance.

3.2.2 Hydrostatic Pressure

Using hydrostatic pressure as a perturbant has advantages over other methods, such as chemical or temperature.[117, 118] The use of hydrostatic pressure mostly affects the overall volume of the system without changing the internal energy of the analyte and the solvent system. Applying pressure changes the distances or volumes of the components of the system at high pressures (>100 kilobar)[118] while keeping the total energy almost constant.[119] Hydrostatic pressure causes a shift in equilibrium for the system with the smallest volume, according to Le Chatelier's principle.[120] At lower pressures (<2 kilobar), volume changes associated with solvation are observed. Ionic interactions are destabilized due to pressure packing water molecules around charges and results in a volume reduction on the order of 25 mL/mol.[121, 122] Hydrophobic interactions are also disrupted under high pressure due to a dense packing of water molecules, with a volume change on the order of 20 mL/mol.[122] In order to calculate the pressure dependence of refractive indices we need to combine standard equations of optics and thermodynamics into a theoretical model. The Lorentz-Lorentz equation relates density to refractive index:

$$R_{LL} = \frac{n^2 - 1}{n^2 + 2}\frac{1}{\rho} = \frac{4\pi}{3}\alpha' N_A \tag{3.1}$$

where R_{LL}represents the Lorentz-Lorentz constant, n represents the refractive index, ρ represents the fluid density, α'represents the polarizability volume, and N_A represents Avogadros number.[108, 123] The Lorentz-Lorentz equation is an extension of the Clausius-Mosotti equation in the region of optical frequencies and links Maxwells theory with the atomistic theory of matter.[123] The isothermal compressibility can be calculated by using the following equation that relates changes in density and pressure:

$$\beta_T = \frac{1}{\rho_\circ} * \frac{\Delta\rho}{\Delta P} \tag{3.2}$$

where β_T represents the isothermal compressibility and P represents the applied pressure.

3.3 Methods

3.3.1 Materials

Sucrose, sodium chloride (NaCl), ethanol, and all other chemicals were purchased from Sigma Aldrich (St. Louis, MO, USA). BIND sensor chips were graciously provided by Dr. Brian Cunningham. The pressure bomb and the high pressure cuvette were machined in the Life Sciences Machine Shop. Buffers were prepared with 18 MΩ deionized water and filtered prior to use.

3.3.2 High Pressure Cuvette and Apparatus

Analyte solutions were inside of a custom designed cuvette manufactured out of polycarbonate. The cuvette was designed so that it could hold a BIND Assay grating sensor that would be cut out of 96-well plate backing. The grating is mounted in the cuvette, on top of a sealing O-ring, and then sealed with a faceplate that is held together by four screws. The cuvette has a liquid reservoir that allows the fluid to come into contact

with the sensor. A fluid-filled cap is placed on the stem of the cuvette. The details of the cuvette are shown in Figure 3.1. As the cuvette is inside the pressure chamber and the pressure is increased, the cap slides down the stem, increasing the pressure inside of the cuvette as well. Using this method, there is no difference in the pressure on both sides of the BIND Assay grating sensor, causing distortions in the sensor geometry. The cuvette was housed inside a high pressure bomb machined out of steel with quartz windows designed based on previously published work.[118, 124] Hydrostatic pressure was generated by a single stage pump (High Pressure Equipment, Erie, PA) using absolute ethanol as the pressurizing fluid. Refractive index changes were monitored by measuring the shift of the peak of the reflected resonant wavelengths (PWV). (Figure 3.2)

3.3.3 BIND Assay Sensors

The sensors are fabricated on a material with a low refractive index that is coated with a thin layer of a higher refractive index material, as previously described.[76] Briefly, the sensors utilize a one-dimensional surface grating structure. Using deep-UV lithography, the sensors were fabricated on plastic substrate and then coated with a thin layer of titanium oxide. The grating period is 550 nm and the depth of the grating is 170 nm. The thickness of the titanium oxide coating is 120 nm. The sensors are fabricated on sheets that fit the backs of standard 96-well plates, and single sensors are then cut out from the sheets, cleaned using a serial ethanol and water rinse, and mounted inside the high-pressure cuvette, which is detailed above.

3.4 Results and Discussion

3.4.1 BIND Assay Verification

In order to verify that the BIND Assay sensor was accurately measuring the refractive index as it was mounted inside the cuvette and placed inside the pressure cell, the refractive index of several concentrations of NaCl was first measured and the measured

values compared to the calculated values. This was repeated for four different sensors and in order to account for any discrepancies in mounting and orientation, the relative difference in refractive index from pure water is what was recorded instead of absolute refractive index. As can be seen in Figure 3.3, the slope of measured Δn vs. calculated Δn is close to 1 and the measured values correspond to the calculated values.

The same set of measurements was repeated for several concentrations of sucrose and compared to calculated values. Again, the measurements were repeated for two different sensors, so the difference in refractive index rather than the absolute refractive index is used. The slope of measured Δn vs. calculated Δn is close to 1 and the measured values correspond to the calculated values. Additionally, in order to eliminate any possible interactions between charged ions and the grating coating, solutions of ethanol and water were examined. In order to minimize interactions between the plastic sensor and the ethanol inside, only concentrations of 50% ethanol and lower were used. Two unique sensors were used in four separate trials, which resulted in the averaged data points presented. Again, the slope of measured Δn vs. calculated Δn is close to 1 and the measured values correspond to the calculated values.

This set of experiments validates the use of the BIND Assay sensors for the purpose of measuring the change in refractive index. All of these experiments were done in ambient pressure and temperature and there was no external pressure applied to the sensors. However it is crucial to demonstrate the utility of the method and instrumentation before applying pressure. These experiments showed that by modulating the concentration of salts in the solution, the sensors were able to detect the changes in refractive index. This was accomplished using solutions with known refractive indices. The sensors were additionally able to detect changes in refractive index with solutions which contained no charged species, eliminating any interactions between the grating coating and charged ions.

3.4.2 Compressibility

To calculate the compressibility of the same solutions, the change in PWV was monitored as pressure was increased from 0 to 21,000 psi. The PWV was recorded in pressure jumps

of 3,000 psi until the final pressure was reached. The PWV was then converted into refractive index[125] and plotted on a graph against pressure. (Figure 3.6) The compressibility of these solutions was calculated using the Lorentz-Lorentz equation (Equation 3.1) combined with the isothermal compressibility equation (Equation 3.2). (Table 3.1) Interestingly, while the compressibility initially increases from pure water, as the concentration of NaCl continues increasing, the compressibility of the solutions first increase, then reaches a plateau, and eventually starts dropping.

The pressure dependence of the refractive index of various concentrations of sucrose solutions was also measured in the same fashion. (Figure 3.7) The compressibility of these solutions is calculated using the Lorentz-Lorentz equation combined with the isothermal compressibility equation. (Table 3.2) The results show that as with solutions of NaCl, the refractive index of sucrose solutions increases both with increasing concentration and with increasing pressure. In contrast to the compressibility of NaCl, the results show that as the concentration of sucrose increases, the compressibility of the solution also increases and does not reach plateau or come back down.

Finally, the pressure dependence of the refractive index of aqueous solutions of ethanol was measured. Higher concentrations of ethanol were not measured since an increase in concentration of ethanol combined with an increase in pressure caused degradation of the plastic component of the sensor. This was most likely caused by a partial dissolution of the plastic substrate on which the sensor is fabricated. (Figure 3.8) The compressibility calculations show that the compressibility does increase with increasing ethanol concentration. (Table 3.3) This behavior is expected, as the compressibility of pure ethanol is almost three times that of pure water.[126] Again, this is in contrast to the NaCl solutions measured above.

3.5 Conclusions

This chapter demonstrates the implementation of a resonant optical biosensor under hydrostatic pressure for measuring changes in refractive index and calculating compressibility of solutions of NaCl, sucrose, and ethanol. An experimental set-up was

built and tested using solutions of different refractive indices. Initially, the BIND Assay sensors were were verified to be accurately measuring refractive indices of the three solutions. After verifying, the pressure dependence and compressibility of the solutions using the BIND Assay sensors under hydrostatic pressure from 0 to 21,000 psi was measured. The Lorentz-Lorentz equation combined with the isothermal compressibility was used to calculate the compressibility of these solutions. Based on these results, we have shown that the BIND Assay sensors are a practical system to be used under hydrostatic pressure to detect changes in refractive index. Additionally, this experimental set up could be used to study other systems of interest under hydrostatic pressure, such as thin films[108], and molecular recognition events.[109, 110] Future works employing this system can be combined with the Nanodisc technology in order to explore the molecular recognition events of membrane proteins, which is further addressed in the last chapter.

3.6 Figures and Tables

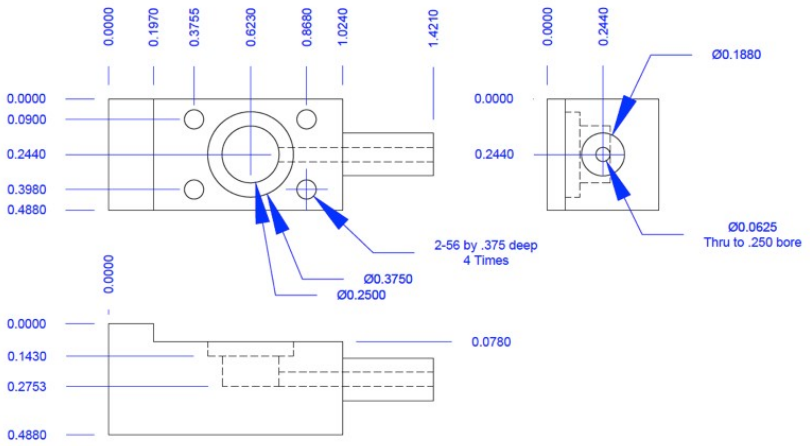

Figure 3.1: A schematic of the custom-machined cuvette used in the high pressure bomb. The cuvette is machined out of polycarbonate. The sensor is placed on top of the hole present in the middle of the cuvette, with a faceplate holding it down. The faceplate is held down by 4 screws. A pressure cap goes on top of the stem, pressurizing the inside of the cuvette as the the pressure outside builds up.

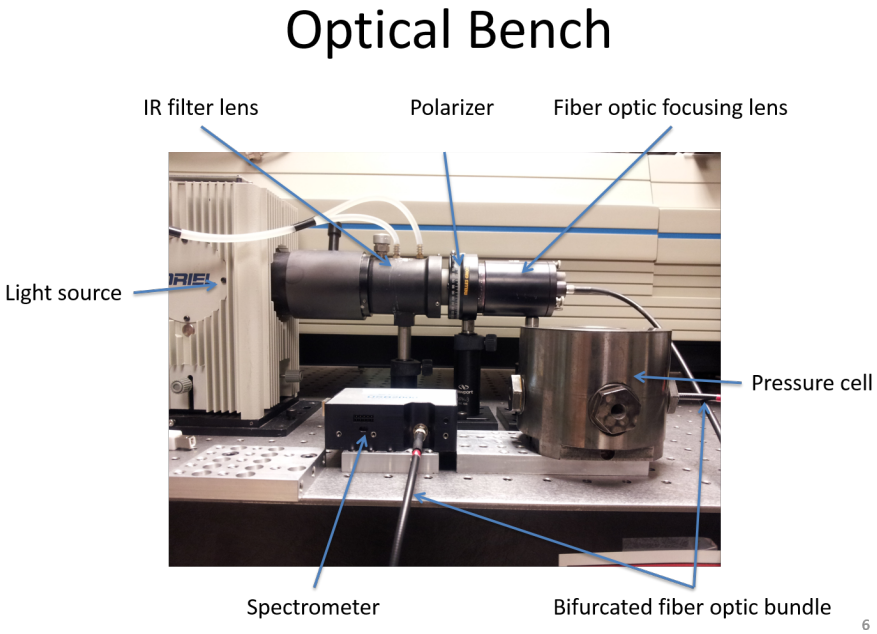

Figure 3.2: Diagram of the high pressure apparatus. The light source is an Oriel tungsten halogen lamp. The light passes through an IR filter, then is polarized, and is focused into a fiber optic cable. The cable focus the light onto the sensor inside the pressure cell through the window and measures the reflected light.

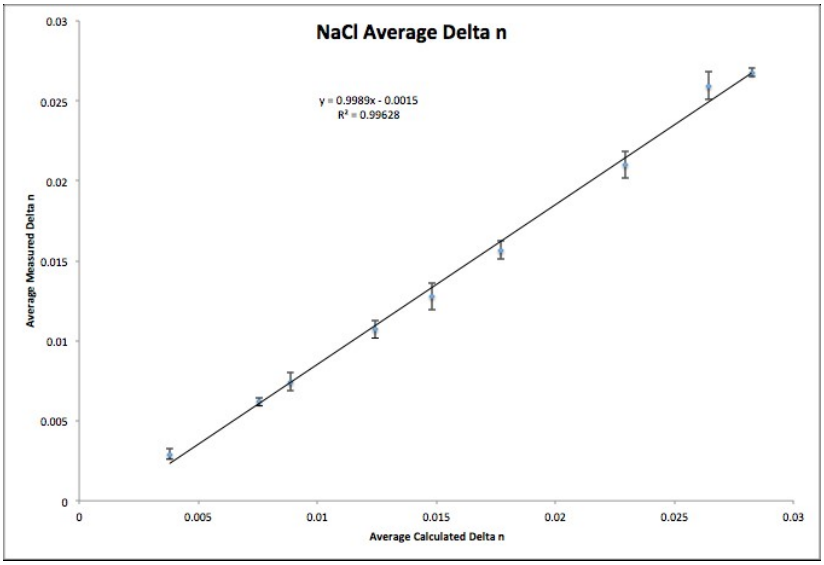

Figure 3.3: A comparison between measured Δn values and calculated Δn values for NaCl.

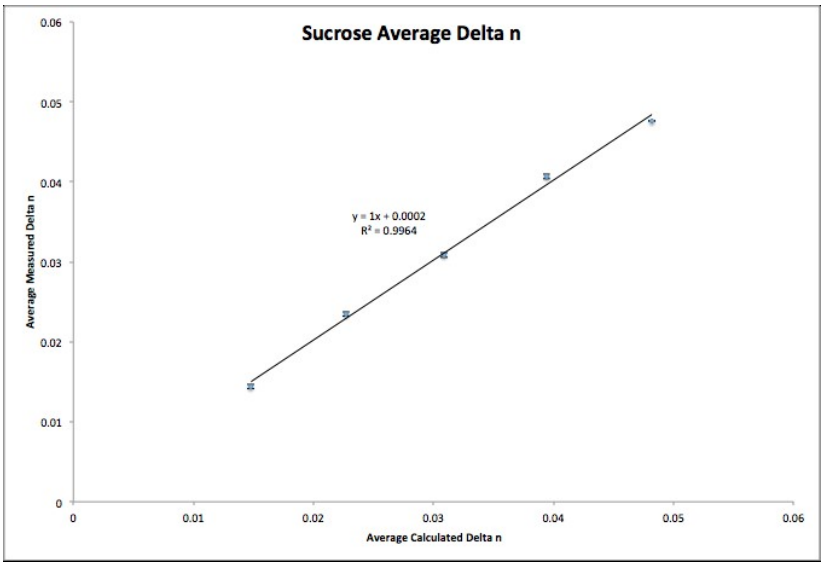

Figure 3.4: A comparison between measured Δn values and calculated Δn values for Sucrose.

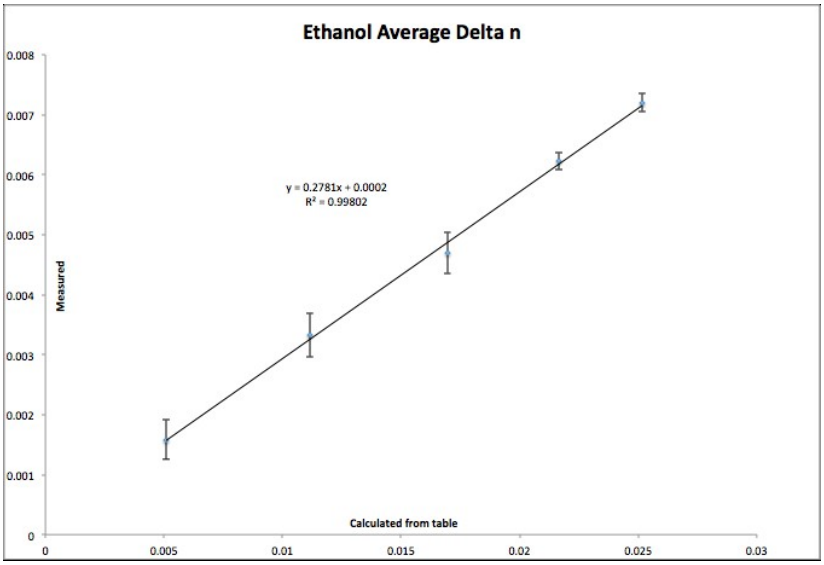

Figure 3.5: A comparison between measured Δn values and calculated Δn values for Ethanol.

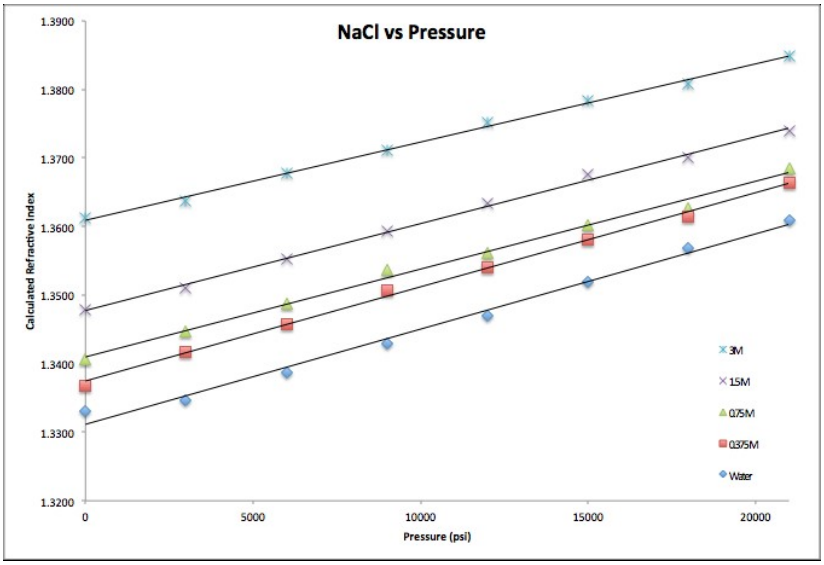

Figure 3.6: Calculated refractive index values at different pressures for NaCl.

Table 3.1: Compressibility of NaCl

Concentration of NaCl (% *by wt.*)	**Compressibility** ($x10^{-10}m^2/N$)
0	4.4
2	5.6
4	4.9
8	4.9
16	4.2

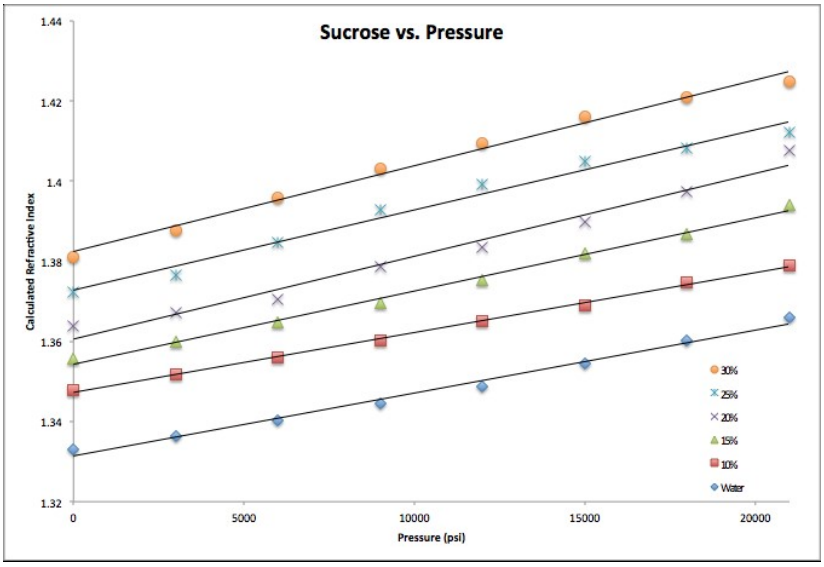

Figure 3.7: Calculated refractive index values at different pressures for sucrose.

Table 3.2: Compressibility of sucrose

Concentration of Sucrose (% *by wt.*)	**Compressibility** ($x10^{-10}m^2/N$)
0	4.4
10	5.4
15	6.2
20	6.3
25	7.3
30	7.6

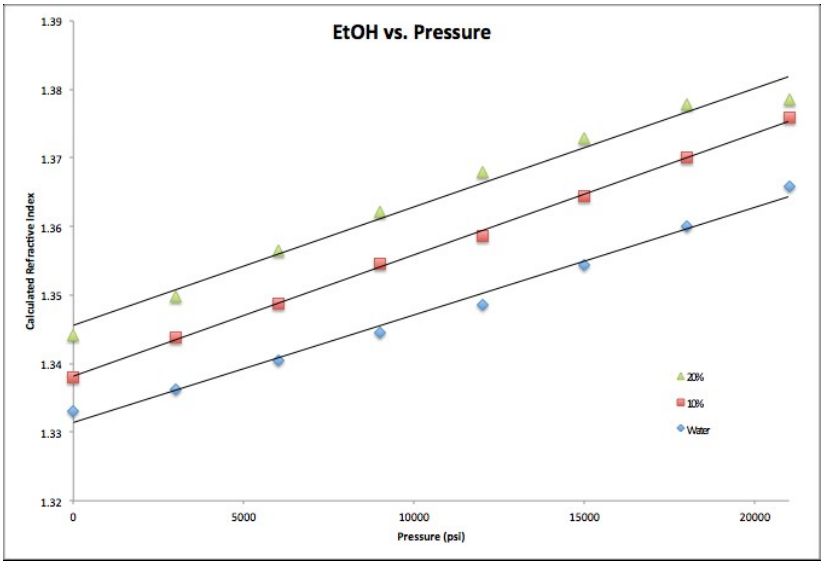

Figure 3.8: Calculated refractive index values at different pressures for ethanol.

Table 3.3: Compressibility of ethanol

Concentration of Ethanol (% *by wt.*)	**Compressibility** ($x10^{-10}m^2/N$)
0	4.4
10	6.8
20	7.1

CHAPTER 4

INTERFACING DNA-LABELED NANODISCS WITH PHOTONIC MICRORING RESONATORS

4.1 Introduction

Nanodiscs have previously been interfaced with a variety of surface-based biosensors, including SPR and silicon photonic microring resonators.[25, 66, 68] However, the published studies utilizing Nanodiscs on biosensors have a need for improved methods. First, most studies have focused on a single protein-protein or protein-lipid interaction. For example, SPR studies have examined the interaction between blood coagulation factors and PS lipid head groups[29, 43]. Commercial SPR instruments are limited in their multiplex capabilities, utilizing one or two channel sensor chips. This inherently limits the number of studies performed on a single chip and shows a need for improved multiplexity of instruments. Multiplexing has been partially addressed by coupling Nanodiscs with the silicon photonic microring resonators[68] but this method requires depositing Nanodiscs by hand onto the sensor chips. This hand deposition method is prone to user error and also limits the number of different Nanodisc types which can be spotted onto the chip, as the dimensions of the chip are small. The need for a system which has high multiplexity, high throughput, and limits manual manipulation is required for systems involving multiple targets. A system incorporating all of these features would decrease analysis time, reagent consumption, and reduce variability between trials.

Silicon photonic microring resonators are biosensors which rely on the optical coupling of internally reflected light from a linear waveguide into micrometer sized ring waveguides. The evanescent wave generated from the internally guided light probes the environment around the wave guide and monitors for a shift in optical density, or refractive index, which would result from a biomolecular interaction near the surface of the waveguide. The

evanescent wave penetrates the surface of the rarer medium, in this case the solution, and decays exponentially with distance from the surface of the waveguide. A shift in refractive index is displayed as a shift in the resonance wavelength and the change is continuously monitored and measured. These biosensors are incredibly scalable, highly multiplexable, and easily manufactured using well-established semiconductor fabrication methods.[127] Microring resonator biosensors have been previously used for studying protein-protein interactions, detecting nucleic acids, and measuring biomolecular binding kinetics parameters.[128, 129, 130] A study detailing the coupling of Nanodiscs to this biosensor platform by using physisorption for the immobilization strategy has been previously published and this work seeks to build upon the previously published methods.[68]

This chapter details the extension of the previously published work by utilizing the specific sequence recognition of complementary DNA strands. An important advantage of this approach is that DNA is remarkably robust in contrast to proteins and complementary antibodies when it comes to long term storage. Sensor chips can be functionalized with DNA, and then dried and stored long term under conditions which would denature proteins and antibodies. Another advantage of using DNA as the attachment strategy is the capacity of DNA to allow extraordinarily high levels of multiplexing - strands which have n bases can encode up to 4^n unique sequences. For example, this study employs labels which are 21 base pairs in length, allowing for close to 200,000 unique identities of labels. Nanodiscs were labeled using ssDNA by an initial chemical modification of a cysteine mutant of MSP with a heterofunctional crosslinker. The crosslinker provides an *N*-Hydroxysuccinimide (NHS) group, which covalently binds to an amine terminated ssDNA chain, as well as a reactive maleimide group, which can react with a thiol group of a cysteine residue present on the MSP. Using this strategy, eight different MSP variants were created with eight unique DNA sequences. The complementary ssDNA was immobilized to the biosensor surface using a molecular printing system, limiting the manual manipulation of the assay. The functionalization of the microring resonator chips with eight different Nanodisc systems provided a multiplexed platform for elucidating the binding parameters of blood coagulation factors and charged lipids. This work not only builds upon the previously published methods, it also lays the groundwork for multiplexed,

high-throughput assays utilizing lipid bilayers of varying composition.

4.2 Methods

4.2.1 Materials

The lipids 1-palmitoyl-2-oleoyl-*sn*-glycero-3-phosphocholine (POPC), 1-palmitoyl-2-oleoyl-*sn*-glycero-3-[phospho-L-serine] (POPS), 1,2- dimyristoyl-*sn*-glycero-3-phosphocholine (DMPC), and 1,2-dimyristoyl-*sn*-glycero-3-phospho-L-serine (DMPS) were purchased from Avanti Polar Lipids (Alabaster, AL, USA). The cysteine mutant, MSP1D1_D73C was expressed and purified as described previously.[30, 31] Tissue factor (TF) was generously provided by the research group of Prof. James Morrissey. The crosslinker m-maleimidobenzoyl-N-hydroxysuccinimide ester (MBS), bis(sulfosuccinimidyl)suberate (BS3), StartingBlock Blocking Buffer, and Tris(2-carboxyethyl)phosphine hydrochloride (TCEP) were purchased from ThermoFisher Scientific (Waltham, MA, USA). Single stranded DNA (ssDNA), terminated with a reactive, primary amine group was purchased from Integrated DNA Technologies (Coralville, IA, USA). Vivaspin Protein Concentrator Spin Columns were purchased from GE Life Sciences (Pittsburg, PA, USA). (3-Aminopropyl)triethoxysilane (APTES), Ethylenediaminetetraacetic acid (EDTA), sodium cholate, dimethyl sulfoxide (DMSO), Amberlite XAD-2 hydrophobic beads, and all other chemicals were purchased from Sigma Aldrich (St. Louis, MO, USA). Buffers were prepared with 18 MΩ deionized water and filtered prior to use.

4.2.2 MSP Labeling with ssDNA

When received, MBS is dissolved in anhydrous DMSO at a concentration of 159 mM and kept as a stock solution, stored in a sealed desiccator at 4 °C. Stock MBS is diluted down to 5 mM prior to use in reaction to prevent precipitation in an aqueous buffer. DNA is dissolved in PBS buffer 1 (10 mM PBS, 3 mM EDTA, pH 8) to a concentration of 100 μM.

MBS and DNA are combined at a ratio of 100:1 MBS:DNA and final concentrations of 1 mM MBS and 10 μM DNA. The reaction is incubated on a shaker at room temperature for 30 minutes. During that reaction time, the cysteine residue of MSP1D1_D73C is reduced through the use of TCEP. This is accomplished by adding TCEP and cholate to a solution of MSP with final molar ratios of 1:5:25 of cholate:MSP:TCEP. The MSP-cholate reaction is allowed to proceed on a shaker at room temperature for 15 minutes. After the MBS-DNA reaction has been incubated for 30 minutes a buffer exchange is performed, using Vivaspin 5,000 MWCO concentrator spin columns into PBS buffer 2 (10 mM PBS, 3 mM EDTA, pH 6.5). The buffer exchange also accomplishes the removal of excess crosslinker. After buffer exchange, MSP and DNA are combined such that the molar ratios are 1:10 of MSP:DNA and the reaction is incubated on a shaker at room temperature for two hours. It is important to note that a low concentration of MSP will produce low labeling efficiency, so the concentration of MSP is kept $\geq$ 75 μM. Labeling was confirmed and efficiency was estimated via gel electrophoresis. The labeled MSP can be separated from the unlabeled DNA via size exclusion chromatography (SEC).

4.2.3 Nanodisc Self-Assembly and Purification

Preparation of Nanodiscs with POPS[29] and TF[43] have been previously described in detail and the same general protocol was followed. Briefly, for Nanodiscs containing a mixed system of POPC:POPS, lipids were combined in the appropriate ratios from chloroform stocks, dried under nitrogen, dessicated overnight, and re-suspended in sodium cholate containing buffer. The solubilized lipids were combined with DNA-labeled MSP1D1_D73C at the appropriate ratio. At this point, for Nanodiscs requiring the addition of tissue factor, a Triton X-100 solubilized stock of TF was added to the solution at the ratio of 10:1 of MSP:TF. For "empty" Nanodiscs, no additional reagents are necessary. Detergent removal was accomplished with Amberlite XAD-2 beads. Samples were purified via a Superdex 200 Increase SEC column (1.6 x 30 cm) at flow rate of 0.75 mL/min and the appropriate peak fractions collected and pooled. The concentration of Nanodisc solutions was determined by a Bradford assay.

4.2.4 Purification of TF-Nanodiscs

Nanodiscs with incorporated TF were purified from "empty" Nanodiscs containing only lipids. This is accomplished through a genetically encoded HPC4 tag on the TF protein. After the Nanodiscs were assembled and purified on the Superdex column, $CaCl_2$ was added to the samples, so that the final concentration was 2 mM. Samples were loaded on an HPC4 resin column equilibrated in HBS-50 buffer (30 mM HEPES, 50 mM NaCl, 5 mM $CaCl_2$). The column was washed with 3 mL of HBS-50 to wash away empty Nanodiscs. The bound discs were then eluted with 2 mL of HBS-50 containing 5 mM EDTA. A buffer exchange was performed through dialysis to remove calcium and EDTA and put the Nanodiscs into PBS buffer. The concentration of Nanodiscs was again determined with a Bradford assay.

4.2.5 Microring Resonator Chips and Instruments

Microring resonator instrumentation and sensor chips were obtained from Genalyte, Inc. (San Diego, CA) and have been described previously.[128, 130] Arrays of silicon photonic microrings were fabricated of silicon oxide substrates using well established and characterized semiconductor fabrication methods. Each 6x6 mm microchip contained 128 microrings, each ring 30 μm in diameter, 500 nm wide and 200 nm tall, with adjacent linear waveguides. Input and output diffractive grating couplers at the end of the linear waveguides allow independent measurements to be made at each ring using a tunable cavity diode laser centered at λ=1560 nm. Light is coupled from the linear waveguide into the microring only at wavelengths that travel at an integer multiple of wavelengths around the ring, with the resonance condition given by:

$$m\lambda = 2\pi r n_{eff} \tag{4.1}$$

where, m is an integer, r is the microring radius, and n_{eff} is the effective refractive index sampled by the evanescent wave. Bio-molecular binding events close to the ring surface cause a change in local refractive index and are measured as a shift in the resonance peak

wavelength (PWV) in units of Δpm. The magnitude of the wavelength shift is directly proportional to the amount of bound analyte. Solution is flowed over the surface through a custom-built microfluidic chamber that features channels defined by a 0.007 inch thick Mylar gasket (RMA Laser, El Caljon, CA, USA). Total shifts were quantified at saturation of the Nanodisc or binding protein sample.

4.2.6 Functionalization of Resonator Chips

Chips were initially immersed in acetone for 2 minutes with continuous shaking at room temperature. The chips were then immersed in acetone with 5% (3-Aminopropyl)triethoxysilane (APTES) for 4 minutes with continuous shaking at room temperature in order to provide a reactive amine on the surface. Afterwards, the chips were immersed in fresh acetone for 2 minutes to remove excess APTES, fresh isopropanol for 2 minutes, and dried under nitrogen. The chips were hand-spotted with 20 μL of 5 mM BS3 in 2 mM acetic acid solution, allowed to incubate for 3 minutes and washed under water and dried with nitrogen. *Note:Functionalization should be completed within 20 minutes of dissolving the BS3 in acetic acid.* DNA was spotted onto the ring resonators using the Nano eNabler Molecular Printing System (Bioforce Nanosciences, Ames, IA) with a concentration of 100 μM. After spotting DNA, the chips were immersed in StartingBlock Blocking Buffer and allowed to incubate for 1 hour under continuous shaking at room temperature. Excess solution was removed and chips were rinsed with 18 MΩ water and dried and stored in a sealed desiccator at 4 °C until ready to be used. Nanodiscs were immobilized on the microchip substrate by flowing Nanodisc solution through 1-, 2-, or 4-channel microfluidic gaskets. After immobilization of Nanodiscs, the chips were blocked by flowing 2% bovine serum albumin (BSA) solution to prevent nonspecific binding to the silica surface. A flow rate of 10 μL/min was used for all steps.

4.3 Results and Discussion

4.3.1 DNA-Labeled MSP

Labeling of the MSP with DNA was achieved through the use of a heterofunctional crosslinker. The crosslinker which was used in this study was chosen based on several characteristics. First, the crosslinker had to react with both the DNA and the MSP in order to link them, but not in such a way that it would crosslink the molecules to another of the same kind. This required two reactive groups on the crosslinker. One of the groups, the maleimide, would react with the cysteine residue of the MSP mutant, while the other group, the N-Hydroxysuccinimide (NHS), would react with the primary amine-modified ssDNA. The labeling was achieved by following the protocol outlined in the methods section. The labeling reaction was further optimized by adjusting concentrations of all the reagents. After optimization, an estimated labeling efficiency of >80% was achieved. (Figure 4.1) After labeling was complete, a separation of labeled MSP from unlabeled MSP was possible via SEC.(Figure 4.2) Prior to self assembling discs, the labeled MSP was separated and collected.

4.3.2 Nanodisc Loading on Chips

After self-assembly and purification, the Nanodiscs were immobilized on a functionalized microring resonator chip. The chip was functionalized according to the methods outlined above. In order to minimize the materials used, only two DNA strands were used on the chip, A and B, as a proof of concept. The Nanodiscs which were in the flow channel were only labeled with DNA strand B. As the Nanodiscs started flowing across the chip, only the sensors with the complementary DNA strand had a shift in PWV. The rest of the rings did not observe a shift in PWV therefore no binding was observed on those rings. (Figure 4.3) This shows that only the rings with the complementary DNA showed binding of Nanodiscs. The other rings, which either had non-complementary DNA or no DNA attached, did not show any binding of Nanodiscs. Therefore, this validates the method and shows that it is possible to use this method in order to address individual rings with

individual species of Nanodiscs labeled with ssDNA.

4.3.3 Annexin Binding to Anionic Lipids

In order to determine whether Nanodiscs immobilized on the surface of the rings were viable for monitoring specific interactions, binding of annexin was monitored for the channels containing POPC and POPC:POPS Nanodiscs. Annexins interact with membranes in a calcium dependent manner which allows for the interaction between proteins and anionic lipids such as POPS.[131] Binding of annexin was only observed on microrings functionalized with Nanodiscs that contained anionic POPS lipids (Figure 4.4). Switching to calcium-free buffer immediately caused dissociation of the bound annexin from the POPC:POPS Nanodiscs, demonstrating the calcium-dependence of this interaction. The data shown here establishes the utility of DNA-labeled Nanodiscs on the microring resonator array as an effective strategy for addressable immobilization of lipid bilayers for biomolecular interaction assays.

4.4 Conclusions

In this chapter, it was demonstrated that Nanodiscs can be labeled using ssDNA and then interfaced to photonic microring resonator chips utilizing the specific recognition of ssDNA strands. By combining the two novel technologies of Nanodiscs and microring resonators, a high throughput, high-multiplexity phospholipid array was created that could be used to elucidate the details of a variety of biological membrane events. This strategy offers the ability to individually address microring resonators with specific species of Nanodiscs, without using hand spotting techniques. Nanodiscs were successfully chemically labeled with individual DNA strands by utilizing the single cysteine mutant scaffold protein and a crosslinking strategy. The microring resonator chips were then labeled with complementary DNA strands and the binding of labeled Nanodiscs to the complementary DNA immobilized on the resonators was observed. The binding was specific and very little nonspecific binding of non-complementary DNA was observed. The utility of the developed

assay was demonstrated by monitoring the binding of annexin to POPS:POPC Nanodiscs. Binding of annexin to POPS-containing Nanoidscs was seen, while no binding was seen of annexin to POPC-only Nanodiscs.

This work presents an extension of the work initially demonstrating the coupling of Nanodiscs and photonic microring resonators.[68] This implementation of the assay provides higher multiplexity and provides the potential for having an unrivaled complexity of lipid bilayers on a single chip. Current generation microring resonator chips contain 128 individually addressable rings, providing the opportunity for a single chip assay containing as many as 128 different Nanodisc populations. This number is easily achievable using the DNA-labeling approach and the only bottleneck is the size of the chip itself. Furthermore, this assay presents an opportunity to create arrays that can continuously monitor the binding kinetics of multiple species of target proteins or pharmaceuticals. This supports a shift toward personalized, bedside medical devices, able to continuously monitor vital statistics.

4.5 Figures and Tables

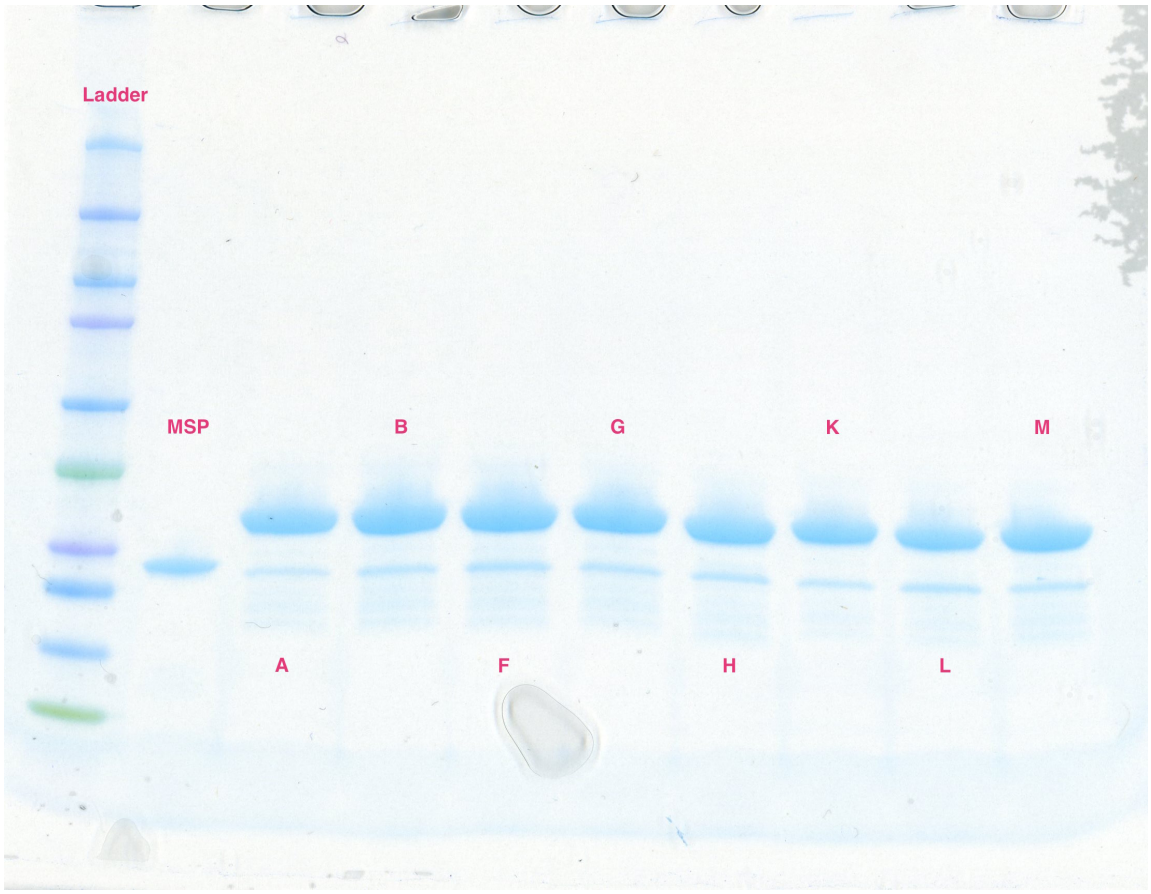

Figure 4.1: SDS-Page gel showing the that the MSP has been labeled with the ssDNA. Lane one is the protein ladder. Lane 2 is unlabeled MSP. Lanes 3 through 10 are the products of the labeling reaction. The thicker bands shows the DNA-labeled MSP and the thinner bands show the unlabeled MSP. The labeling efficiency is >80%.

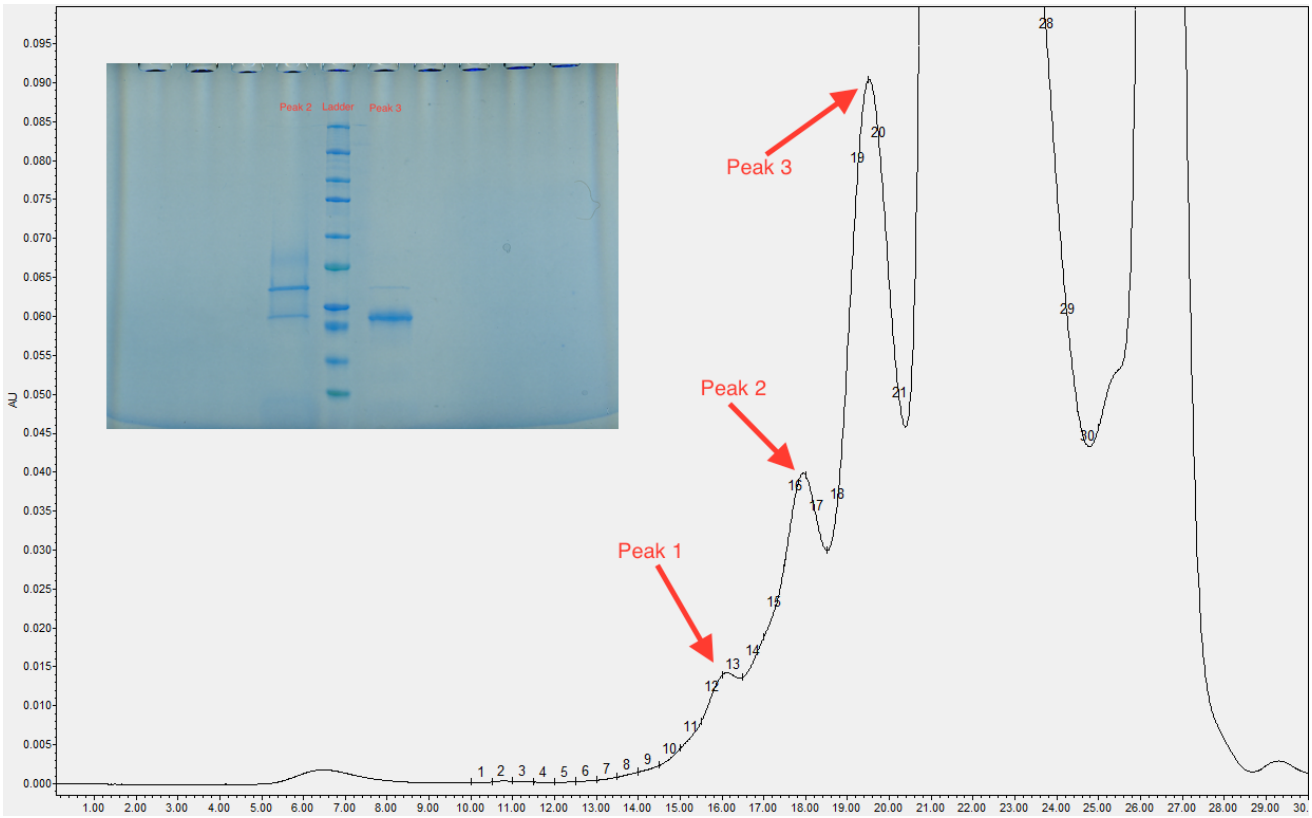

Figure 4.2: SEC chromatogram showing the separation of DNA-labeled vs. unlabeled MSP. The inset shows that the majority of the first peak is DNA-labeled MSP, whereas the majority of the second peak is unlabeled MSP.

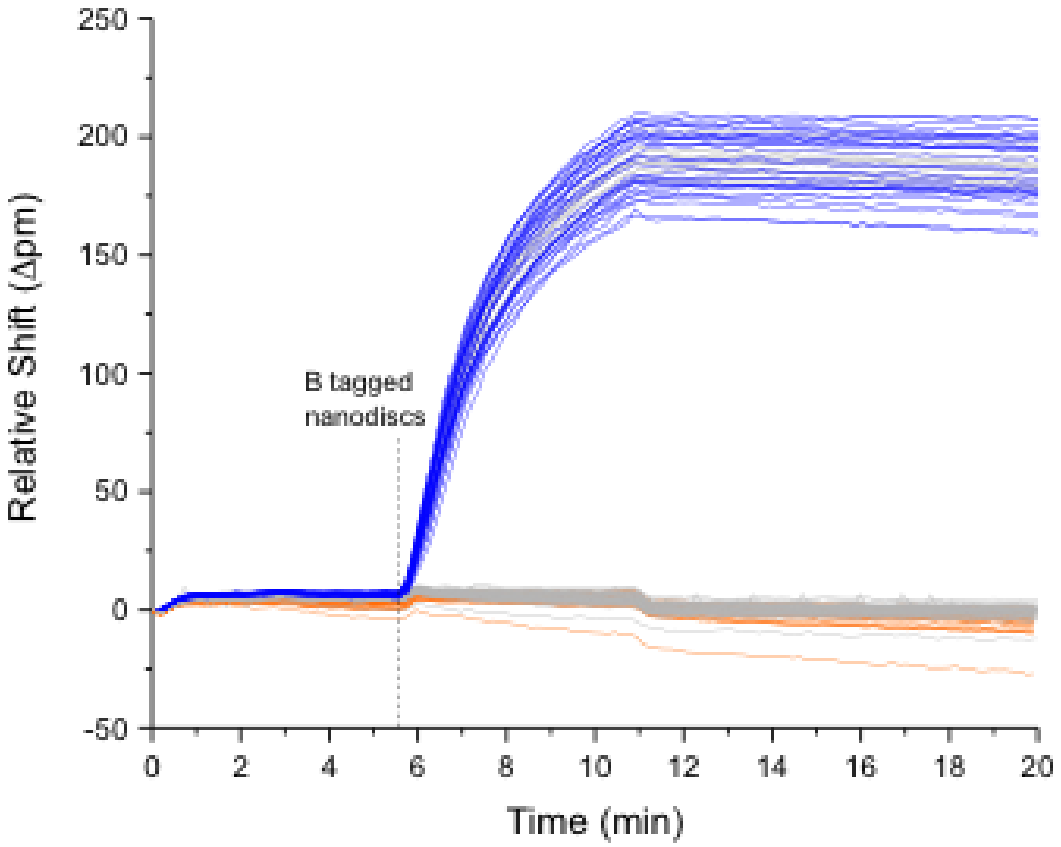

Figure 4.3: Output of the ring resonator instrument showing Nanodiscs labeled with DNA B strands bound to rings with the complementary DNA and did not bind to the rings labeled with a different DNA strand. The blue traces represent the rings with strand B attached to them. The orange traces represent the rings with strand A attached to them. The gray traces represent control rings with no DNA attached to them.

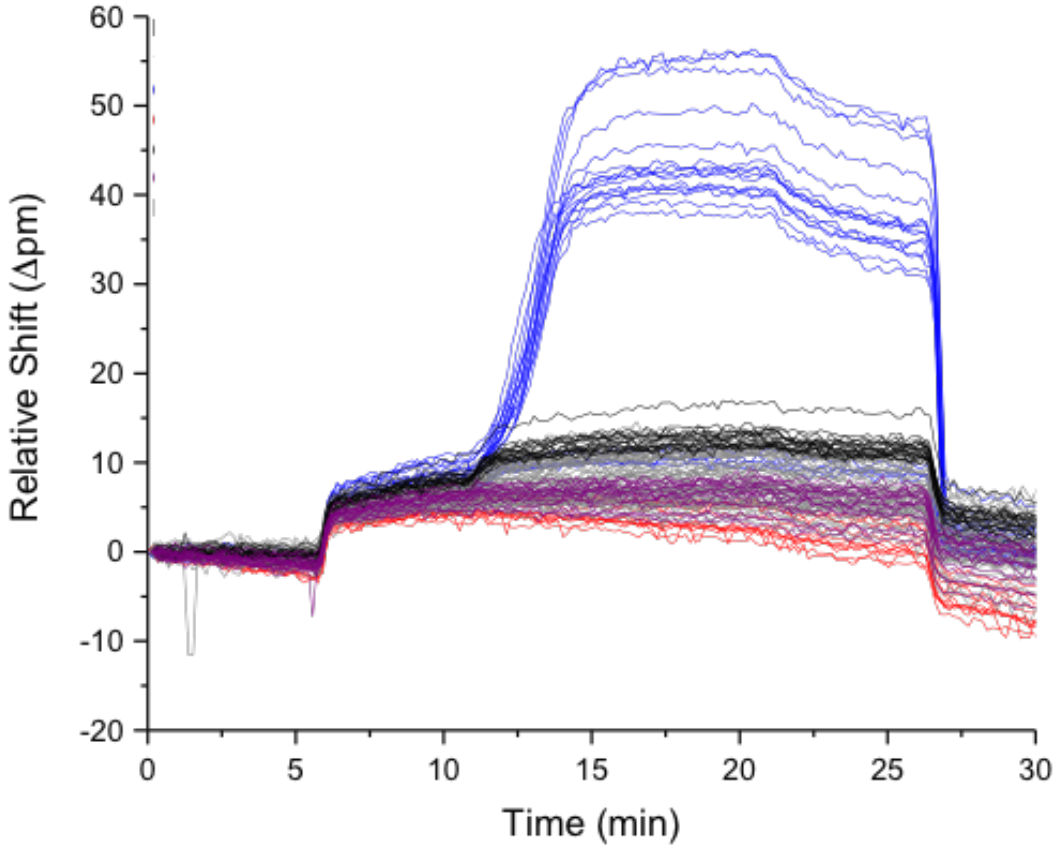

Figure 4.4: Output of the ring resonator instrument showing annexin binding to discs with POPS:POPC and no binding to discs with only POPC. The blue traces represent rings with POPS:POPC Nanodiscs attached to them. Switching to calcium-free buffer immediately caused dissociation of the bound annexin from the POPC:POPS Nanodiscs, as can be seen around 22 minutes.

Table 4.1: Sequences and melting temperatures of the eight ssDNA labels used in this work. The sequences were designed so that the melting temperatures would be similar, ensuring that the hybridization strengths of the molecules are similar.

Label	**Sequence**	$\mathbf{T}_m$ **(°C)**
A	5'-NH3-AAT CCT GGA GCT AAG TCC GTA-3'	55.0
B	5'-NH3-AGC CTC ATT GAA TCA TGC CTA-3'	54.0
F	5'-NH3-AAT CAG GTA AGG TTC ACG GTA-3'	53.3
G	5'-NH3-TGC TCG GGA AGG CTA CTC CTA-3'	58.6
H	5'-NH3-ACG CAC CGC AGT TTG GTC AAT-3'	60.1
K	5'-NH3-ATA ATC TAA TTC TGG TCG CGG-3'	52.3
L	5'-NH3-AGT GAT TAA GTC TGC TTC GGC-3'	55.0
M	5'-NH3-AAC AGG TTC AGA ATC CTC GAC-3'	56.9

CHAPTER 5

DEVELOPMENT OF MICROFLUIDIC PLATFORM FOR THE ASSEMBLY OF NANODISCS

5.1 Introduction

Membrane proteins are usually expressed at low levels throughout the natural proteome of organisms and their recombinant over-expression in host cells is often difficult and costly.[6] This creates a limitation on available material for biomolecular studies involving membrane proteins. The process is further complicated by a greater initial requirement for material in order to optimize incorporation of the target proteins into Nanodiscs - a process inherent to all systems of solubilization. Even though recent molecular biology advancements have simplified construction of DNA sequences for expression, the Nanodisc incorporation optimization, and therefore protein production, remain a bottleneck in the process.[132] In order to decrease sample volume requirements, there is a need for a platform which can rapidly and efficiently prepare and purify small volumes of Nanodisc-incorporated membrane proteins. Small scale studies are needed for cost- and time-effective screening of assay conditions prior to scaling up reactions.[133, 134, 135]

The Nanodisc platform has become an integral and powerful method that has been optimized for the solubilization of membrane proteins. However, the incorporation of each target membrane protein has to be individually optimized. This is often a time and sample consuming procedure but is necessary in order to achieve maximum Nanodisc incorporation as well to maximize the retention of activity in the target protein. The optimization usually involves the screening of several detergents, screening multiple species of lipids, as well as adjusting the ratios of lipids and target protein. Multiple membrane proteins have been successfully incorporated into Nanodiscs,[28, 62, 136] though several other target proteins have proven to be difficult and efforts into incorporation have been

fruitless up to this point. The division in success of incorporation of target proteins has been primarily due to the low availability of starting materials and a need for optimization, therefore a dire need exists for a system which uses small volumes of sample and is able to reliably optimize the incorporation of target proteins into Nanodiscs.

Microfluidic systems have emerged as a robust and reliable platform for the miniaturization of existing tools in molecular biology in order to increase speed and throughput as well as decrease sample cost.[137, 138] In addition to the small size, the ability to add multiple functions and multiple assays on a single device and modularity of microfluidic systems has advanced automation in protein processing and characterization studies.[139] The size and production simplicity of microfluidic technology inherently make the approach amenable to creating modular, multi-step purification systems on a single device. Microfluidic systems have been applied to a variety of problems, including protein purification, protein extraction, point-of-care diagnostics, and chemical and biological analysis.[140, 141, 142, 143] Such devices have incorporated multiple channels, separation columns, micro-reactors, and even cell lysis chambers.[144]

This work details the development of a microfluidic platform for the assembly of Nanodiscs. The device is fabricated out of polydimethylsiloxane (PDMS) and glass slides, with a mixing channel and a channel for the removal of detergent. The design of the device is modular, such that multiple purification steps can be incorporated on a single device, including metal affinity and size purification. The device can be used to generate Nanodiscs, both empty - having no target membrane protein - and with an incorporated protein. Because of the intrinsic property of handling small volumes of materials, this device is extremely applicable in the optimization of target protein incorporation. It is shown that Nanodiscs come out of the device in a matter of minutes, with and without incorporated protein. Additionally, a continuous gradient can be programmed such that optimization of ratios can be achieved on the fly, without preparing multiple samples, requiring multiple steps of purification and analysis.

5.2 Methods

5.2.1 Materials

The lipids 1-palmitoyl-2-oleoyl-*sn*-glycero-3-phosphocholine (POPC), 1-palmitoyl-2-oleoyl-*sn*-glycero-3-[phospho-L-serine] (POPS), 1,2- dimyristoyl-*sn*-glycero-3-phosphocholine (DMPC), and 1,2-dimyristoyl-*sn*-glycero-3-phospho-L-serine (DMPS) were purchased from Avanti Polar Lipids (Alabaster, AL, USA). The scaffold protein, MSP1D1 was expressed and purified as described previously.[30, 31] CYP3A4 was expressed with a histidine affinity tag from the NF-14 construct in the pCWOri+ vector, purified, and incorporated into POPC Nanodisc lipid bilayers as previously described.[41, 83, 102, 103] Pierce Detergent Removal Resin was purchased from ThermoFisher Scientific (Waltham, MA, USA). Ethylenediaminetetraacetic acid (EDTA), sodium cholate, dimethyl sulfoxide (DMSO), Amberlite XAD-2 hydrophobic beads, and all other chemicals were purchased from Sigma Aldrich (St. Louis, MO, USA). Buffers were prepared with 18 MΩ deionized water and filtered prior to use.

5.2.2 Microfluidic Design and Fabrication

Microfluidic devices were designed to incorporate a mixing channel as well as detergent removal channel. The mixing channel is in a serpentine shape capable of mixing the three separate components that are introduced in the three inlets. The detergent removal channel incorporates posts to enhance structural stability. The device master was designed in AutoCAD (Autodesk Inc., San Rafael, CA) and a mask was printed by . The masters were made by spin coating SU8-2100 on a wafer to produce a thickness of . The mask design was transferred using standard photolithography techniques. Feature height was validated using optical profilometry. PDMS was poured on top of the master, air bubbles removed via vacuum, and subsequently cured at 80 °C for two hours. The PDMS was removed from the master, cut out to individual devices, and holes punched for inlet and outlet ports. Glass slides were cleaned in a plasma cleaner and the PDMS adhered to the cleaned glass slides. Standard silicone tubing was used for the connection between syringes

and device inlets as well as the outlet of the devices.

5.2.3 Microfluidic Assembly of Nanodiscs

Non-Mixing In order to assemble empty Nanodiscs, a solution of detergent-solubilized lipids and purified MSP1D1 was flowed across a device, filled with detergent removal resin. Flow rates were constant, set at 30 μL/min, and controlled by infusion syringe pumps (Harvard Apparatus, Holliston, MA). In order to assemble CYP3A4 into Nanodiscs on the device, a solution of detergent-solubilized lipids, purified MSP1D1, and purified, detergent-solubilized CYP3A4 was flowed across the device. All solutions and device were under temperature-controlled conditions, depending on the identity of the lipid used so that the temperature was slightly above the transition temperature. The eluent was collected in 50 μL fractions and characterized by SEC and AFM.

Mixing In order to assemble empty Nanodiscs, three solutions were flowed into separate channels: detergent-solubilized lipids, purified MSP1D1, and buffer. The three separate channels combine into a serpentine, mixing channel which mixes the three constituents before flowing into the detergent removal channel. The three solutions are placed into separate syringes and each syringe is controlled by an infusion syringe pump to have a constant flow rate of 10 μL/min. Incorporating CYP3A4 into Nanodiscs with a mixing channel calls for a similar protocol, changing the buffer solution to a solution of detergent-solubilized CYP3A4 in the third channel. All solutions and device were under temperature-controlled conditions, depending on the identity of the lipid used so that the temperature was slightly above the transition temperature.The eluent was collected in 50 μL fractions and characterized by SEC.

Lipid Gradient Mixing To assemble empty Nanodiscs, three solutions were flowed into separate channels: detergent-solubilized lipids, purified MSP1D1, and buffer. The three separate channels combine into a serpentine, mixing channel which mixes the three constituents before flowing into the detergent removal channel. The three solutions are

placed into separate syringes and each syringe is controlled by an infusion syringe pump. Syringes not containing lipids were flowed at a constant rate of 10 μL/min while the syringe containing lipids was flown utilizing a programmed gradient beginning at 6.92 μL/min and ending at 13.08 μL/min over the span of 8 minutes and 20 seconds. The same conditions were repeated for the assembly of CYP3A4-Nanodiscs, replacing the buffer channel with detergent-solubilized CYP3A4. All solutions and device were under temperature-controlled conditions, depending on the identity of the lipid used so that the temperature was slightly above the transition temperature.The eluent was collected in 50 μL fractions and characterized by SEC.

5.2.4 Colorimetric Quantitation of Detergent Removal

The amount of cholate and CHAPS present in solution can be determined colorimetrically, as described in a published method.[145] Briefly, to quantify the amount of detergent being removed by the detergent removal resin packed in the microfluidic device, buffer containing 100 mM sodium cholate was flowed through resin bed and 10 μL fractions were collected in individual polypropylene tubes, diluted to 50 μL and 800 μL of concentrated sulfuric acid was added. A standard curve was made by preparing 50 μL samples of buffer with concentrations of sodium cholate ranging from 1 mM to 100 mM before 800 μL of concentrated sulfuric acid was added. Using the standard curve, the concentration of sodium cholate of the collected fractions was determined by using a plate reader and measuring absorbance at 390 nm of 200 μL of each sample on a 96-well plate.

5.2.5 Nanodisc Characterization by SEC

After elution from the microfluidic devices, Nanodiscs were characterized by SEC. Fractions collected from the microfluidic device were injected onto a Superdex 200 Increase column (1.6 x 30 cm) (GE Healthcare, Pittsburgh, PA) at a flow rate of 0.75 mL/min and absorbance monitoring at 280 nm. The resulting chromatograms were compared to a chromatogram of a standard mixture of proteins - Bovine Serum Albumin (BSA), Bovine

Liver Catalase, Ferritin, and Thyroglobulin - with hydrodynamic radii in the range of interest.

5.2.6 Nanodisc Characterization by AFM

AFM images were obtained with a Cypher ES Environmental AFM (Asylum Research, Santa Barbara, CA) equipped with a fluid cell. To form the surface of Nanodiscs, mica was glued to 10 mm steel disks and cleaved with cellophane tape. Samples of 10 μL Nanodiscs were applied followed by 10-20 μL of imaging buffer (10 mM Tris-HCl pH 7.4, 0.15 M NaCl, 10 mM $MgCl_2$). The use of a PAP pen (Ted Pella Inc., Redding, CA) to circumscribe an area of mica with a hydrophobic border has been found useful to prevent flow of solution off the mica. After 10 min, several milliliters of imaging buffer were passed through the cell to remove any unadsorbed material and the sample was mounted on the imaging stage. Contact imaging was done under imaging buffer using the thin-legged 310 μm cantilever having a nominal spring constant of 0.01 N/m.

5.3 Results and Discussion

5.3.1 Design and Fabrication of Microfluidic Devices

Devices were fabricated using standard photolithography and PDMS methods. Regular devices include three inlet ports, a mixing channel in a serpentine shape, consisting of tight turns and wedge shaped inlets. After the mixing channel, a detergent removal channel is included, with a height and width of 1 cm each and a depth of 200 μm totalling a volume of 20 μL. (Figure 5.1). The detergent removal channel has posts spaced throughout the channel for vertical support. The channel is filled with detergent removal resin using the resin port. The port is integrated in the device in order to prevent clogging of other channels. Additionally, the channel contains resin capture posts on both the inlet and the outlet. (Figure 5.3) The capture regions serve two purposes - to first capture and contain all of the resin in the channel and second to distribute the initial flow through the entirety

of the channel. The large device (Figure 5.2) is identical to the regular device, with the only exception being that the detergent removal channel is larger. Specifically, the channel is the same width (1 cm) but longer (3 cm), with the depth of the channel remaining the same, with a total bed volume of 60 μL, allowing for the processing of a larger volume.

To prepare the devices for self assembly, they are initially washed with 18 MΩ deionized water. The detergent removal channel is filled with Pierce Detergent Removal resin under positive pressure and the silicone tubing is clamped. The entire device is rinsed with a series of water, methanol and water for 20 minutes at each rinse. The rinsing is accomplished using a syringe pump flowing at a constant 20 μL/min. After the final rinse of water, the device is equilibrated with buffer for 20 minutes at a constant rate of 20 μL/min. At this point devices are ready for the assembly of Nanodiscs.

5.3.2 Colorimetric Determination of Detergent Removal

To quantitate the detergent removal capability of the device and the resin, a colorimetric method was employed, based on a previously published method.[145] The reaction is between concentrated sulfuric acid and the hydroxyl group of the cholate ring. (Figure 5.5) The reaction results in an intense absorption peak centered at 389 nm. A solution of 100 mM sodium cholate was flowed through the device and samples of 10 μL were collected from the outlet port into Eppendorf vials. The samples were diluted up to 50 μL and 800 μL of concentrated sulfuric acid was added to each tube. To measure the absorbance, three 100 μL fractions were put into individual wells on a 96-well plate. The absorbance was measured and averaged over the three wells. The absorbance generated at 389 nm was stable, increasing by only 5% over 4 h.

Using this method, it was determined that a small device could reliably completely remove cholate from approximately 250 μL of reconstitution mixture. (Figure 5.6) The process was repeated for the similar bile salt detergent 3-[(3-cholamidopropyl)dimethylammonio]-1-propanesulfonate (CHAPS), a detergent that is commonly used in membrane protein studies for its non-denaturing properties.[146] A solution of 10% CHAPS was flowed over the device and 5 μL fractions were collected and

diluted up to 50 μL before adding 800 μL concentrated sulfuric acid. The results from the assay are similar to those of cholate, with the device capable of completely removing CHAPS from approximately 200 μL of reconstitution mixture. These results show that the devices are capable of completely removing two common detergents used in protein purification in a short amount of time. This validates the devices for the use of removing detergent and assembling Nanodiscs on a short time scale.

5.3.3 Nanodisc Characterization by SEC

Nanodiscs were characterized using SEC by first calibrating the column using a mixture of four proteins - Bovine Serum Albumin (BSA), Bovine Liver Catalase, Ferritin, and Thyroglobulin - with hydrodynamic radii in the range of interest. The concentrations of the proteins were normalized so that they would produce peaks of approximately equal intensity on the chromatogram. The absorbance at 280 nm was monitored over time. Well-formed, tightly-packed Nanodiscs display a single, narrow peak between the third and fourth peak of the standards. Nanodiscs with too few lipids display a shoulder or peak to the right of the characteristic Nanodisc peak, indicating smaller species, or free MSP. If the ratio of lipids to MSP is too high, shoulders and peaks to the left of the characteristic peak are observed, indicating aggregates that are too large to be Nanodiscs. (Figure 5.7) Nanodiscs coming off the microfluidic device were characterized by SEC, displaying a characteristic peak, just as expected. At the optimal lipid:MSP ratio, the peak is narrow and at the expected retention time, indicating well-formed Nanodiscs.

5.3.4 Nanodisc Characterization by AFM

Nanodiscs were further characterized using AFM to show the formation of discs immediately after eluting off the microfluidic device. Qualitatively, it can be seen that Nanodiscs have formed on the microfluidic device. The AFM images show that a small amount of aggregates have formed as well, but the population is primarily well formed Nanodiscs. This observation supports the idea that the microfluidic is capable of

assembling Nanodiscs in a matter of minutes, using small volumes of reagents, an inherent advantage of microfluidic systems. (Figure 5.8)

5.3.5 CYP3A4-Nanodiscs on a Microfluidic Device

To demonstrate the utility of the microfluidic devices in assembling Nanodiscs with an incorporated membrane protein, CYP3A4 was incorporated into DMPC Nanodiscs on the microfluidic devices. This was accomplished using all three of the ports on the device and having the concentration ratio be 1:20:90 CYP3A4:MSP:DMPC. The initial characterization was performed by SEC, scanning at 280 nm for the general protein absorbance and at 417 nm for the heme group of CYP3A4. The chromatogram trace revealed that CYP3A4 seemed to be incorporated into the Nanodiscs, coming out at the beginning of the characteristic peak and the "empty" Nanodiscs coming a few seconds later. (Figure 5.9) This is expected as Nanodiscs containing CYP3A4 have a slightly larger hydrodynamic radius than those without incorporated protein.

5.3.6 Lipid Gradient Optimization

To further reduce the time and materials requirements of target incorporation, a lipid gradient was developed. While holding the concentrations of all materials constant, the flow rate of MSP and buffer/target are held constant and the flow rate of the lipid channel is varied, according to a programmed gradient. This, in turn, produces a continuous gradient of lipid:MSP:target ratios that can be used to determine the optimal ratio for target incorporation. To characterize the Nanodiscs produced by the gradient, 25 μL fractions were collected and characterized by SEC. To show that the gradient can be applied in either direction, a gradient started at a low ratio of lipids to MSP and increased, while a different device started a gradient at a high lipid to MSP ratio and decreased with time. This was also in order to account for the resin detergent removal capacity. Both gradients showed that the optimal ratio for DMPC Nanodiscs is somewhere around 90 lipid molecules to 1 MSP molecule. (Figures 5.10 and 5.11)

5.4 Conclusions

A modular microfluidic device has been designed and shown to assemble Nanodiscs, both with and without target proteins incorporated into them, by handling small volumes of reagents, having available on-chip mixing of reagents, as well as a purification channel. At this point in time, the purification channel is a wide channel filled with detergent removal resin, facilitating the self-assembly process of Nanodiscs. The device has further been shown to produce Nanodiscs by employing a lipid gradient, both starting at a low lipid to MSP ratio and going up as well as starting at a high lipid to MSP ratio and going down. The incorporation of a gradient aspect to the microfluidic platform further reduces sample volume and time cost and increases the utility of these devices in optimizing protocols for the incorporation of target proteins. Using the microfluidic system developed in this work, the conditions for inserting a target protein can be optimized by simultaneously screening several detergents, while varying the lipid ratio using a gradient and collecting small volumes for analysis. This can be accomplished in a short amount of time, using small volumes of sample, and reducing the need for production of precious target proteins. The devices are furthermore modular and can be implemented in series or in conjunction with other analytical devices.

5.5 Figures and Tables

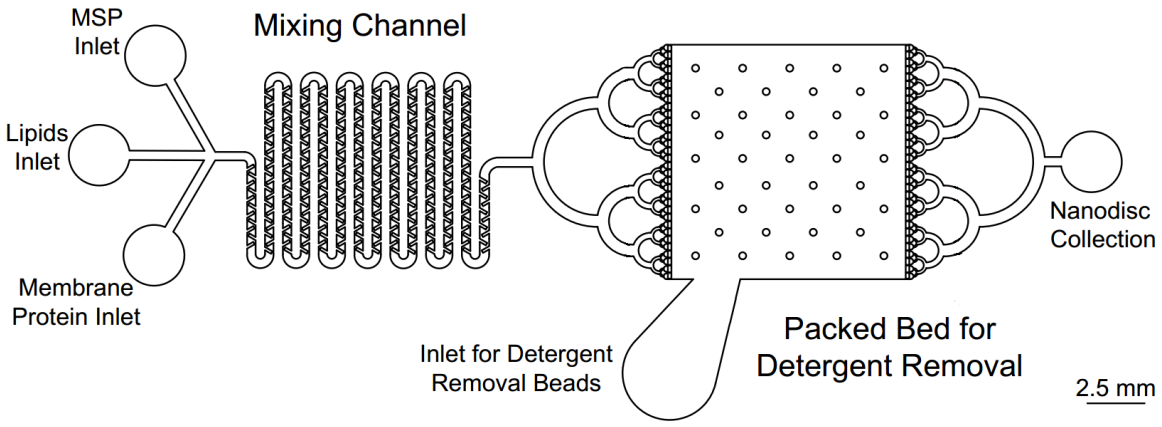

Figure 5.1: Schematic of the microfluidic device used in this study. The device has three inlet ports, a mixing channel, a detergent removal channel, and a Nanodisc outlet port.

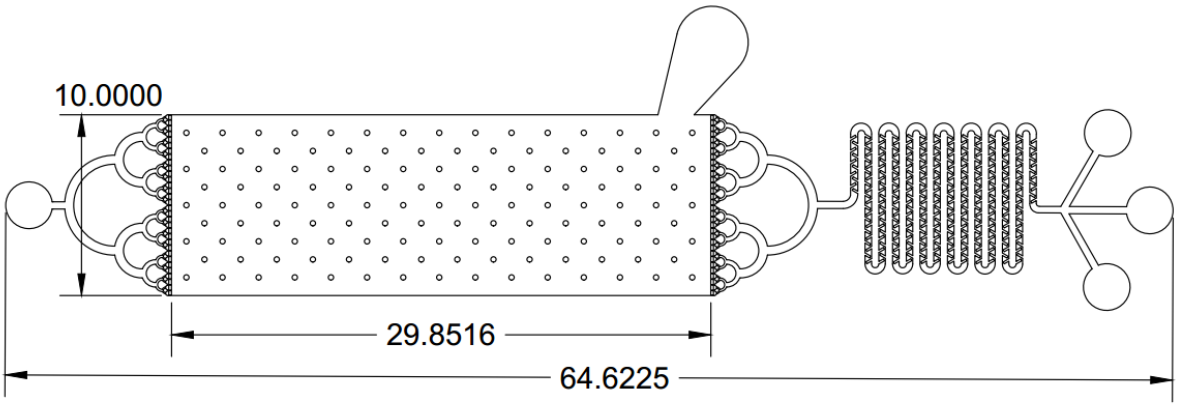

Figure 5.2: Schematic of the large device used in this study. The large device is similar to the smaller devices, with the only difference being the larger detergent removal channel.

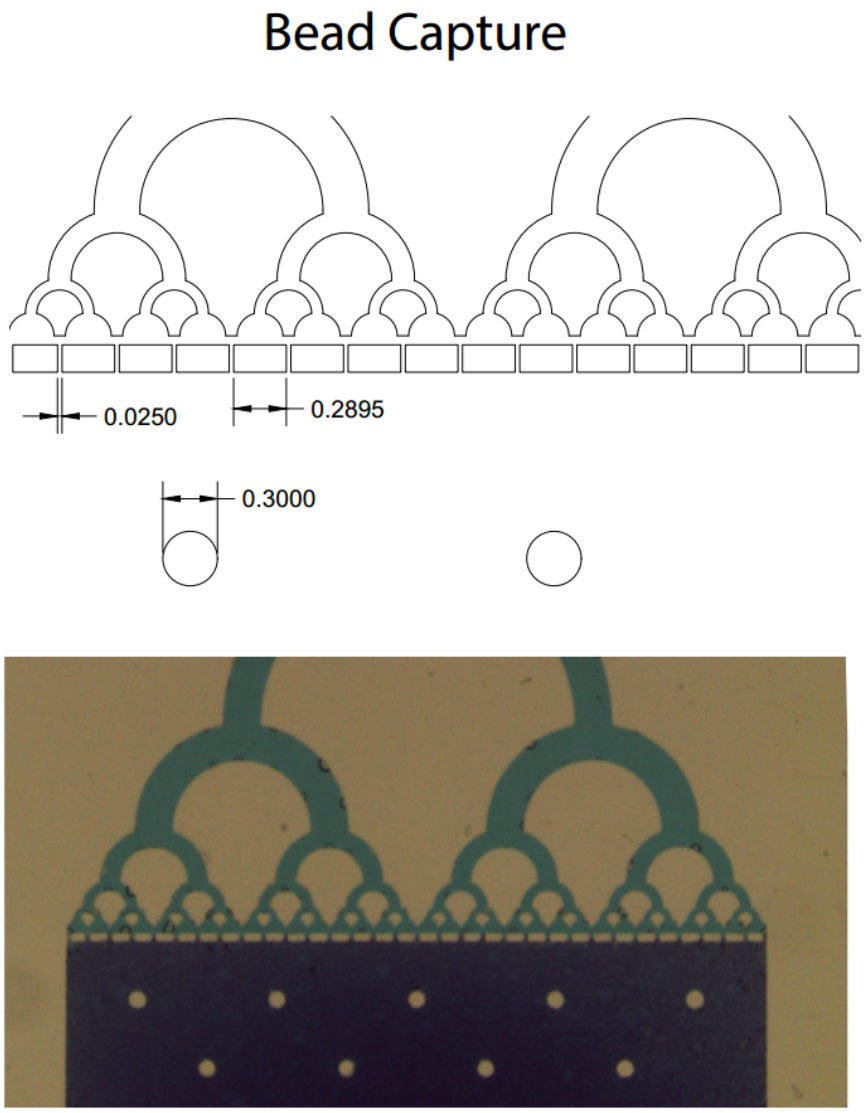

Figure 5.3: Zoomed-in schematic of the bead capture region. The bottom picture is an actual picture of the device colored with dye. This shows the distribution of the solution over the entire bed of resin, with the support posts clearly visible.

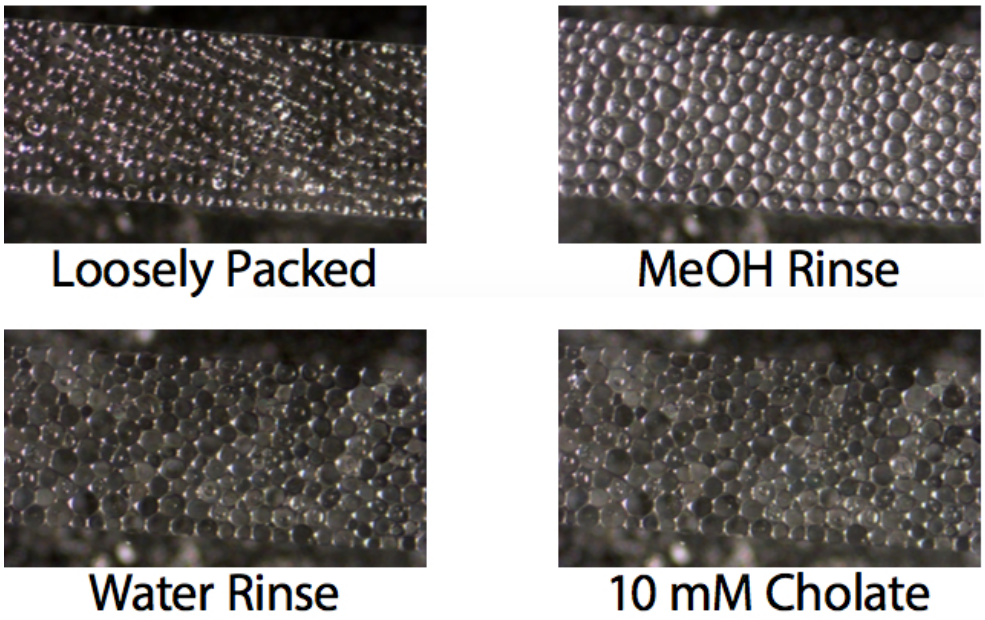

Figure 5.4: Zoomed-in pictures of the resin beads within the device after treatments with water, methanol, and after flowing detergent through the resin bed.

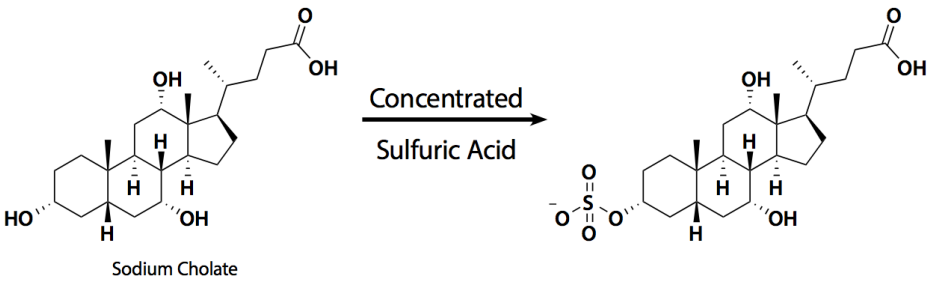

Figure 5.5: The reaction which occurs between sodium cholate and concentrated sulfuric acid that is behind the colorimetric quantitation assay.

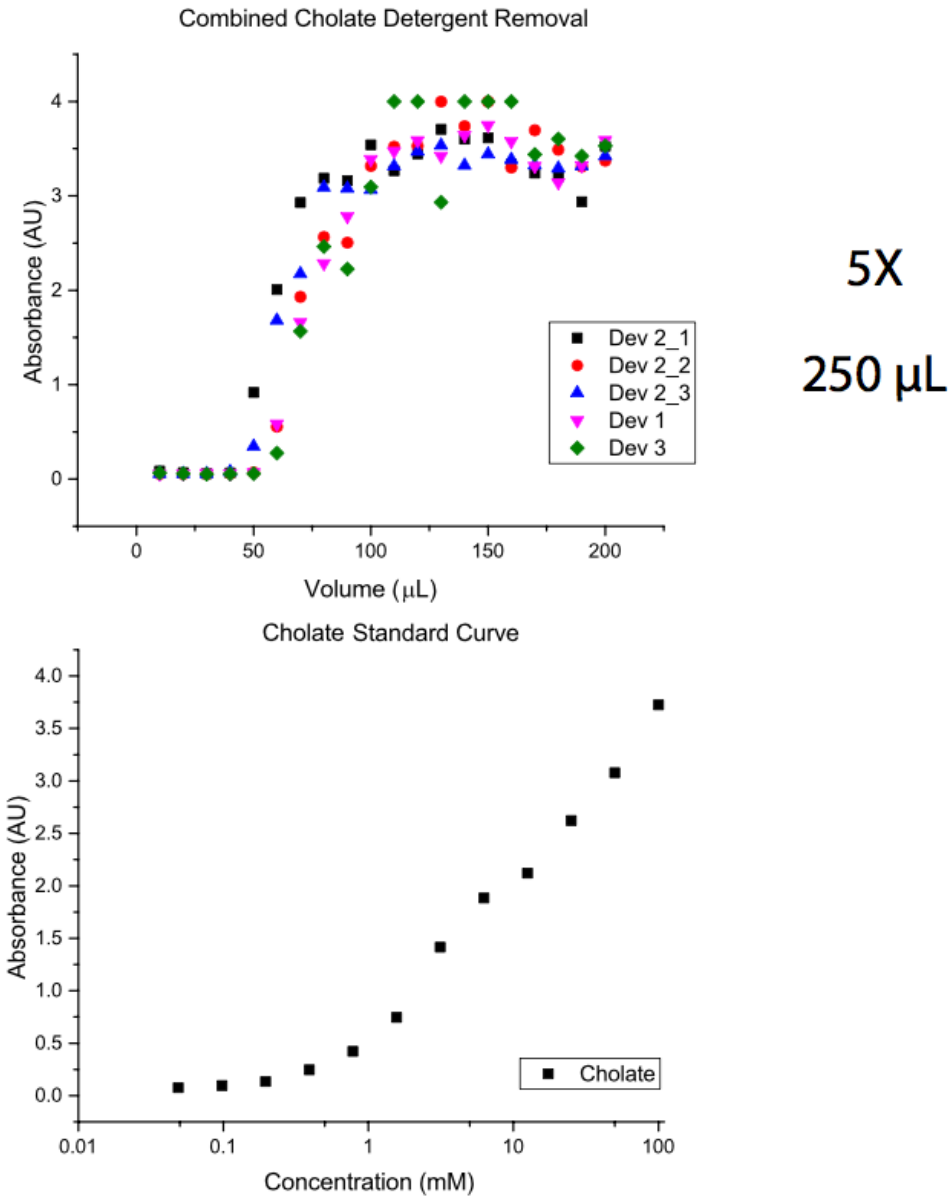

Figure 5.6: The small device is able to remove detergent from 250 μL of solution before we see a change in absorbance. The solution which was put through the device in these experiments was 100 mM cholate while the solution used in Nanodisc assembly is 20 mM cholate.

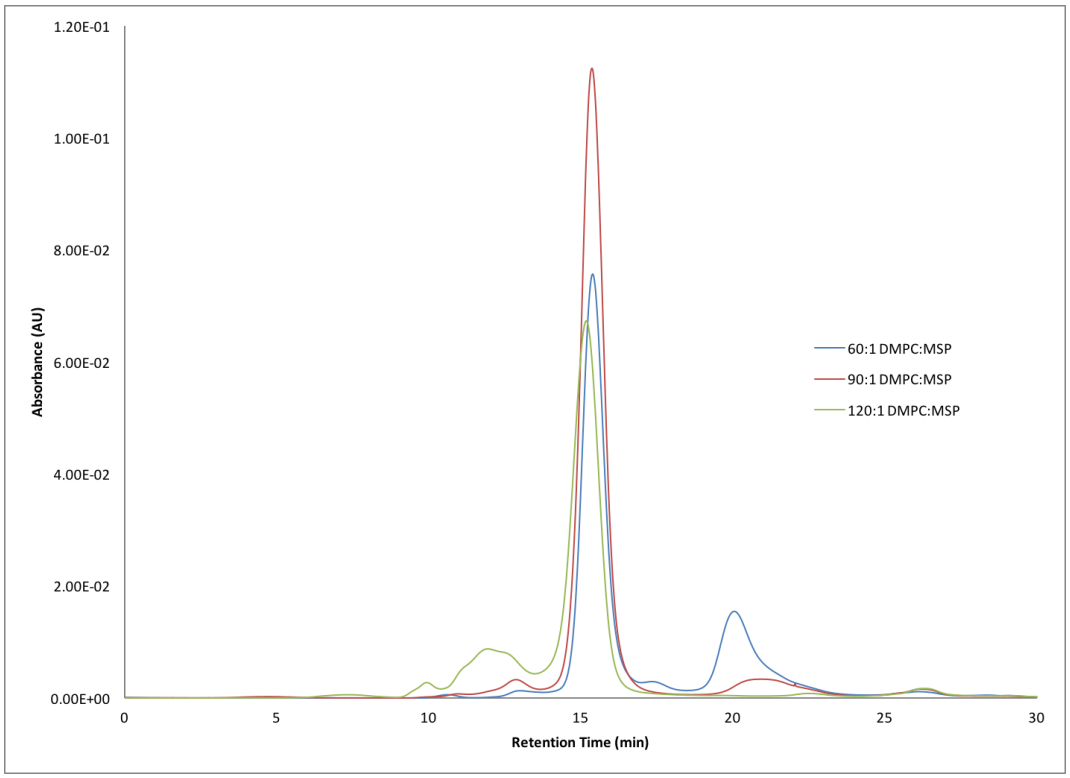

Figure 5.7: Representative chromatogram traces of three preparations of Nanodiscs - underlipidated (60:1), tight-packed (90:1), and overlipidated (120:1). As can be seen, a lower than optimal ratio produces peaks to the right of the characteristic peak, indicating free MSP. An optimal ratio produces a single, narrow, characteristic peak. A higher than optimal ratio produces peaks to the left of the characteristic peak, indicating the presence of aggregate species.

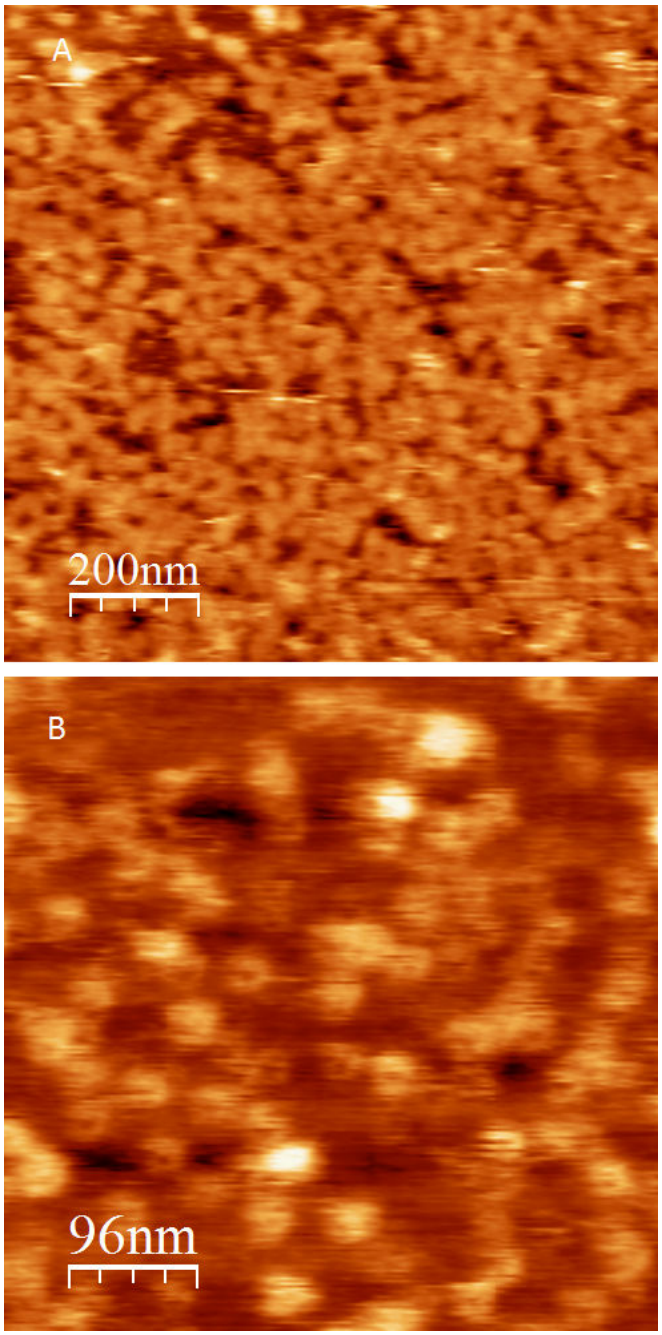

Figure 5.8: An AFM scan of DMPC Nanodiscs produced by the microfluidic device. The Nanodiscs are not purified in any way, which is why we see some aggregates. The scan size is 1 x 1 μm for image A and 500 x 500 nm for image B.

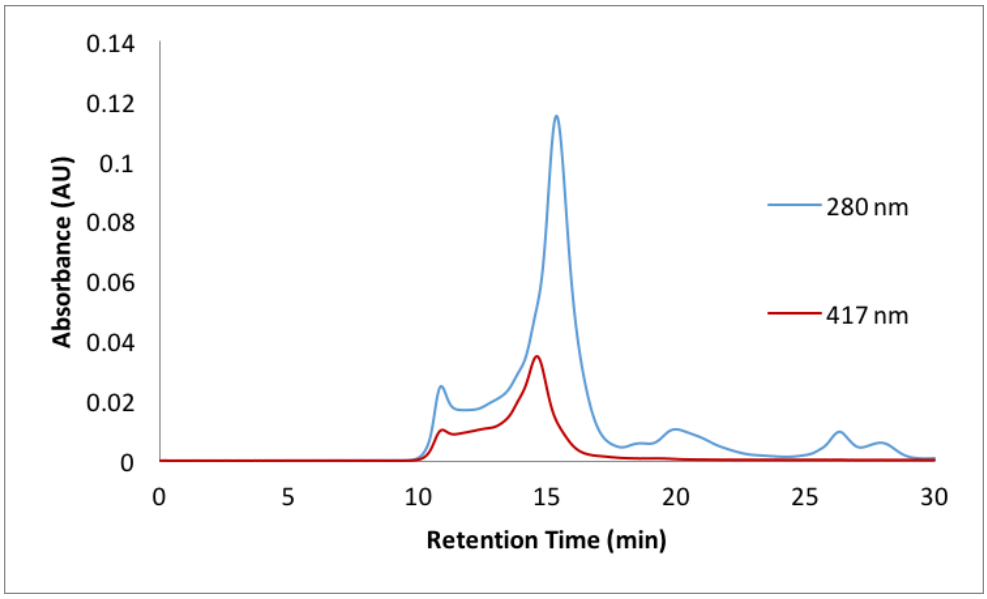

Figure 5.9: Size exclusion chromatogram showing the purification of Nanodiscs with CYP3A4 incorporated in them immediately after going through the microfluidic device. The chromatogram shows monitoring at 417 nm and at 280 nm. The trace at 417 shows that Nanodisc-incorporated CYP3A4 comes out at the beginning of the characteristic Nanodisc peak, indicating that CYP3A4 is embedded in the Nanodiscs and "filled" Nanodiscs show a slightly larger hydrodynamic radius than "empty" Nanodiscs.

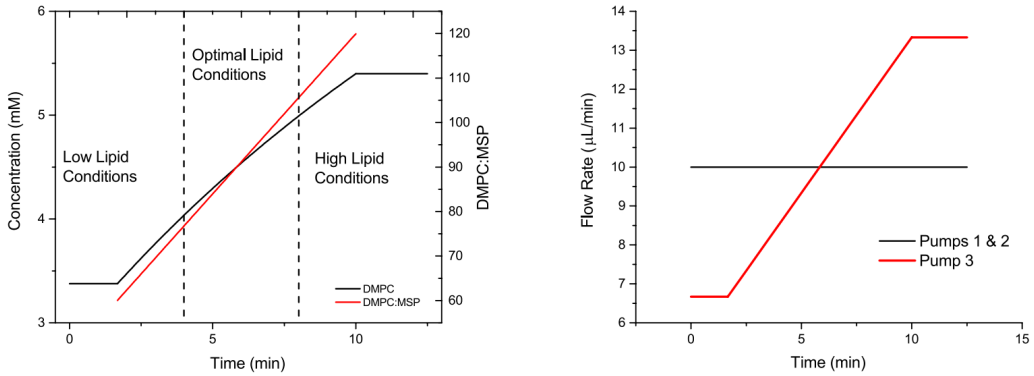

Figure 5.10: Two graphs showing how the lipid gradient works. The first chart shows the concentration of lipid as it changes and how the ratio of lipid to MSP changes over time. The second chart shows the flow rate of all three pumps over time.

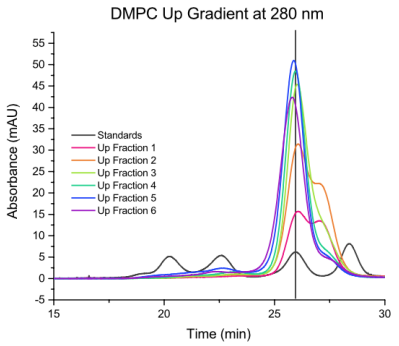

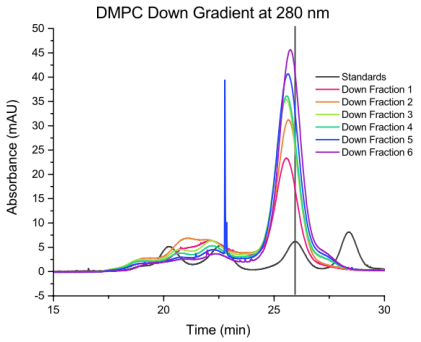

DMPC Up Gradient		
Time	Flow Rate (µL/min)	Lipid:MSP
00:00:00	6.67	60
00:01:40	6.67	60
00:10:00	13.33	120
00:12:30	13.33	120

DMPC Down Gradient		
Time	Flow Rate (µL/min)	Lipid:MSP
00:00:00	13.33	120
00:01:40	13.33	120
00:10:00	6.67	60
00:12:30	6.67	60

Figure 5.11: Chromatogram traces showing the analysis of DMPC Nanodiscs formed using the programmed gradient. On the left, the gradient starts at a low lipid ratio and increases. On the right, the gradient starts at a high lipid ratio and decreases.

CHAPTER 6

DEVELOPMENT OF A NANODISC DELIVERY PLATFORM FOR MRI-OPTICAL IMAGING

6.1 Introduction

Noninvasive imaging of cells *in vivo* is crucial for different clinical applications, including cancer detection[147], cell tracking[148], and detecting disease markers[149]. Methods for noninvasive imaging include ultrasound, computed tomography (CT), positron emission tomography (PET), and magnetic resonance imaging (MRI). Of these methods, MRI is the best suited for studies over long periods of time as it does not use ionizing radiation or radioactive tracers and provides high resolution images.[150, 151] MRI contrast agents are often employed for an enhanced signal, with Gd(III) complexes being the most common in clinical settings.[152] These agents provide a positive image contrast by decreasing the proton spin-lattice relaxation time (T1) of water protons.[153] However, these Gd(III) complexes usually provide low sensitivity which necessitates the use of higher concentrations. Higher concentrations can lead to complications when used *in vivo* due to toxicity, with cases of anaphylactoid reactions reported.[154]

A series of lipohilic Gd(III) contrast agents were synthesized by Thomas Meade and coworkers[155] for the enhanced labeling of cells. The compounds are composed of one or three Gd(III) chelates, attached to a set of lipophilic alkyl chains, similar to those present in the tails of lipid molecules. These contrast agents displayed a significant improvement in MRI contrast as well as a significant increase in retention by two different cell lines over the commercially available compounds. Furthermore, the compounds displayed relatively

Reproduced in part with permission from Carney, C.E.; Lenov, I.L.; Baker, C.J.; MacRenaris, K.W.; Eckermann, A.L.; Sligar, S.G.; and Meade T.J. Nanodiscs as a Modular Platform for Multimodal MR-Optical Imaging *Bioconjugate Chemistry* **2015** *26* (5), 899-905 Copyright 2015 American Chemical Society. The published version may be found online at http://pubs.acs.org/doi/abs/10.1021/acs.bioconjchem.5b00107. This chapter includes significant contributions, including data and figures, from Christiane Carney.

low toxicities *in vitro*. However, while the increase in contrast was appreciable, the delivery system consisted of solubilizing the agents in a detergent and incubating cells with the solution, which means that it wasn't easily amenable to the attachment of any peripheral fluorophores or targeting groups. Furthermore, a higher degree of control over size and stability of the delivery agent is required for the implementation *in vivo*.

Incorporation of Gd(III) into nanoparaticles has been utilized as a means to improve the sensitivity and imaging contrast. Nanoparticles offer several advantageous characteristics including high loading capacity per particle, modular syntehsis for the application of multimodal and targeting moieties, and enhancements in efficacy of the contrast agents.[156] Several metal-based nanoparticles have been used as MR contrast agents; however, these metallic nanoparticles have been implicated in toxicity due to the generation of reactive oxygen species generation and releasing of toxic ions.[157, 151] In contrast, antigenically neutral nanoparticles have been explored as MRI contrast agents, including liposomoes and high-density lipoprotein (HDL) particles.[70, 71] These nanoparticles offer similar advantages as their metal-based counterparts, without the additional toxic side effects. These nanoparticles have been successfully used for cell labeling and tumor imaging *in vivo*. [158, 159] Additionally, polymeric delivery agents have been explored as biocompatible alternatives, offering a more modular design.[160, 161] Even though these particles are capable of serving as therapeutic delivery agents, they still lack the stoichiometric control as well as the uniformity present in Nanodiscs.

This chapter details the development of a Nanodisc delivery agent for MRI contrast agents using Gd(III) complex molecules. Nanodiscs display a greater stability, higher monodispersity, and much greater stoichiometric control compared to liposomes or detergent-based systems. They have been used in applications varying from the solublization of membrane proteins for structural studies[36, 40, 162] to the delivery of therapeutic phospholipids for the inhibition of respiratory syncytial virus (RSV) *in vivo*.[45] Nanodiscs have additionally been coupled to analytical systems, accounting for a very thorough biophysical characterization.[33, 162] The modularity of Nanodiscs allows for not only the loading of a variety of lipids and lipophilic molecules but also the attachment of fluorophores and targeting groups to the MSP. The incorporation of the Gd(III) chelate

contrast agents into TMR-labeled Nanodiscs was optimized to generate water-soluble nanoparticles that label cells with high efficiency and produce a significant contrast enhancement. The labeling of cells with the contrast agents was examined and quantitated at high and low fields, while the stability and proliferation of the cells was also monitored.

6.2 Methods

6.2.1 Materials

The lipids 1,2- dimyristoyl-*sn*-glycero-3- phosphocholine (DMPC) were purchased from Avanti Polar Lipids (Alabaster, AL, USA). The cysteine mutant, MSP1D1_D73C was expressed and purified as described previously.[30, 31] Tetramethylrhodamine-5-(and -6) C2 maleimide (TMR) was purchased from Anaspec, Inc (Fremont, CA, USA). Multimeric and monomeric Gd(III) chelating contrast agents were synthesized and graciously provided by Christiane Carney. (Figure 6.1) Tris(2-carboxyethyl)phosphine hydrochloride (TCEP) and Pierce 660 nm Protein Assay Reagent were purchased from ThermoFisher Scientific (Waltham, MA, USA). Ethylenediaminetetraacetic acid (EDTA), sodium cholate, dimethyl sulfoxide (DMSO), chloroform, Amberlite XAD-2 hydrophobic beads, and all other chemicals were purchased from Sigma Aldrich (St. Louis, MO, USA). Buffers were prepared with 18 MΩ deionized water and filtered prior to use.

6.2.2 Labeling MSP with TMR

MSP labeling was carried out in tris buffered saline (TBS) buffer (50 mM Tris/HCl pH 7.4, 0.3 M NaCl). MSP1D1_D73C was reconstituted to a concentration of 100 μM in TBS. Sodium cholate was added with a final concentration of 10 μM. TMR was dissolved in anhydrous DMSO. MSP1D1_D73C was reduced with 4 molar equivalents of TCEP and incubated at room temperature for 15 minutes. TMR dissolved in DMSO was added to the reduced MSP1D1_D73C so that the final molar ratio would be 10:1 of TMR:MSP. The mixture was incubated at room temperature for 4 hours and then overnight at 4 °C. The

following day, one volume equivalent of XAD-2 hydrophobic beads was added to the solution and shaken at room temperature for 4 hours. Excess dye was completely removed on a G-25 column. Concentration of MSP1_D73C labeled with TMR can be measured spectrophotometrically by using 280 nm total protein absorption and using a 0.3 correction factor to account for the absorption of the TMR dye.

6.2.3 Incorporation of Gd(III) chelate into Nanodiscs

Gd(III) chelate was dissolved in chloroform at a concentration of 10 mM. The general self-assembly procedure of Nanodiscs with incorporated Gd(III) chelates is as described previously.[30] Briefly, desired ratios of lipids and Gd(III) chelate were measured out into a glass tube, mixed together, and dried under N_2. The mixture of lipids and contrast agents was further dried in a vacuum desiccator overnight. The mixture was reconstituted with 0.1 M sodium cholate so that the final concentration of sodium cholate would be twice that of the total lipid/chelate concentration. Labeled MSP1D1_D73C was added to the mixture in a ratio of 90:1 lipid:protein. The mixture was incubated at 25 °C for 20 minutes before adding XAD-2 hydrophobic beads for the removal of detergent. The reconstitution mixture was incubated at 25 °C overnight. The hydrophobic beads were removed using a disposable column and samples were purified via a Superdex 200 Increase column (1.6 x 30 cm). Total Nanodisc concentration was measured using a Pierce 660 nm Protein Assay.

6.2.4 Cell Labeling

Either 25,000 HeLa cells or 30,000 MCF7 cells were seeded in a 24-well plate for labeling experiments. Cells were incubated with multimeric or monomeric Nanodiscs in media at concentrations of 01 μM (Nanodisc concentration) for 24 h (180 μL dose). Cells were washed with 2 x 500 μL PBS, detached with trypsin, and centrifuged at 1000g for 5 min at 4 °C. The media was aspirated and the cells were re-suspended in 200 μL media. An aliquot of 50 μL was used for cell counting and 130 μL was used for analysis of Gd(III) content by ICP-MS.

6.2.5 Relaxivity Measurements

For 1.41 T relaxivity measurements, solutions of ND1 and ND2 were prepared in 20 mM Tris buffer (pH 7.4). T1 and T2 were determined on a Bruker mq60 minispec NMR spectrometer at 1.41 T (60 MHz) and 37 °C using an inversion recovery pulse sequence with 4 averages, 15 s repetition time, and 10 data points (Bruker Canada; Milton, Ontario, Canada). For 7 T relaxivity measurements, MR imaging and T1 measurements were performed using a Bruker Pharmscan 7 T imaging spectrometer according to previously described methods.[155] Briefly, a rapid-acquisition rapid-echo (RARE-VTR) T1-map pulse sequence, with static TE (11 ms), variable TR (150, 250, 500, 750, 1000, 2000, 4000, 6000, 8000, and 10000 ms) values, field of view (FOV) = 25 x 25 mm^2, matrix size (MTX) = 256 x 256, number of axial slices = 4, slice thickness (SI) = 1.0 mm, and averages (NEX) = 3 was used. Relaxivity at 7 T was determined using serially diluted solutions of multimeric and monomeric Nanodiscs.

6.3 Results and Discussion

6.3.1 Labeling MSP with TMR and Optimization of Loading

The labeling of MSP with TMR was accomplished through using maleimide-cysteine reaction chemistry, as outlined above. Complexes 1 and 2 were incorporated into TMR-tagged Nanodiscs according to Figure 6.2. Specifically, MSP was labeled with TMR at Cys73. The tagged MSP was combined with a cholate-solubilized solution of DMPC phospholipids and either complex 1 or 2 at molar ratios of 1:(90-X):180:X (MSP:lipid:cholate:amount of 1 or 2). The cholate was removed with XAD-2 hydrophobic beads and the resulting Nanodiscs were purified on an SEC column calibrated using a standard mixture of four proteins - Bovine Serum Albumin (BSA), Bovine Liver Catalase, Ferritin, and Thyroglobulin - with hydrodynamic radii in the range of interest. Based on the calibration, the retention time for Nanodiscs with a diameter of 10 nm is between bovine liver catalase and BSA.

The maximum loading of complexes 1 and 2 into Nanodiscs was determined by assembling particles with varied molar ratios of 1 and 2. For both constructs, a maximum of 30% contrast agent loading relative to total lipid content (i.e., phospholipids + 1 or 2) was achieved. Consequently, the loading percentages correspond to 137 ± 14 Gd(III) ions per Nanodisc for multimeric Nanodiscs and 48 ± 8 for monomeric Nanodiscs. These values represent an increase in Gd(III) loading on lipid-based particles with similarly sized HDL particles achieving only 22 Gd(III)/particle.[163] T1 relaxivity was determined at low (1.41 T) and high (7 T) magnetic field strengths. Both multimeric Nanodiscs and monomeric Nanodiscs have relaxivities of 17 mM^{-1} s^{-1} at 1.41 T (37 °C), which is comparable to other lipid-based particles that typically report a relaxivity of 10-30 mM^{-1} s^{-1}.[164] Relaxivities at 7 T (25 °C) are 3.1 mM^{-1} s^{-1} ± 0.1 for multimeric Nanodiscs and 4.2 mM^{-1} s^{-1} ± 0.2 for monomeric Nanodiscs. Additionally, the stability and shelf life Nanodiscs was explored. Nanodiscs were determined to be stable for at least 2 weeks in buffer and at least 1 week in cell media at a temperature of 4 °C.

6.3.2 Labeling of Cells using Gd(III) Nanodiscs

The ability of both varieties of Nanodiscs to label cells was investigated with HeLa and MCF7 cells. All experiments were performed with a 24 h incubation time at concentrations that maintained ≥90% cell viability. Confocal laser scanning microscopy was used to determine cellular localization of TMR-tagged MSP. Microscopy images showed intracellular accumulation of the Nanodiscs (Figure 6.3). The localization of contrast agent-doped Nanodiscs was compared to that of Nanodisc controls without Gd(III) contrast agent. From these images, it does not appear that incorporation of complexes 1 and 2 into Nanodiscs significantly affects intracellular accumulation. As complexes 1 and 2 are not covalently attached to the TMR-tagged MSP, the localization of these contrast agents was determined using cell fractionation. Briefly, the membrane and cytosol of the cells were separated and analyzed for Gd(III) content by ICP-MS. These data show that both multimeric and monomeric Nanodiscs show approximately 7-fold greater accumulation in the membrane compared to the cytosol. (Figure 6.4) This suggests that

the lipids and the contrast agents in the Nanodiscs can freely exchange with the lipids present in the cell membrane.

The enhanced cellular retention of multimeric Nanodiscs in both cell lines (Figure 6.5) suggests that these Nanodiscs may be used for cell tracking applications where it is critical that contrast agents remain associated with cells for longer periods of time. Examples of such applications include fate-mapping transplanted stem cells and monitoring developmental events. The lower retention of monomeric Nanodiscs indicates that these Nanodiscs are better suited for applications where clearance of the contrast agent is desired such as detection of cancer and disease markers. Therefore, the Nanodiscs can be tailored to specific imaging applications by altering the lipophilic contrast agent incorporated into the particles. This attribute further shows the modularity of the Nanodiscs and provides opportunities for further research. Additionally, Nanodiscs are not limited by type of phospholipid used, allowing for a rational design approach, using lipids with shorter or longer tails, based on the imaging application desired.

6.3.3 Magnetic Resonance Imaging

To investigate the ability of Nanodiscs to enhance T1-weighted contrast of cell populations, MR images of HeLa cell pellets were acquired at 7 T (Figure 6.7). Cells were labeled with Nanodiscs containing no agent (0.6 μM), multimeric Nanodiscs (0.2 M, 30 μM Gd(III)), monomeric Nanodiscs (0.6 μM, 30 μM Gd(III)), and clinically approved ProHance (30 μM). The most significant contrast enhancement was observed in cells treated with monomeric Nanodiscs showing a 66% reduction of T1 compared to untreated cells. Cells labeled with the multimeric Nanodiscs showed a 25% reduction. As expected, no significant contrast enhancement was observed with cells treated with Nanodiscs containing no agent or ProHance. These results are consistent with the cell labeling trends observed in Figure 6.6. Overall, these results show that monomeric Nanodiscs are a viable and promising option for labeling cells for use in cell imaging.

6.4 Conclusions

Multimeric and monomeric lipophilic MR contrast agents were incorporated into TMR-tagged Nanodiscs to generate bimodal agents for cellular imaging. Multimeric Nanodsics achieved 3-fold higher Gd(III)/Nanodisc loading than those containing monomeric agents. Despite the higher concentration of Gd(III)/Nanodisc, multimeric Nanodiscs did not label cells as effectively as monomeric Nanodiscs. Cellular retention studies showed that 50% or greater of the initial multimeric agent remained associated with cells for 72 h, whereas the monomeric agent leached from cells at a much faster rate. This indicates that multimeric Nanodiscs may be useful for long-term cell tracking studies while monomeric Nanodiscs are more appropriate for applications that require the rapid clearance of the contrast agent from cells. These results suggest that the Nanodisc system can be tailored for the specific needs of the study or application. Additionally, this work showed that monomeric Nanodiscs produced significant contrast enhancement of cell populations at 7 T suggesting that these Nanodiscs may be useful for *in vivo* applications.

Using Nanodiscs as therapeutic delivery agents is a concept that is just beginning to be explored. Previous work using Nanodiscs as delivery agents focused on using therapeutic lipids.[45] This work shows that Nanodiscs can be used as delivery agents for imaging applications as well, utilizing a bimodal imaging platform of both MRI and optical fluorescence. This work illustrates that Nanodiscs are capable of delivering lipophilic compounds into cell membranes more efficiently than detergent-based systems. Nanodiscs have the additional advantages over current delivery systems employing liposomes of stoichiometric control and longer shelf life. The Nanodisc delivery agents can further be tailored by varying the type of lipids being used or employing different labels on the MSP, whether they are fluorophores or a targeting moieties. These advantages open up the field of therapeutic and imaging delivery agents with a vast set of possibilities to be explored.

6.5 Figures and Tables

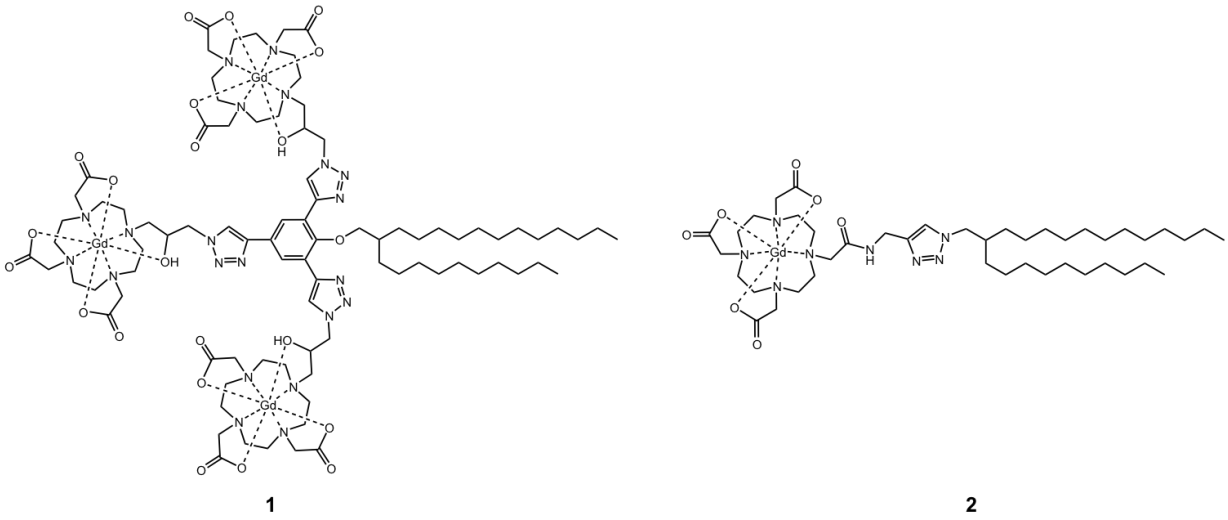

Figure 6.1: Structures of lipophilic contrast agents for incorporation into nanodiscs. Complex 1 is multimeric and contains three Gd(III) chelates, while 2 is monomeric and contains a single Gd(III) chelate.

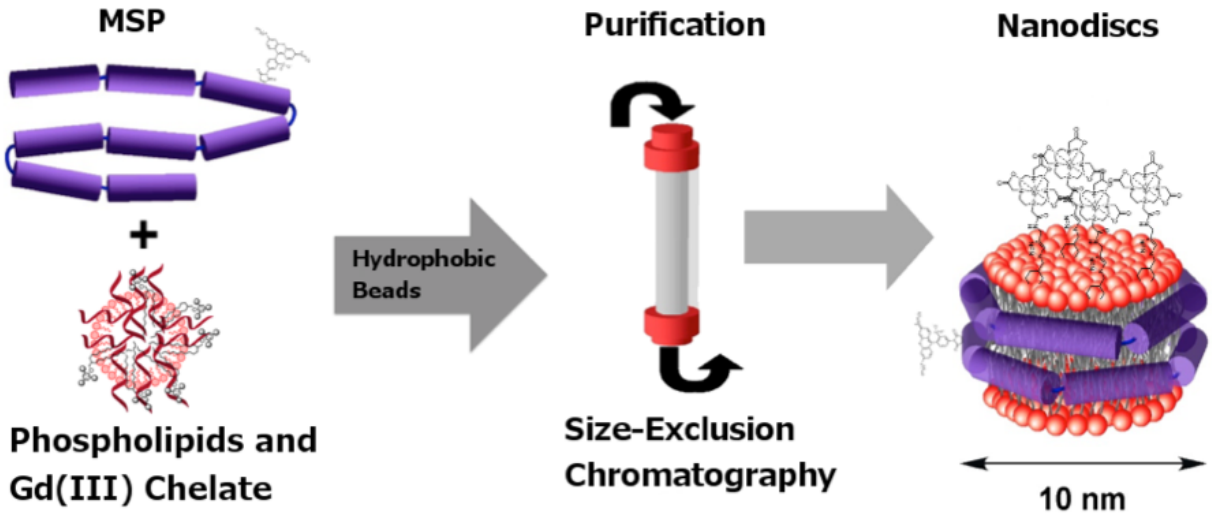

Figure 6.2: A diagram showing the basic procedure of assembling and purifying Nanodiscs with the Gd(III) chelate.

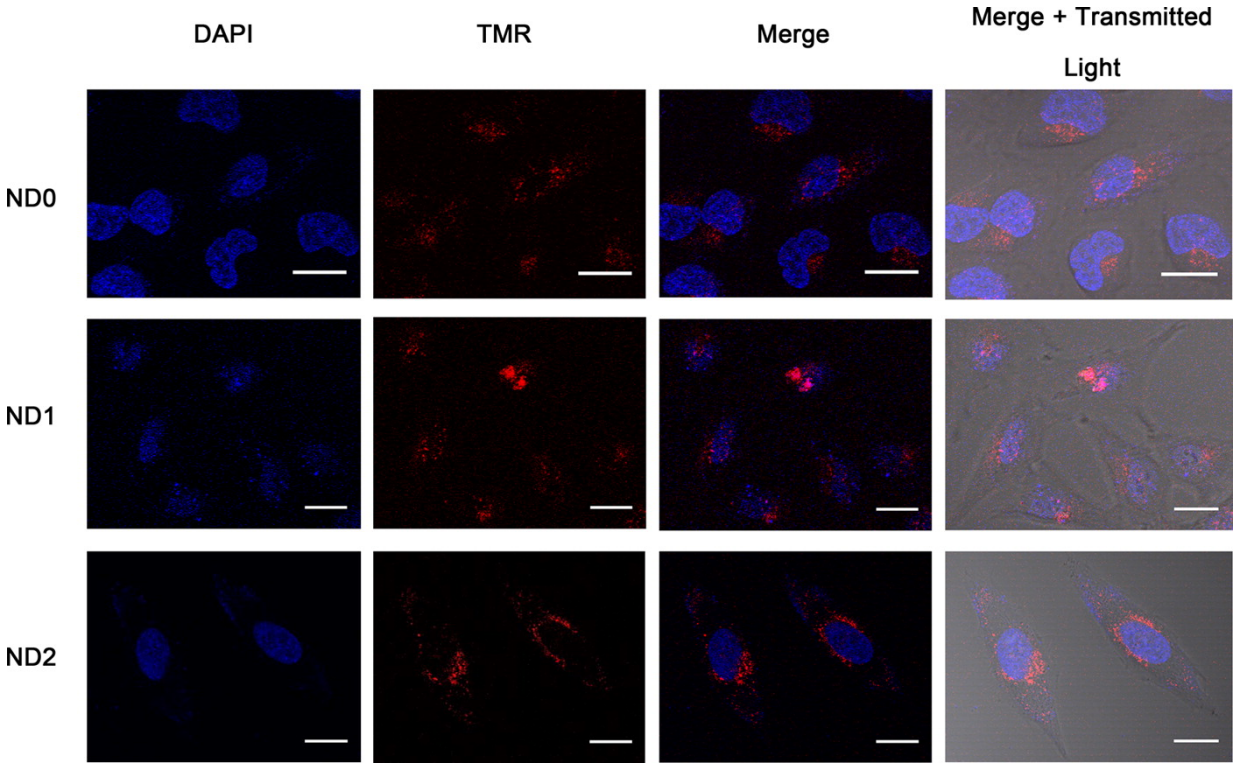

Figure 6.3: Confocal micrographs of HeLa cells incubated with 1 μM of empty, multimeric, and monomeric Nanodiscs show intracellular accumulation. Blue = DAPI, Red = TMR. Scale bar = 20 μm.

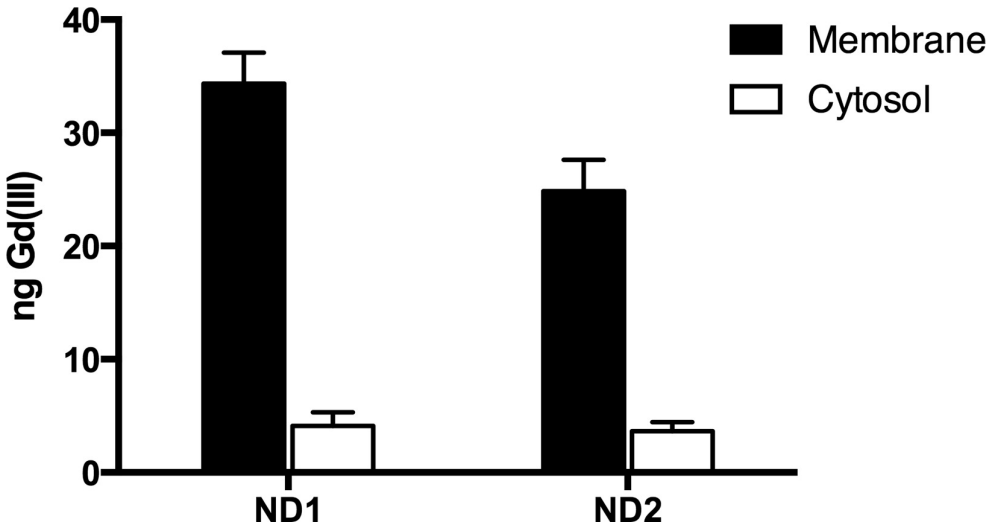

Figure 6.4: Fractionation data showing that contrast agent accumulated more in the cell membrane as opposed to the cytosolic fraction. This data suggests that an exchange between lipids and contrast agents happens between Nanodiscs and cell membrane

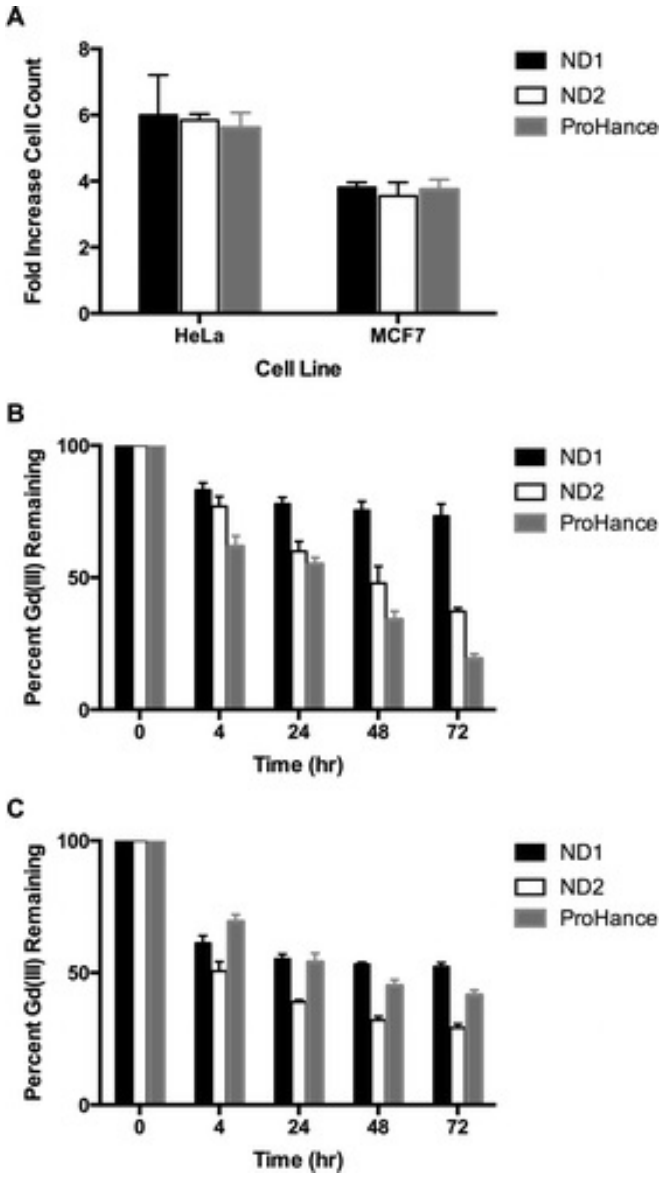

Figure 6.5: Cellular proliferation and retention of HeLa and MCF7 cells treated with concentrations of multimeric (45 μM Gd(III)), monomeric (25 μM Gd(III)), and ProHance (2 mM) chosen to equalize cell labeling. (A) Cellular proliferation was measured as the fold increase in cell number between time = 0 and 72 h. No significant change in proliferation was observed. (B) Cellular retention in HeLa cells was determined by measuring the Gd(III) content in the media at 4, 24, 48, and 72 h after labeling. Multimeric Nanodiscs show the greatest retention in HeLa cells. (C) Cellular retention was also determined in MCF7 cells. Similar retention was observed for multimeric Nanodiscs and ProHance while monomeric Nanodiscs were retained least effectively by cells. Error bars represent the standard deviation of triplicate experiments.

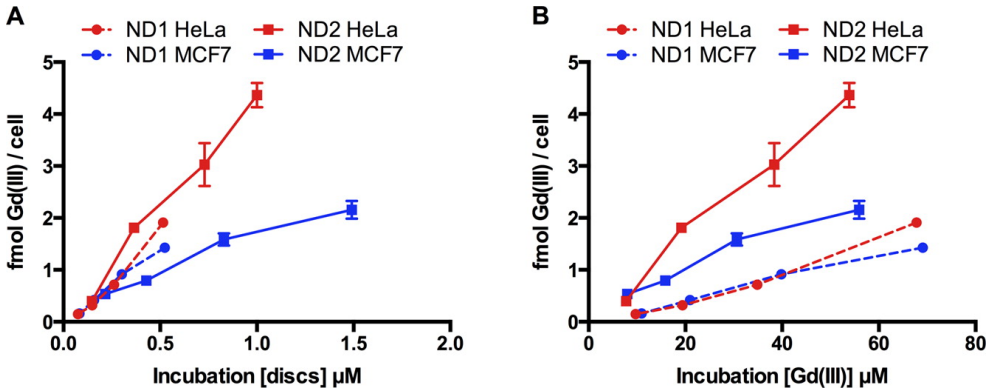

Figure 6.6: Cell uptake of multimeric and monomeric Nanodiscs was determined in HeLa (red) and MCF7 (blue) cells at varied incubation concentrations. (A) Uptake at variable Nanodisc incubation concentrations shows the same labeling for multimeric and monomeric Nanodiscs. (B) Uptake at variable Gd(III) incubation concentrations shows that monomeric Nanodiscs attains higher cell labeling. Error bars represent the standard deviation of triplicate experiments.

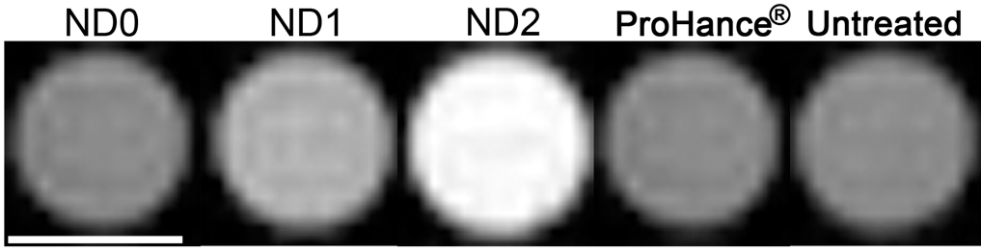

	ND0	ND1	ND2	Prohance	Control
Fmol Gd(III) per cell	0.01	1.7	4.1	0.09	0.01
T_1 (ms)	2201 ± 150	1660 ± 138	749 ± 74	2202 ± 102	2215 ± 163

Figure 6.7: T1-weighted cell pellet images of HeLa cells incubated with empty Nanodiscs, multimeric Nanodiscs, monomeric Nanodiscs, and Prohance acquired at 7 T. TE = 11 ms, TR = 500 ms, MTX = 256 x 256, and slice thickness is 1.0 mm. Scale bar represents 1 mm. Error bars represent standard deviation of the mean of 4 slices. These images show that at incubation concentrations of 30 μM Gd(III), monomeric Nanodiscs produce the greatest image contrast.

CHAPTER 7

CONCLUSIONS AND FUTURE WORKS

This work examines and describes the benefits and applications of using Nanodiscs in the study of membrane interactions. Events involving the membrane, and specifically membrane proteins, play a central role in biochemistry and pharmacology, therefore a deeper understanding of the mechanisms behind these events is crucial for the advancements of these fields. Previous efforts in the study of membrane proteins have encountered challenges when it comes to considering all the variables of solibilizing membrane proteins. Nanodiscs, however, have provided a monodisperse platform for the solubilization of membrane proteins that offers a native lipid bilayer, unparalleled stoichiometric control, and is extremely modular with the ability to be tailored to specific needs. Details have been provided throughout the previous chapters that describe the development of analytical systems employing Nanodiscs as well as the development of systems that can be further combined with Nanodiscs for the biophysical characterization of membrane-specific events.

The development and use of a linear dichroism instrument in order to calculate the orientation of heme-containing CYP's incorporated in Nanodiscs was described in Chapter 2. The work takes advantage of the ability of Nanodiscs to lay flat on silicon surfaces, as has been shown in previous studies.[30] Nanodiscs further allow for the incorporation of membrane proteins in a native-like lipid bilayer environment, preserving the activity and natural conformation of the protein. Combining Nanodiscs with LD spectroscopy allowed for the determination of the orientation of three different CYP enzymes within a POPC lipid bilayer. The experimental work was complemented by MD simulations that showed the structure and orientation in detail.

While the orientation of the enzymes within the lipid bilayer is an important step into

further understanding the mechanism of substrate recruitment, there are other biologically relevant factors that should also be considered. Lipid composition is usually a variable that is simplified in structural studies, often employing the use of only one lipid, while cellular membranes are often complicated and are composed of multiple lipid species.[165] Because of the specific interactions between the globular domain of the protein and the lipid head groups, an exploration into the effect of differently charged lipid species on the orientation of these enzymes would lead to a better understanding of the topology of the protein. Nanodiscs are especially amenable to such studies because of the ease of control over lipid composition. Additionally, CYP17 has been known to go through conformational and activity changes due to interactions with Cytochrome b_5.[166, 167] These studies would imply that CYP's can experience a change in orientation based on their interactions with redox partners. Studies of multiple-protein systems are warranted and feasible using the Nanodisc platform.

Nanodiscs can further be used in biophysical characterization of molecular recognition events as probed hydrostatic pressure in a system similar to that described in Chapter 3. In that chapter, a method to study the refractive index change based on increasing hydrostatic pressure was developed. The instrument was validated and calibrated using solutions of known refractive indices at atmospheric pressure prior to observing changes under pressure. The system is well suited for probing biomolecular interactions under pressure primarily because the BIND Assay chips are used and specialized optics or geometries are not required, unlike SPR.[108] The system can be further utilized in the study of molecular recognition events. Hydrostatic pressure has been previously used to study protein-protein and protein-nucleic acid interactions.[110, 168, 169] Using the current instrument and method, it is possible to employ Nanodiscs in the study of protein-lipid interactions. Tavoosi and coworkers showed that Factor VII gets activated through the GLA domain in a Ca^{2+} dependent fashion.[170] Using this method, it would be possible to elucidate the mechanism behind this activation and its dependence on Ca^{2+}. In order to further explore the lipid-membrane interactions present in the blood coagulation cascade in a high-throughput fashion a lipid assay with individually addressable sensors was designed. Chapter 4 describes the development of methods for creating robust, multiplexed arrays of

Nanodiscs on the basis of DNA-encoding. Nanodiscs were chemically labeled with ssDNA by utilizing the single cysteine mutant scaffold protein, MSP1D1_D73. The resulting Nanodisc arrays were thoroughly characterized and shown to exhibit specific binding through DNA base pair recognition. Furthermore, the utility of these arrays was demonstrated by monitoring the binding of annexin to POPS phospholipids. To further expand the utility and application of this assay, it will be applied to the study of protein-protein and protein-membrane interactions in the blood coagulation cascade. Factor VII is known to be activated by both anionic phospholipids as well as the enzyme cofactor Tissue Factor. However, details behind the activation mechanism are not known and they need to be unraveled. Using the combination of Nanodiscs with photonic microring resonators, it is indeed possible to easily create a highly multiplex-able assay with multiple lipid compositions and multiple Tissue Factor concentrations on the same sensor chip. Going beyond the study of the mechanism behind blood coagulation, this platform presents a powerful approach for highly multiplexed studies of biomolecular interactions occurring at the membrane surface.

To further increase the speed and reduce sample requirements of biomolecular assays involving Nanodiscs, a modular platform for the handling of small volumes has been developed. Chapter 5 describes the implementation and optimization of a microfluidic device for the assembly of Nanodiscs. This device is capable of assembling Nanodiscs in a matter of minutes, while using microliter volumes of reagents. The initial validation and proof of the device was established by assembling "empty" Nanodiscs, which did not have a target membrane protein incorporated. The work then focused on incorporating CYP3A4 in order to show that the device could be used to optimize volumes and ratios of lipids, target protein, and scaffold protein, as well as showing that detergent screens were possible on the device. The microfluidic platform employed a gradient of lipid:MSP:target ratios for the optimization of starting materials, utilizing small volumes of protein. Further development of this platform will explore incorporating membrane protein targets which have yet to be inserted into Nanodiscs. Furthermore, the microfluidic device is modular and this advantage can be leveraged to include multiple steps of purification, including affinity and size purification. This method has the potential not only to decrease the cost

of optimizing target protein incorporation, but also presents an opportunity for the development of therapeutic and diagnostic Nanodiscs.

Nanodiscs have previously been used to deliver therapeutic phospholipids to treat RSV. Within this work, Nanodiscs were used to deliver imaging agents and provide a means for cell tracking, as described in Chapter 6. Nanodiscs were labeled with a fluorophore, using maleimide-cysteine chemistry on the cysteine mutant of the scaffold protein, and an MRI contrast agent was incorporated into the bilayer. This construct, when used for the incubation of cells, produced a contrast higher than clinically available agents and was validated in two different cell lines. Since the construct did not include any targeting moieties, a step forward would be to use a targeting molecule in order to selectively label cells. Nanodiscs present a very modular platform, having the ability to use single point mutations within the membrane protein to introduce reactive residues for the chemical attachment of molecules of interest. Taking advantage of this idea, it is possible to introduce a targeting label, such as cyclo(RGD) in order to target over-expressed integrins on certain cancer cell lines. This would provide a platform for the enhanced labeling of cancer cells, as well as the potential for the selective delivery of therapeutic compounds. Furthermore, efforts have gone into combining delivery agents with microfluidic approaches[171], a concept which can be implemented with Nanodisc microfluidic approaches.

Nanodiscs are emerging as a key tool in biochemical and biophysical research studies. The possess critical advantages over similar solubilization systems and present the potential to be integrated with multiple analytical systems, including spectroscopic methods, biosensors, and even mass spectrometry. Furthermore, Nanodiscs are just beginning to be utilized as therapeutic and imaging compound delivery agents - an area which has a lot of room for expansion and research. Additionally, the development of Nanodisc-solubilized membrane protein libraries has recently been accomplished[172, 173] and has opened the door to new and innovative techniques within biochemical and pharmaceutical research. The innovations and applications of Nanodiscs present the opportunity for great expansion within the bio-analytical field of research.

REFERENCES

[1] Antonina Andreeva, Dave Howorth, Cyrus Chothia, Eugene Kulesha, and Alexey G. Murzin, "SCOP2 prototype: a new approach to protein structure mining", *Nucleic Acids Research*, vol. 42, no. D1, pp. D310–D314, jan 2014.

[2] Anders Krogh, Björn Larsson, Gunnar von Heijne, and Erik L.L Sonnhammer, "Predicting transmembrane protein topology with a hidden markov model: application to complete genomes11Edited by F. Cohen", *Journal of Molecular Biology*, vol. 305, no. 3, pp. 567–580, jan 2001.

[3] John P Overington, Bissan Al-Lazikani, and Andrew L Hopkins, "How many drug targets are there?", *Nature Reviews Drug Discovery*, vol. 5, no. 12, pp. 993–996, dec 2006.

[4] Markus Almén, Karl JV Nordström, Robert Fredriksson, and Helgi B. Schiöth, "Mapping the human membrane proteome: a majority of the human membrane proteins can be classified according to function and evolutionary origin", *BMC Biology*, vol. 7, no. 1, pp. 50, 2009.

[5] Gunnar von Heijne, "Membrane-protein topology", *Nature Reviews Molecular Cell Biology*, vol. 7, no. 12, pp. 909–918, dec 2006.

[6] Florent Bernaudat, Annie Frelet-Barrand, Nathalie Pochon, Sébastien Dementin, Patrick Hivin, Sylvain Boutigny, Jean-Baptiste Rioux, Daniel Salvi, Daphné Seigneurin-Berny, Pierre Richaud, Jacques Joyard, David Pignol, Monique Sabaty, Thierry Desnos, Eva Pebay-Peyroula, Elisabeth Darrouzet, Thierry Vernet, and Norbert Rolland, "Heterologous Expression of Membrane Proteins: Choosing the Appropriate Host", *PLoS ONE*, vol. 6, no. 12, pp. e29191, dec 2011.

[7] G. von Heijne, "The membrane protein universe: what's out there and why bother?", *Journal of Internal Medicine*, vol. 261, no. 6, pp. 543–557, jun 2007.

[8] Jean-Jacques Lacapère, Eva Pebay-Peyroula, Jean-Michel Neumann, and Catherine Etchebest, "Determining membrane protein structures: still a challenge!", *Trends in Biochemical Sciences*, vol. 32, no. 6, pp. 259–270, jun 2007.

[9] David Drew, Linda Fröderberg, Louise Baars, and Jan-Willem L de Gier, "Assembly and overexpression of membrane proteins in Escherichia coli", *Biochimica et Biophysica Acta (BBA) - Biomembranes*, vol. 1610, no. 1, pp. 3–10, feb 2003.

[10] Aditi Das and Stephen G. Sligar, "Modulation of the Cytochrome P450 Reductase Redox Potential by the Phospholipid Bilayer", *Biochemistry*, vol. 48, no. 51, pp. 12104–12112, dec 2009.

[11] Anthony G. Lee, "How lipids affect the activities of integral membrane proteins", *Biochimica et Biophysica Acta (BBA) - Biomembranes*, vol. 1666, no. 1-2, pp. 62–87, nov 2004.

[12] Hildur Palsdottir and Carola Hunte, "Lipids in membrane protein structures", *Biochimica et Biophysica Acta (BBA) - Biomembranes*, vol. 1666, no. 1-2, pp. 2–18, nov 2004.

[13] Keon-Hee Kim, Taeho Ahn, and Chul-Ho Yun, "Membrane Properties Induced by Anionic Phospholipids and Phosphatidylethanolamine Are Critical for the Membrane Binding and Catalytic Activity of Human Cytochrome P450 3A4 ", *Biochemistry*, vol. 42, no. 51, pp. 15377–15387, dec 2003.

[14] A.G Lee, "Lipidprotein interactions in biological membranes: a structural perspective", *Biochimica et Biophysica Acta (BBA) - Biomembranes*, vol. 1612, no. 1, pp. 1–40, may 2003.

[15] R. Michael Garavito and Shelagh Ferguson-Miller, "Detergents as Tools in Membrane Biochemistry", *Journal of Biological Chemistry*, vol. 276, no. 35, pp. 32403–32406, aug 2001.

[16] Marc le Maire, Philippe Champeil, and Jesper V Møller, "Interaction of membrane proteins and lipids with solubilizing detergents", *Biochimica et Biophysica Acta (BBA) - Biomembranes*, vol. 1508, no. 1-2, pp. 86–111, nov 2000.

[17] Annela M. Seddon, Paul Curnow, and Paula J. Booth, "Membrane proteins, lipids and detergents: not just a soap opera", *Biochimica et Biophysica Acta (BBA) - Biomembranes*, vol. 1666, no. 1-2, pp. 105–117, nov 2004.

[18] Jan Knol, Klaas Sjollema, and Bert Poolman, "Detergent-Mediated Reconstitution of Membrane Proteins ", *Biochemistry*, vol. 37, no. 46, pp. 16410–16415, nov 1998.

[19] L Veenhoff, "Unidirectional Reconstitution into Detergent-destabilized Liposomes of the Purified Lactose Transport System of Streptococcus thermophilus", *Journal of Biological Chemistry*, vol. 271, no. 26, pp. 15358–15366, jun 1996.

[20] Michael Edidin, "The State of Lipid Rafts: From Model Membranes to Cells", *Annual Review of Biophysics and Biomolecular Structure*, vol. 32, no. 1, pp. 257–283, jun 2003.

[21] Reinhard Krämer, Sascha Nicklisch, and Vera Ott, "Use of Liposomes to Study Cellular Osmosensors", in *Liposomes*, Volkmar Weissig, Ed., pp. 21–30. Humana Press, Totowa, NJ, 2010.

[22] Gustav Schonfeld and Barbara Pfleger, "The Structure of Human High Density Lipoprotein and the Levels of Apolipoprotein A-I in Plasma as Determined by Radioimmunoassay", *Journal of Clinical Investigation*, vol. 54, no. 2, pp. 236–246, aug 1974.

[23] Joan B Karlin, Dawn J Juhn, J I Starr, Angelo M. Scanu, and Arthur H. Rubenstein, "Measurement of human high density lipoprotein apolipoprotein A-1 in serum by radioimmunoassay.", *Journal of lipid research*, vol. 17, no. 1, pp. 30–7, jan 1976.

[24] David Atkinson and Donald M Small, "Recombinant Lipoproteins: Implications for Structure and Assembly of Native Lipoproteins", *Annual Review of Biophysics and Biophysical Chemistry*, vol. 15, no. 1, pp. 403–456, jun 1986.

[25] Robert O Ryan, "Nanobiotechnology applications of reconstituted high density lipoprotein", *Journal of Nanobiotechnology*, vol. 8, no. 1, pp. 28, 2010.

[26] Brett A. Chromy, Erin Arroyo, Craig D. Blanchette, Graham Bench, Henry Benner, Jenny A. Cappuccio, Matthew A. Coleman, Paul T. Henderson, Angie K. Hinz, Edward A. Kuhn, Joseph B. Pesavento, Brent W. Segelke, Todd A. Sulchek, Ted Tarasow, Vicki L. Walsworth, and Paul D. Hoeprich, "Different Apolipoproteins Impact Nanolipoprotein Particle Formation", *Journal of the American Chemical Society*, vol. 129, no. 46, pp. 14348–14354, nov 2007.

[27] Timothy H Bayburt, Joseph W Carlson, and Stephen G Sligar, "Reconstitution and Imaging of a Membrane Protein in a Nanometer-Size Phospholipid Bilayer", *Journal of Structural Biology*, vol. 123, no. 1, pp. 37–44, sep 1998.

[28] T.K. Ritchie, Y.V. Grinkova, T.H. Bayburt, I.G. Denisov, J.K. Zolnerciks, W.M. Atkins, and S.G. Sligar, "Reconstitution of Membrane Proteins in Phospholipid Bilayer Nanodiscs", in *Methods in Enzymology*, vol. 464, chapter 11, pp. 211–231. Elsevier Masson SAS, 2009.

[29] Andrew W Shaw, Vincent S Pureza, Stephen G Sligar, and James H Morrissey, "The Local Phospholipid Environment Modulates the Activation of Blood Clotting", *Journal of Biological Chemistry*, vol. 282, no. 9, pp. 6556–6563, dec 2006.

[30] Timothy H. Bayburt, Yelena V. Grinkova, and Stephen G. Sligar, "Self-Assembly of Discoidal Phospholipid Bilayer Nanoparticles with Membrane Scaffold Proteins", *Nano Letters*, vol. 2, no. 8, pp. 853–856, aug 2002.

[31] I G Denisov, Y V Grinkova, A A Lazarides, and S G Sligar, "Directed Self-Assembly of Monodisperse Phospholipid Bilayer Nanodiscs with Controlled Size", *Journal of the American Chemical Society*, vol. 126, no. 11, pp. 3477–3487, mar 2004.

[32] Timothy H Bayburt and Stephen G Sligar, "Single-molecule height measurements on microsomal cytochrome P450 in nanometer-scale phospholipid bilayer disks", *Proceedings of the National Academy of Sciences*, vol. 99, no. 10, pp. 6725–6730, may 2002.

[33] Michael T. Marty, Hao Zhang, Weidong Cui, Robert E. Blankenship, Michael L. Gross, and Stephen G. Sligar, "Native Mass Spectrometry Characterization of Intact Nanodisc Lipoprotein Complexes", *Analytical Chemistry*, vol. 84, pp. 121017091907007, oct 2012.

[34] Nicholas Skar-Gislinge, Søren A. R. Kynde, Ilia G. Denisov, Xin Ye, Ivan Lenov, Stephen G. Sligar, and Lise Arleth, "Small-angle scattering determination of the shape and localization of human cytochrome P450 embedded in a phospholipid nanodisc environment", *Acta Crystallographica Section D Biological Crystallography*, vol. 71, no. 12, pp. 2412–2421, dec 2015.

[35] Timothy H Bayburt and Stephen G Sligar, "Self-assembly of single integral membrane proteins into soluble nanoscale phospholipid bilayers", *Protein Science*, vol. 12, no. 11, pp. 2476–2481, jan 2009.

[36] Natanya R. Civjan, Timothy H. Bayburt, Mary A. Schuler, and Stephen G. Sligar, "Direct solubilization of heterologously expressed membrane proteins by incorporation into nanoscale lipid bilayers.", *BioTechniques*, vol. 35, no. 3, pp. 556–60, 562–3, sep 2003.

[37] Li-zhi Mi, Michael J Grey, Noritaka Nishida, Thomas Walz, Chafen Lu, and Timothy A Springer, "Functional and Structural Stability of the Epidermal Growth Factor Receptor in Detergent Micelles and Phospholipid Nanodiscs ", *Biochemistry*, vol. 47, no. 39, pp. 10314–10323, sep 2008.

[38] Rong Yan, Xi Mo, Angel M. Paredes, Kesheng Dai, Francois Lanza, Miguel A. Cruz, and Renhao Li, "Reconstitution of the Platelet Glycoprotein Ib-IX Complex in Phospholipid Bilayer Nanodiscs", *Biochemistry*, vol. 50, no. 49, pp. 10598–10606, dec 2011.

[39] Bradley J. Baas, Ilia G. Denisov, and Stephen G. Sligar, "Homotropic cooperativity of monomeric cytochrome P450 3A4 in a nanoscale native bilayer environment", *Archives of Biochemistry and Biophysics*, vol. 430, no. 2, pp. 218–228, oct 2004.

[40] Javier L Baylon, Ivan L Lenov, Stephen G Sligar, and Emad Tajkhorshid, "Characterizing the Membrane-Bound State of Cytochrome P450 3A4: Structure, Depth of Insertion, and Orientation", *Journal of the American Chemical Society*, vol. 135, no. 23, pp. 8542–8551, jun 2013.

[41] Ilia G Denisov, Bradley J Baas, Yelena V Grinkova, and Stephen G Sligar, "Cooperativity in Cytochrome P450 3A4: LINKAGES IN SUBSTRATE BINDING, SPIN STATE, UNCOUPLING, AND PRODUCT FORMATION", *Journal of Biological Chemistry*, vol. 282, no. 10, pp. 7066–7076, dec 2006.

[42] James H Morrissey, Rebecca L Davis-Harrison, Narjes Tavoosi, Ke Ke, Vincent Pureza, John M Boettcher, Mary C Clay, Chad M Rienstra, Y Zenmei Ohkubo, Taras V Pogorelov, and Emad Tajkhorshid, "Protein-Phospholipid interactions in blood clotting", *Thrombosis Research*, vol. 125, pp. S23–S25, apr 2010.

[43] James Morrissey and Nigel Mackman, "Tissue factor and factor VIIa: Understanding the molecular mechanism", *Thrombosis Research*, vol. 122, pp. S1–S2, jan 2008.

[44] Christiane E. Carney, Ivan L. Lenov, Catherine J. Baker, Keith W. MacRenaris, Amanda L. Eckermann, Stephen G. Sligar, and Thomas J. Meade, "Nanodiscs as a Modular Platform for Multimodal MR-Optical Imaging", *Bioconjugate Chemistry*, vol. 26, no. 5, pp. 899–905, may 2015.

[45] Stephen Sligar, Numata, Yelena Grinkova, Hong Wei Chu, Voelker, and Mitchell, "Nanodiscs as a therapeutic delivery agent: inhibition of respiratory syncytial virus infection in the lung", *International Journal of Nanomedicine*, vol. 8, pp. 1417, apr 2013.

[46] Timothy H. Bayburt, Andrew J. Leitz, Guifu Xie, Daniel D. Oprian, and Stephen G. Sligar, "Transducin Activation by Nanoscale Lipid Bilayers Containing One and Two Rhodopsins", *Journal of Biological Chemistry*, vol. 282, no. 20, pp. 14875–14881, may 2007.

[47] N. Akkaladevi, L. Hinton-Chollet, H. Katayama, J. Mitchell, L. Szerszen, S. Mukherjee, E. P. Gogol, B. L. Pentelute, R. J. Collier, and M. T. Fisher, "Assembly of anthrax toxin pore: Lethal-factor complexes into lipid nanodiscs", *Protein Science*, vol. 22, no. 4, pp. 492–501, apr 2013.

[48] Jens Frauenfeld, James Gumbart, Eli O van der Sluis, Soledad Funes, Marco Gartmann, Birgitta Beatrix, Thorsten Mielke, Otto Berninghausen, Thomas Becker, Klaus Schulten, and Roland Beckmann, "Cryo-EM structure of the ribosomeSecYE complex in the membrane environment", *Nature Structural & Molecular Biology*, vol. 18, no. 5, pp. 614–621, may 2011.

[49] Feng Ye, Guiqing Hu, Dianne Taylor, Boris Ratnikov, Andrey A Bobkov, Mark A McLean, Stephen G Sligar, Kenneth A Taylor, and Mark H Ginsberg, "Recreation of the terminal events in physiological integrin activation", *The Journal of Cell Biology*, vol. 188, no. 1, pp. 157–173, jan 2010.

[50] Franz Hagn, Manuel Etzkorn, Thomas Raschle, and Gerhard Wagner, "Optimized Phospholipid Bilayer Nanodiscs Facilitate High-Resolution Structure Determination of Membrane Proteins", *Journal of the American Chemical Society*, vol. 135, no. 5, pp. 1919–1925, feb 2013.

[51] Aleksandra Kijac, Amy Y Shih, Andrew J Nieuwkoop, Klaus Schulten, Stephen G Sligar, and Chad M Rienstra, "LipidProtein Correlations in Nanoscale Phospholipid Bilayers Determined by Solid-State Nuclear Magnetic Resonance", *Biochemistry*, vol. 49, no. 43, pp. 9190–9198, nov 2010.

[52] Aleksandra Z Kijac, Ying Li, Stephen G Sligar, and Chad M Rienstra, "Magic-Angle Spinning Solid-State NMR Spectroscopy of Nanodisc-Embedded Human CYP3A4 ", *Biochemistry*, vol. 46, no. 48, pp. 13696–13703, dec 2007.

[53] Mohammad T Mazhab-Jafari, Christopher B Marshall, Peter B Stathopulos, Yoshihiro Kobashigawa, Vuk Stambolic, Lewis E Kay, Fuyuhiko Inagaki, and Mitsuhiko Ikura, "Membrane-Dependent Modulation of the mTOR Activator Rheb: NMR Observations of a GTPase Tethered to a Lipid-Bilayer Nanodisc", *Journal of the American Chemical Society*, vol. 135, no. 9, pp. 3367–3370, mar 2013.

[54] Michael T Marty, Aditi Das, and Stephen G Sligar, "Ultra-thin layer MALDI mass spectrometry of membrane proteins in nanodiscs", *Analytical and Bioanalytical Chemistry*, vol. 402, no. 2, pp. 721–729, jan 2012.

[55] Michael T Marty, Hao Zhang, Weidong Cui, Michael L Gross, and Stephen G Sligar, "Interpretation and Deconvolution of Nanodisc Native Mass Spectra", *Journal of The American Society for Mass Spectrometry*, vol. 25, no. 2, pp. 269–277, feb 2014.

[56] Christine M Hebling, Christopher R Morgan, Darrel W Stafford, James W Jorgenson, Kasper D Rand, and John R Engen, "Conformational Analysis of Membrane Proteins in Phospholipid Bilayer Nanodiscs by Hydrogen Exchange Mass Spectrometry", *Analytical Chemistry*, vol. 82, no. 13, pp. 5415–5419, jul 2010.

[57] Timothy H. Bayburt, Yelena V. Grinkova, and Stephen G. Sligar, "Assembly of single bacteriorhodopsin trimers in bilayer nanodiscs", *Archives of Biochemistry and Biophysics*, vol. 450, no. 2, pp. 215–222, jun 2006.

[58] Ilia G Denisov, Thomas M Makris, Stephen G Sligar, and Ilme Schlichting, "Structure and Chemistry of Cytochrome P450", *Chemical Reviews*, vol. 105, no. 6, pp. 2253–2278, jun 2005.

[59] Antoinette Chougnet, Yelena Grinkova, David Ricard, Stephen Sligar, and Wolf-D. Woggon, "Fluorescent Probes for Rapid Screening of Potential DrugDrug Interactions at the CYP3A4 Level", *ChemMedChem*, vol. 2, no. 5, pp. 717–724, may 2007.

[60] Ilia G Denisov, Mark A McLean, Andrew W Shaw, Yelena V Grinkova, and Stephen G Sligar, "Thermotropic Phase Transition in Soluble Nanoscale Lipid Bilayers", *The Journal of Physical Chemistry B*, vol. 109, no. 32, pp. 15580–15588, aug 2005.

[61] Andrew W Shaw, Mark A McLean, and Stephen G Sligar, "Phospholipid phase transitions in homogeneous nanometer scale bilayer discs", *FEBS Letters*, vol. 556, no. 1-3, pp. 260–264, jan 2004.

[62] Michael Gregory, Piotr J. Mak, Stephen G. Sligar, and James R. Kincaid, "Differential Hydrogen Bonding in Human CYP17 Dictates Hydroxylation versus Lyase Chemistry", *Angewandte Chemie International Edition*, vol. 52, no. 20, pp. 5342–5345, may 2013.

[63] A Luthra, M Gregory, Y V Grinkova, I G Denisov, and S G Sligar, "Nanodiscs in the Studies of Membrane-Bound Cytochrome P450 Enzymes", in *Cytochrome P450 Protocols*, R Ian Phillips, A Elizabeth Shephard, and R Paul Ortiz de Montellano, Eds., pp. 115–127. Humana Press, Totowa, NJ, 2013.

[64] Jirí Homola, "Present and future of surface plasmon resonance biosensors", *Analytical and Bioanalytical Chemistry*, vol. 377, no. 3, pp. 528–539, oct 2003.

[65] Priyabrata Pattnaik, "Surface Plasmon Resonance: Applications in Understanding ReceptorLigand Interaction", *Applied Biochemistry and Biotechnology*, vol. 126, no. 2, pp. 079–092, 2005.

[66] Jonas Borch, Federico Torta, Stephen G. Sligar, and Peter Roepstorff, "Nanodiscs for Immobilization of Lipid Bilayers and Membrane Receptors: Kinetic Analysis of Cholera Toxin Binding to a Glycolipid Receptor", *Analytical Chemistry*, vol. 80, no. 16, pp. 6245–6252, aug 2008.

[67] Edgar D Goluch, Andrew W Shaw, Stephen G Sligar, and Chang Liu, "Microfluidic patterning of nanodisc lipid bilayers and multiplexed analysis of protein interaction", *Lab on a Chip*, vol. 8, no. 10, pp. 1723, oct 2008.

[68] Courtney D Kuhnline Sloan, Michael T. Marty, Stephen G. Sligar, and Ryan C. Bailey, "Interfacing Lipid Bilayer Nanodiscs and Silicon Photonic Sensor Arrays for Multiplexed ProteinLipid and ProteinMembrane Protein Interaction Screening", *Analytical Chemistry*, vol. 85, no. 5, pp. 2970–2976, mar 2013.

[69] Theresa M Allen and Pieter R Cullis, "Drug Delivery Systems: Entering the Mainstream", *Science*, vol. 303, no. 5665, pp. 1818–1822, mar 2004.

[70] S Dean Allison, "Liposomal Drug Delivery", *Journal of Infusion Nursing*, vol. 30, no. 2, 2007.

[71] Robert M Fielding, "Liposomal Drug Delivery", *Clinical Pharmacokinetics*, vol. 21, no. 3, pp. 155–164, 2012.

[72] André Bernard, Bruno Michel, and Emmanuel Delamarche, "Micromosaic Immunoassays", *Analytical Chemistry*, vol. 73, no. 1, pp. 8–12, jan 2001.

[73] Jing Su, Michelle R. Bringer, Rustem F. Ismagilov, and Milan Mrksich, "Combining Microfluidic Networks and Peptide Arrays for Multi-Enzyme Assays", *Journal of the American Chemical Society*, vol. 127, no. 20, pp. 7280–7281, may 2005.

[74] Yongtae Kim, Francois Fay, David P Cormode, Brenda L Sanchez-Gaytan, Jun Tang, Elizabeth J Hennessy, Mingming Ma, Kathryn Moore, Omid C Farokhzad, Edward Allen Fisher, Willem J M Mulder, Robert Langer, and Zahi A Fayad, "Single Step Reconstitution of Multifunctional High-Density Lipoprotein-Derived Nanomaterials Using Microfluidics", *ACS Nano*, vol. 7, no. 11, pp. 9975–9983, nov 2013.

[75] F Peter Guengerich, "Cytochrome P450 and Chemical Toxicology", *Chemical Research in Toxicology*, vol. 21, no. 1, pp. 70–83, jan 2008.

[76] Brian Cunningham, Jean Qiu, Bo Lin, Peter Li, and Jane Pepper, "A plastic colorimetric resonant optical biosensor for multiparallel detection of label-free biochemical interactions", in *Proceedings of IEEE Sensors*. 2002, vol. 1, pp. 212–216, IEEE.

[77] Brian Cunningham, Jean Qiu, Peter Li, and Bo Lin, "Enhancing the surface sensitivity of colorimetric resonant optical biosensors", *Sensors and Actuators B: Chemical*, vol. 87, no. 2, pp. 365–370, dec 2002.

[78] Vlad Cojocaru, Peter J Winn, and Rebecca C Wade, "The ins and outs of cytochrome P450s", *Biochimica et Biophysica Acta (BBA) - General Subjects*, vol. 1770, no. 3, pp. 390–401, mar 2007.

[79] Karin Schleinkofer, Sudarko, Peter J Winn, Susanne K Lüdemann, and Rebecca C Wade, "Do mammalian cytochrome P450s show multiple ligand access pathways and ligand channelling?", *EMBO reports*, vol. 6, no. 6, pp. 584–589, jun 2005.

[80] Susanna K Lüdemann, Valère Lounnas, and Rebecca C Wade, "How do substrates enter and products exit the buried active site of cytochrome P450cam? 1. Random expulsion molecular dynamics investigation of ligand access channels and mechanisms", *Journal of Molecular Biology*, vol. 303, no. 5, pp. 797–811, nov 2000.

[81] Swati Prasad, Shyamalava Mazumdar, and Samaresh Mitra, "Binding of camphor to Pseudomonas putida cytochrome P450 cam : steady-state and picosecond time-resolved fluorescence studies", *FEBS Letters*, vol. 477, no. 3, pp. 157–160, jul 2000.

[82] F. Peter Guengerich, "CYTOCHROME P-450 3A4: Regulation and Role in Drug Metabolism", *Annual Review of Pharmacology and Toxicology*, vol. 39, no. 1, pp. 1–17, apr 1999.

[83] Natilie A. Hosea, Grover P. Miller, and F. Peter Guengerich, "Elucidation of Distinct Ligand Binding Sites for Cytochrome P450 3A4 ", *Biochemistry*, vol. 39, no. 20, pp. 5929–5939, may 2000.

[84] Pamela A. Williams, Jose Cosme, Vandana Sridhar, Eric F. Johnson, and Duncan E. McRee, "Mammalian Microsomal Cytochrome P450 Monooxygenase", *Molecular Cell*, vol. 5, no. 1, pp. 121–131, 2000.

[85] Thomas L. Poulos, Barry C. Finzel, and Andrew J. Howard, "High-resolution crystal structure of cytochrome P450cam", *Journal of Molecular Biology*, vol. 195, no. 3, pp. 687–700, jun 1987.

[86] Irina F Sevrioukova and Thomas L Poulos, "Structural and Mechanistic Insights into the Interaction of Cytochrome P4503A4 with Bromoergocryptine, a Type I Ligand", *Journal of Biological Chemistry*, vol. 287, no. 5, pp. 3510–3517, jan 2012.

[87] Daniel J Frank, Ilia G Denisov, and Stephen G Sligar, "Mixing apples and oranges: Analysis of heterotropic cooperativity in cytochrome P450 3A4", *Archives of Biochemistry and Biophysics*, vol. 488, no. 2, pp. 146–152, aug 2009.

[88] Dmitri R Davydov, James R Halpert, Jean-Paul Renaud, and Gaston Hui Bon Hoa, "Conformational heterogeneity of cytochrome P450 3A4 revealed by high pressure spectroscopy", *Biochemical and Biophysical Research Communications*, vol. 312, no. 1, pp. 121–130, dec 2003.

[89] Dmitri R Davydov, Bradley J Baas, Stephen G Sligar, and James R Halpert, "Allosteric Mechanisms in Cytochrome P450 3A4 Studied by High-Pressure Spectroscopy: Pivotal Role of Substrate-Induced Changes in the Accessibility and Degree of Hydration of the Heme Pocket ", *Biochemistry*, vol. 46, no. 26, pp. 7852–7864, jul 2007.

[90] Patrik Rydberg, Thomas H Rod, Lars Olsen, and Ulf Ryde, "Dynamics of Water Molecules in the Active-Site Cavity of Human Cytochromes P450", *The Journal of Physical Chemistry B*, vol. 111, no. 19, pp. 5445–5457, may 2007.

[91] Karel Berka, Tereza Hendrychová, Pavel Anzenbacher, and Michal Otyepka, "Membrane Position of Ibuprofen Agrees with Suggested Access Path Entrance to Cytochrome P450 2C9 Active Site", *The Journal of Physical Chemistry A*, vol. 115, no. 41, pp. 11248–11255, oct 2011.

[92] Vlad Cojocaru, Kia Balali-Mood, Mark S P Sansom, and Rebecca C Wade, "Structure and Dynamics of the Membrane-Bound Cytochrome P450 2C9", *PLoS Computational Biology*, vol. 7, no. 8, pp. e1002152, aug 2011.

[93] Karel Berka, Markéta Paloncýová, Pavel Anzenbacher, and Michal Otyepka, "Behavior of Human Cytochromes P450 on Lipid Membranes", *The Journal of Physical Chemistry B*, vol. 117, no. 39, pp. 11556–11564, oct 2013.

[94] Ying-Lu Cui, Qiao Xue, Qing-Chuan Zheng, Ji-Long Zhang, Chui-Peng Kong, Jing-Rong Fan, and Hong-Xing Zhang, "Structural features and dynamic investigations of the membrane-bound cytochrome P450 17A1", *Biochimica et Biophysica Acta (BBA) - Biomembranes*, vol. 1848, no. 10, pp. 2013–2021, oct 2015.

[95] Jiho Park, Luke Czapla, and Rommie E. Amaro, "Molecular Simulations of Aromatase Reveal New Insights Into the Mechanism of Ligand Binding", *Journal of Chemical Information and Modeling*, vol. 53, no. 8, pp. 2047–2056, aug 2013.

[96] Ilan Chabay, "Optical waveguides. Photon plumbing for the chemistry lab: fiber optics, waveguides, and evanescent waves as tools for chemical analysis", *Analytical Chemistry*, vol. 54, no. 9, pp. 1071A–1080A, aug 1982.

[97] Lee Kang and Raymond E. Dessy, "Slab Waveguides in Chemistry", *Critical Reviews in Analytical Chemistry*, vol. 21, no. 6, pp. 377–388, jan 1990.

[98] N. J. Harrick, "Electric Field Strengths at Totally Reflecting Interfaces", *Journal of the Optical Society of America*, vol. 55, no. 7, pp. 851, jul 1965.

[99] D. M. Cropek and Paul W. Bohn, "Surface molecular orientations determined by electronic linear dichroism in optical waveguide structures", *The Journal of Physical Chemistry*, vol. 94, no. 16, pp. 6452–6457, aug 1990.

[100] Louise Karle Hanson, William a Eaton, Stephen G Sligar, I C Gunsalus, Martin Gouterman, and Charles R Connell, "Origin of the anomalous Soret spectra of carboxycytochrome P-450", *Journal of the American Chemical Society*, vol. 98, no. 9, pp. 2672–2674, apr 1976.

[101] Marvin W. Makinen and William A. Eaton, "POLARIZED SINGLE CRYSTAL ABSORPTION SPECTRA OF CARBOXY- AND OXYHEMOGLOBIN", *Annals of the New York Academy of Sciences*, vol. 206, no. 1 The Chemical, pp. 210–222, oct 1973.

[102] Tammy L. Domanski, You-Ai He, Kishore K. Khan, Fabienne Roussel, Qinmi Wang, and James R. Halpert, "Phenylalanine and Tryptophan Scanning Mutagenesis of CYP3A4 Substrate Recognition Site Residues and Effect on Substrate Oxidation and Cooperativity ", *Biochemistry*, vol. 40, no. 34, pp. 10150–10160, aug 2001.

[103] E.M.J. Gillam, T. Baba, B.R. Kim, S. Ohmori, and F.P. Guengerich, "Expression of Modified Human Cytochrome P450 3A4 in Escherichia coli and Purification and Reconstitution of the Enzyme", *Archives of Biochemistry and Biophysics*, vol. 305, no. 1, pp. 123–131, aug 1993.

[104] Richard Lonsdale, Sarah L. Rouse, Mark S P Sansom, and Adrian J. Mulholland, "A Multiscale Approach to Modelling Drug Metabolism by Membrane-Bound Cytochrome P450 Enzymes", *PLoS Computational Biology*, vol. 10, no. 7, pp. e1003714, jul 2014.

[105] Ghulam Mustafa, Prajwal P. Nandekar, Xiaofeng Yu, and Rebecca C. Wade, "On the application of the MARTINI coarse-grained model to immersion of a protein in a phospholipid bilayer", *The Journal of Chemical Physics*, vol. 143, no. 24, pp. 243139, dec 2015.

[106] Veronika Navrátilová, Markéta Paloncýová, Michaela Kajšová, Karel Berka, and Michal Otyepka, "Effect of Cholesterol on the Structure of Membrane-Attached Cytochrome P450 3A4", *Journal of Chemical Information and Modeling*, vol. 55, no. 3, pp. 628–635, mar 2015.

[107] Yoshihiro Ohta, Suguru Kawato, Hiroko Tagashira, Shigeki Takemori, and Shiro Kominami, "Dynamic structures of adrenocortical cytochrome P-450 in proteoliposomes and microsomes: protein rotation study", *Biochemistry*, vol. 31, no. 50, pp. 12680–12687, dec 1992.

[108] Gerd Kleideiter, Manfred Dieter Lechner, and Wolfgang Knoll, "Pressure dependence of thickness and refractive index of thin PMMA-films investigated by surface plasmon and optical waveguide spectroscopy", *Macromolecular Chemistry and Physics*, vol. 200, no. 5, pp. 1028–1033, may 1999.

[109] K. Rodgers, T. Pochapsky, and S. Sligar, "Probing the mechanisms of macromolecular recognition: the cytochrome b5-cytochrome c complex", *Science*, vol. 240, no. 4859, pp. 1657–1659, jun 1988.

[110] Karla K. Rodgers and Stephen G. Sligar, "Mapping electrostatic interactions in macromolecular associations", *Journal of Molecular Biology*, vol. 221, no. 4, pp. 1453–1460, oct 1991.

[111] Zdzislaw Salamon, H.Angus Macleod, and Gordon Tollin, "Surface plasmon resonance spectroscopy as a tool for investigating the biochemical and biophysical properties of membrane protein systems. II: Applications to biological systems", *Biochimica et Biophysica Acta (BBA) - Reviews on Biomembranes*, vol. 1331, no. 2, pp. 131–152, sep 1997.

[112] Erwin Kretschmann, "Die Bestimmung optischer Konstanten von Metallen durch Anregung von Oberfluchenplasmaschwingungen", *Zeitschrift fur Physik*, vol. 241, no. 4, pp. 313–324, aug 1971.

[113] Abraham Verghese, Blake Charlton, Brooke Cotter, and John Kugler, "A History of Physical Examination Texts and the Conception of Bedside Diagnosis", *Transactions of the American Clinical and Climatological Association*, vol. 122, pp. 290–311, 2011.

[114] Jessica M Strauss, Dietrich V K Jehle, and Beric E Berlioz, "Advancements at the bedside: diagnostic and therapeutic tools", *Clinical Practice*, vol. 11, no. 6, pp. 689–697, dec 2014.

[115] Bo Lin, Jean Qiu, John Gerstenmeier, Peter Li, Homer Pien, Jane Pepper, and Brian Cunningham, "A label-free optical technique for detecting small molecule interactions", *Biosensors and Bioelectronics*, vol. 17, no. 9, pp. 827–834, sep 2002.

[116] Leo L. Chan, Brian T. Cunningham, Peter Y. Li, and Derek Puff, "Self-referenced assay method for photonic crystal biosensors: Application to small molecule analytes", *Sensors and Actuators B: Chemical*, vol. 120, no. 2, pp. 392–398, jan 2007.

[117] Jerson L Silva, Debora Foguel, Andrea T Da Poian, and Peter E Prevelige, "The use of hydrostatic pressure as a tool to study viruses and other macromolecular assemblages", *Current Opinion in Structural Biology*, vol. 6, no. 2, pp. 166–175, apr 1996.

[118] Gregorio Weber and Harry G. Drickamer, "The effect of high pressure upon proteins and other biomolecules", *Quarterly Reviews of Biophysics*, vol. 16, no. 01, pp. 89, feb 1983.

[119] Mark T. Fisher, Ronald E. White, and S. G. Sligar, "Pressure dissociation of a protein-protein electron-transfer complex", *Journal of the American Chemical Society*, vol. 108, no. 21, pp. 6835–6837, oct 1986.

[120] J L Silva and G Weber, "Pressure Stability of Proteins", *Annual Review of Physical Chemistry*, vol. 44, no. 1, pp. 89–113, oct 1993.

[121] Michael GROSS and Rainer JAENICKE, "Proteins under pressure. The influence of high hydrostatic pressure on structure, function and assembly of proteins and protein complexes", *European Journal of Biochemistry*, vol. 221, no. 2, pp. 617–630, apr 1994.

[122] Eddie Morild, "The Theory of Pressure Effects on Enzymes", in *Advances in Protein Chemistry*, vol. 34 of *Advances in Protein Chemistry*, pp. 93–166. Elsevier, 1981.

[123] G Kleideiter, Z Sekkat, M Kreiter, M Dieter Lechner, and W Knoll, "Photoisomerization of disperse red one in films of poly(methyl-methacrylate) at high pressure", *Journal of Molecular Structure*, vol. 521, no. 1-3, pp. 167–178, mar 2000.

[124] Alejandro A. Paladini, "Absolute measurements of fluorescence polarization at high pressures", *Review of Scientific Instruments*, vol. 52, no. 3, pp. 419, mar 1981.

[125] Brian Cunningham, Peter Li, Bo Lin, and Jane Pepper, "Colorimetric resonant reflection as a direct biochemical assay technique", *Sensors and Actuators B: Chemical*, vol. 81, no. 2-3, pp. 316–328, jan 2002.

[126] Henry V Kehiaian David R. Lide, *CRC Handbook of Themophysical and Thermochemical Data*, CRC Press, 1994.

[127] Adam L Washburn, Joseph Gomez, and Ryan C Bailey, "DNA-Encoding to Improve Performance and Allow Parallel Evaluation of the Binding Characteristics of Multiple Antibodies in a Surface-Bound Immunoassay Format", *Analytical Chemistry*, vol. 83, no. 9, pp. 3572–3580, may 2011.

[128] Matthew S Luchansky, Adam L Washburn, Teresa A Martin, Muzammil Iqbal, L Cary Gunn, and Ryan C Bailey, "Characterization of the evanescent field profile and bound mass sensitivity of a label-free silicon photonic microring resonator biosensing platform", *Biosensors and Bioelectronics*, vol. 26, no. 4, pp. 1283–1291, dec 2010.

[129] Matthew S Luchansky and Ryan C Bailey, "Silicon Photonic Microring Resonators for Quantitative Cytokine Detection and T-Cell Secretion Analysis", *Analytical Chemistry*, vol. 82, no. 5, pp. 1975–1981, mar 2010.

[130] Adam L. Washburn, Matthew S. Luchansky, Melinda S. McClellan, and Ryan C. Bailey, "Label-free, multiplexed biomolecular analysis using arrays of silicon photonic microring resonators", *Procedia Engineering*, vol. 25, pp. 63–66, 2011.

[131] Patrick Raynal and Harvey B Pollard, "Annexins: the problem of assessing the biological role for a gene family of multifunctional calcium- and phospholipid-binding proteins", *Biochimica et Biophysica Acta (BBA) - Reviews on Biomembranes*, vol. 1197, no. 1, pp. 63–93, apr 1994.

[132] Isabelle Mus-Veteau, *Heterologous Expression of Membrane Proteins*, vol. 601 of *Methods in Molecular Biology*, Humana Press, Totowa, NJ, 2010.

[133] Marco G Casteleijn, Arto Urtti, and Sanjay Sarkhel, "Expression without boundaries: Cell-free protein synthesis in pharmaceutical research", *International Journal of Pharmaceutics*, vol. 440, no. 1, pp. 39–47, jan 2013.

[134] Steffen Rupp, "Next-generation bioproduction systems: Cell-free conversion concepts for industrial biotechnology", *Engineering in Life Sciences*, vol. 13, no. 1, pp. 19–25, jan 2013.

[135] James F Zawada, Gang Yin, Alexander R Steiner, Junhao Yang, Alpana Naresh, Sushmita M Roy, Daniel S Gold, Henry G Heinsohn, and Christopher J Murray, "Microscale to manufacturing scale-up of cell-free cytokine production-a new approach for shortening protein production development timelines", *Biotechnology and Bioengineering*, vol. 108, no. 7, pp. 1570–1578, jul 2011.

[136] Andrew Leitz, Timothy Bayburt, Alexander Barnakov, Barry Springer, and Stephen Sligar, "Functional reconstitution of β2-adrenergic receptors utilizing self-assembling Nanodisc technology", *BioTechniques*, vol. 40, no. 5, pp. 601–612, may 2006.

[137] Spyridon Gerontas, Michael S. Shapiro, and Daniel G. Bracewell, "Chromatography modelling to describe protein adsorption at bead level", *Journal of Chromatography A*, vol. 1284, pp. 44–52, apr 2013.

[138] Michael S Shapiro, Steve J Haswell, Gary J Lye, and Daniel G Bracewell, "Design and characterization of a microfluidic packed bed system for protein breakthrough and dynamic binding capacity determination", *Biotechnology Progress*, vol. 25, no. 1, pp. 277–285, jan 2009.

[139] Mei He and Amy E Herr, "Automated microfluidic protein immunoblotting", *Nature Protocols*, vol. 5, no. 11, pp. 1844–1856, oct 2010.

[140] George M Whitesides, "The origins and the future of microfluidics", *Nature*, vol. 442, no. 7101, pp. 368–373, jul 2006.

[141] Harold Craighead, "Future lab-on-a-chip technologies for interrogating individual molecules", *Nature*, vol. 442, no. 7101, pp. 387–393, jul 2006.

[142] L. J. Millet, J. D. Lucheon, R. F. Standaert, S. T. Retterer, and M. J. Doktycz, "Modular microfluidics for point-of-care protein purifications", *Lab Chip*, vol. 15, no. 8, pp. 1799–1811, 2015.

[143] Rui Hu, Xiaojun Feng, Pu Chen, Meng Fu, Hong Chen, Lin Guo, and Bi-Feng Liu, "Rapid, highly efficient extraction and purification of membrane proteins using a microfluidic continuous-flow based aqueous two-phase system", *Journal of Chromatography A*, vol. 1218, no. 1, pp. 171–177, jan 2011.

[144] G. Münchow, S Hardt, J P Kutter, and K S Drese, "Electrophoretic partitioning of proteins in two-phase microflows", *Lab Chip*, vol. 7, no. 1, pp. 98–102, 2007.

[145] Andrea Urbani and Tony Warne, "A colorimetric determination for glycosidic and bile salt-based detergents: applications in membrane protein research", *Analytical Biochemistry*, vol. 336, no. 1, pp. 117–124, jan 2005.

[146] Josep Cladera, Jean-Louis Ricaud, Joaquim Villa Verde, and Mireia DuNach, "Liposome Solubilization and Membrane Protein Reconstitution Using Chaps and Chapso", *European Journal of Biochemistry*, vol. 243, no. 3, pp. 798–804, feb 1997.

[147] Ralph Weissleder, "Molecular Imaging in Cancer", *Science*, vol. 312, no. 5777, pp. 1168–1171, may 2006.

[148] Eric T Ahrens and Jeff W M Bulte, "Tracking immune cells in vivo using magnetic resonance imaging", *Nature Reviews Immunology*, vol. 13, no. 10, pp. 755–763, sep 2013.

[149] Tarik F Massoud, "Molecular imaging in living subjects: seeing fundamental biological processes in a new light", *Genes & Development*, vol. 17, no. 5, pp. 545–580, mar 2003.

[150] David E Sosnovik, Eyk A Schellenberger, Matthias Nahrendorf, Mikhail S Novikov, Takashi Matsui, George Dai, Fred Reynolds, Luanda Grazette, Anthony Rosenzweig, Ralph Weissleder, and Lee Josephson, "Magnetic resonance imaging of cardiomyocyte apoptosis with a novel magneto-optical nanoparticle", *Magnetic Resonance in Medicine*, vol. 54, no. 3, pp. 718–724, sep 2005.

[151] M Modo, J.S. Beech, T.J. Meade, S.C.R. Williams, and J Price, "A chronic 1 year assessment of MRI contrast agent-labelled neural stem cell transplants in stroke", *NeuroImage*, vol. 47, pp. T133–T142, aug 2009.

[152] Preeti A Sukerkar, Keith W MacRenaris, Thomas J Meade, and Joanna E Burdette, "A Steroid-Conjugated Magnetic Resonance Probe Enhances Contrast in Progesterone Receptor Expressing Organs and Tumors in Vivo", *Molecular Pharmaceutics*, vol. 8, no. 4, pp. 1390–1400, aug 2011.

[153] éva Tóth, Lothar Helm, and André Merbach, "Relaxivity of Gadolinium(III) Complexes: Theory and Mechanism", in *The Chemistry of Contrast Agents in Medical Magnetic Resonance Imaging*, pp. 25–81. John Wiley & Sons, Ltd, Chichester, UK, feb 2013.

[154] K J Murphy, J A Brunberg, and R H Cohan, "Adverse reactions to gadolinium contrast media: a review of 36 cases.", *American Journal of Roentgenology*, vol. 167, no. 4, pp. 847–849, oct 1996.

[155] Christiane E Carney, Keith W MacRenaris, Daniel J Mastarone, David R Kasjanski, Andy H Hung, and Thomas J Meade, "Cell Labeling via Membrane-Anchored Lipophilic MR Contrast Agents", *Bioconjugate Chemistry*, vol. 25, no. 5, pp. 945–954, may 2014.

[156] Michael A Bruckman, Xin Yu, and Nicole F Steinmetz, "Engineering Gd-loaded nanoparticles to enhance MRI sensitivity via T 1 shortening", *Nanotechnology*, vol. 24, no. 46, pp. 462001, nov 2013.

[157] Amruta Manke, Liying Wang, and Yon Rojanasakul, "Mechanisms of Nanoparticle-Induced Oxidative Stress and Toxicity", *BioMed Research International*, vol. 2013, pp. 1–15, 2013.

[158] David P Cormode, Juan C Frias, Yanqing Ma, Wei Chen, Torjus Skajaa, Karen Briley-Saebo, Alessandra Barazza, Kevin Jon Williams, Willem JM Mulder, Zahi A Fayad, and Edward A Fisher, "HDL as a contrast agent for medical imaging", *Clinical Lipidology*, vol. 4, no. 4, pp. 493–500, aug 2009.

[159] Sander Langereis, Tessa Geelen, Holger Grüll, Gustav J Strijkers, and Klaas Nicolay, "Paramagnetic liposomes for molecular MRI and MRI-guided drug delivery", *NMR in Biomedicine*, vol. 26, no. 7, pp. 728–744, jul 2013.

[160] Eugene Mahon, Anna Salvati, Francesca Baldelli Bombelli, Iseult Lynch, and Kenneth a. Dawson, "Designing the nanoparticle-biomolecule interface for "targeting and therapeutic delivery"", *Journal of Controlled Release*, vol. 161, no. 2, pp. 164–174, 2012.

[161] You Han Bae and Kinam Park, "Targeted drug delivery to tumors: Myths, reality and possibility", *Journal of Controlled Release*, vol. 153, no. 3, pp. 198–205, 2011.

[162] Abhinav Nath, William M Atkins, and Stephen G Sligar, "Applications of Phospholipid Bilayer Nanodiscs in the Study of Membranes and Membrane Proteins ", *Biochemistry*, vol. 46, no. 8, pp. 2059–2069, feb 2007.

[163] Wei Chen, Esad Vucic, Eik Leupold, Willem J M Mulder, David P. Cormode, Karen C. Briley-Saebo, Alessandra Barazza, Edward A. Fisher, Margitta Dathe, and Zahi A. Fayad, "Incorporation of an apoE-derived lipopeptide in high-density lipoprotein MRI contrast agents for enhanced imaging of macrophages in atherosclerosis", *Contrast Media & Molecular Imaging*, vol. 3, no. 6, pp. 233–242, nov 2008.

[164] Willem J M Mulder, Gustav J. Strijkers, Geralda A F van Tilborg, Arjan W. Griffioen, and Klaas Nicolay, "Lipid-based nanoparticles for contrast-enhanced MRI and molecular imaging", *NMR in Biomedicine*, vol. 19, no. 1, pp. 142–164, feb 2006.

[165] Gerrit van Meer, Dennis R Voelker, and Gerald W Feigenson, "Membrane lipids: where they are and how they behave", *Nat Rev Mol Cell Biol*, vol. 9, no. 2, pp. 112–124, feb 2008.

[166] Megh Raj Bhatt, Yogan Khatri, Raymond J Rodgers, and Lisandra L Martin, "Role of cytochrome b5 in the modulation of the enzymatic activities of cytochrome P450 17α-hydroxylase/17,20-lyase (P450 17A1)", *The Journal of Steroid Biochemistry and Molecular Biology*, mar 2016.

[167] D Fernando Estrada, Andria L Skinner, Jennifer S Laurence, and Emily E Scott, "Human Cytochrome P450 17A1 Conformational Selection: MODULATION BY LIGAND AND CYTOCHROME b5", *Journal of Biological Chemistry*, vol. 289, no. 20, pp. 14310–14320, may 2014.

[168] Clifford R Robinson and Stephen G Sligar, "Hydrostatic Pressure Reverses Osmotic Pressure Effects on the Specificity of EcoRI-DNA Interactions", *Biochemistry*, vol. 33, no. 13, pp. 3787–3793, apr 1994.

[169] T.W. Lynch, M.A. McLean, D. Kosztin, K. Schulten, and S.G. Sligar, "High pressure gel mobility shift analysis and molecular dynamics: Investigating specific protein-nucleic acid recognition", in *Trends in High Pressure Bioscience and Biotechnology*, vol. 19, pp. 87–94. Elsevier B.V., 2002.

[170] Narjes Tavoosi, Rebecca L Davis-Harrison, Taras V Pogorelov, Y Zenmei Ohkubo, Mark J Arcario, Mary C Clay, Chad M Rienstra, Emad Tajkhorshid, and James H Morrissey, "Molecular Determinants of Phospholipid Synergy in Blood Clotting", *Journal of Biological Chemistry*, vol. 286, no. 26, pp. 23247–23253, jul 2011.

[171] Mattias Björnmalm, Yan Yan, and Frank Caruso, "Engineering and evaluating drug delivery particles in microfluidic devices", *Journal of Controlled Release*, vol. 190, pp. 139–149, 2014.

[172] Michael T Marty, Kyle C Wilcox, William L Klein, and Stephen G Sligar, "Nanodisc-solubilized membrane protein library reflects the membrane proteome", *Analytical and Bioanalytical Chemistry*, vol. 405, no. 12, pp. 4009–4016, may 2013.

[173] Jahnabi Roy, Holly Pondenis, Timothy M. Fan, and Aditi Das, "Direct Capture of Functional Proteins from Mammalian Plasma Membranes into Nanodiscs", *Biochemistry*, vol. 54, no. 41, pp. 6299–6302, oct 2015.